AL/OE-TR-1994-0060

ARMSTRONG LABORATORY

REVIEW OF PERSONNEL SUSCEPTIBILITY TO LASERS: SIMULATION IN SIMNET-D FOR CTAS-2.0

Shari R. Thomas, Ph.D.

Occupational and Environmental Health Directorate
Optical Radiation Division
8111 18th Street
Brooks AFB, TX 78235-5215

January 1994

Final Technical Report for Period June 1990 - December 1993

Approved for public release; distribution is unlimited.

AIR FORCE MATERIEL COMMAND
BROOKS AIR FORCE BASE, TEXAS

NOTICES

When Government drawings, specifications, or other data are used for any purpose other than in connection with a definitely Government-related procurement, the United States Government incurs no responsibility or any obligation whatsoever. The fact that the Government may have formulated or in any way supplied the said drawings, specifications, or other data, is not to be regarded by implication, or otherwise in any manner construed, as licensing the holder or any other person or corporation; or as conveying any rights or permission to manufacture, use, or sell any patented invention that may in any way be related thereto.

The mention of trade names or commerical products in this publication is for illustration purposes and does not constitute endorsement or recommendation for use by the United Sates Air Force.

The Office of Public Affairs has reviewed this report, and it is releasable to the National Technical Information Service, where it will be available to the general public, including foreign nationals.

This report has been reviewed and is approved for publication.

Government agencies and their contractors registerd with Defense Technical Information Center (DTIC) should direct requests for copies to: DTIC, Building 5, Cameron Station, 5010 Duke Street, Alexandria VA 22304-6145.

Non-goverment agencies may purchase copies of this report from: National Technical Information Service (NTIS), 5285 Port Royal Road, Springfield VA 22161-2103.

Shari R. Thomas

SHARI R. THOMAS, Ph.D.
Project Scientist

Robert M. Cartledge

ROBERT M. CARTLEDGE, Lt Col, USAF, BSC
Chief, Optical Radiation Division

REPORT DOCUMENTATION PAGE

Form Approved
OMB No. 0704-0188

1. AGENCY USE ONLY *(Leave blank)*	2. REPORT DATE	3. REPORT TYPE AND DATES COVERED
	January 1995	June 1990 - December 1993

4. TITLE AND SUBTITLE

Review of Personnel Susceptibility to Lasers: Simulation in SIMNET-D for CTAS-2.0

5. FUNDING NUMBERS

PE - 62202F
PR - 7757
TA - 88
WU - 03

6. AUTHOR(S)

Shari R. Thomas

7. PERFORMING ORGANIZATION NAME(S) AND ADDRESS(ES)

Armstrong Laboratory
Occupational and Environmental Health Directorate
Optical Radiation Division
8111 18th Street
Brooks Air Force Base, Texas 78235-5215

8. PERFORMING ORGANIZATION REPORT NUMBER

AL/OE-TR-1994-0060

9. SPONSORING / MONITORING AGENCY NAME(S) AND ADDRESS(ES)

Visual Psychophysics Branch
Armstrong Laboratory
Occupational and Environmental Health Directorate
Brooks Air Force Base, Texas 78235-5000

10. SPONSORING / MONITORING AGENCY REPORT NUMBER

11. SUPPLEMENTARY NOTES

12a. DISTRIBUTION / AVAILABILITY STATEMENT

Approved for public release; distribution is unlimited.

12b. DISTRIBUTION CODE

13. ABSTRACT *(Maximum 200 words)*

The purpose of this report is to provide an overview of retinal laser bioeffects and document the rationale for their characterization in simulated virtual battlefield networks (i.e., SIMNET-D) for the CTAS 2.0 exercises. Specifically, the goals of this report are to: (a) explain retinal laser bioeffects in layman's terms so that their biological and perceptual consequences can be understood by persons not having vision science backgrounds; (b) recommend methods of ideally simulating retinal laser bioeffects in computerized virtual battlefields given what is currently known about these bioeffects and the present state-of-the-art computer graphics technology; (c) propose a mapping of these ideal simulations to reasonable laser bioeffect simulations that are achievable for the CTAS-2.0 test given the capabilities the computer graphic software that SIMNET-D is known to possess; and (d) recommend methods of simulating laser bioeffects with LEP devices, called electro-optical counter countermeasures (EOCCM), and provide the rationale for these recommendations.

14. SUBJECT TERMS	15. NUMBER OF PAGES
SIMNET-D, CTAS-2.0, retinal bioeffects, virtual battlefields	84
	16. PRICE CODE

17. SECURITY CLASSIFICATION OF REPORT	18. SECURITY CLASSIFICATION OF THIS PAGE	19. SECURITY CLASSIFICATION OF ABSTRACT	20. LIMITATION OF ABSTRACT
Unclassified	Unclassified	Unclassified	SAR

DEDICATION

This report is dedicated to the memory of Arthur Menendez, Ph.D., who disappeared while diving on 5 Jul 92. Dr. Menendez' dedication to laser bioeffects research resulted in many advances in the science. His arduous review of preliminary versions of this document enhanced its quality immensely. Our program's loss of Dr. Menendez has created a tremendous void which will be difficult to overcome.

CONTENTS

Page

LIST OF ACRONYMS ix

INTRODUCTION 1

Background 1

General Comments on CTAS-2.0 and Laser Bioeffects 1

FACTORS DETERMINING VISIBILITY 2

Ambient Environmental Luminance Condition 2
Target Characteristics 4
Retinal Location 4
Contrast Sensitivity 5
Spectral Sensitivity 6
Interaction of Factors Influencing Visibility 7
Models of Human Vision and Laser Bioeffects 8
Visibility with Selective Absorption Filters 9

OVERVIEW OF LASER BIOEFFECTS 11

Veiling Glare 12
Equivalent Background Hypothesis for Modeling Glare 14
Flashblindness 15
General Comments on Biological Damage 17
Classifications of Laser Energy and Damage 19
Classification of Biological Damage 19
Mechanisms of Biological Damage 20
Minimum Visible and Photocoagulation Lesions 22
MVL and Photocoagulation Lesions Effects on Visual Function 22
Hemorrhagic Lesions 23
Hemorrhagic Lesions Effects on Visual Function 24
Other Discussions of Biological Damage Effects on Visual Function 25
Multiple Lesions 25
Summary of Retinal Laser Bioeffects 26

INFLUENCE OF SIMNET WORLD AMBIENT CONDITIONS ON THE PREDICTED LASER BIOEFFECTS FOR CTAS-2.0 27

TECHNICAL CONSIDERATIONS AND SUGGESTIONS FOR THE SIMULATION OF LASER BIOEFFECTS ON SIMNET FOR CTAS-2.0 29

Technical Considerations for Simulating Laser Bioeffects 29
Actual Bioeffects Versus Ideal Simulations 32
Ideal Simulations of Glare 32
Ideal Simulations of Flashblindness 33
Ideal Simulations for Biological Damage 34
Ideal Simulations for Minimum Visible Lesions 35
Ideal Simulations for Hemorrhagic Lesions 35
Ideal Versus Achievable Simulations of Laser Bioeffects 36
Achievable Laser Glare Simulations 36

Achievable Flashblindness Simulations 36
Achievable Biological Damage Simulations 36

FIGURES 38

REFERENCES 59

LIST OF FIGURES

Figure no.		Page
1	Ocular tissue absorption of electromagnetic radiation	38
2	Diagram of the different regions of the retina	39
3	Visual Acuity across the retina	40
4	Sensitivity of the visual system to contrast	41
5	The photopic luminosity function	42
6	Increment threshold spectral sensitivity as a funciton of target size	43
7	Glare effectiveness as a function of angular separation	44
8	The Vos function of glare	45
9	Extraocular scatter effects on the Vos function	46
10	Psychological mechansims for glare and flashblindness	47
11	Variables effecting recover from flashblindness	48
12	Flashblindness scotoma size as a functionfo corneal irradiance of the laser exposure	49
13	The visual acuity of the posterior pole	50
14	Several types of laser lesions	51
15	The MPE energy for visible and near IR wavelengths	52
16	The effect of a foveal scotoma on aiming and tracking	53
17	The effect of multiple scotomas on tracking	54
18	The size of the FOVO by cw laser glare	55
19	Spectral characteristics of several commercial phosphors	56

LIST OF TABLES

Table no.		Page
1	Average values of subject trials	57
2	Measured sizes of ADATS on Video Display	58

FOREWARD

This document is a summary report that was written for Cmdr Dennis McBride of the Advanced Research Projects Agency (ARPA), formerly the Defense Advanced Research Projects Agency, for the Counter Target Acquisition Systems (Phase II) force-on-force simulated battle test (CTAS-2.0) performed between Sep and Nov 90. The purpose of the original report was to provide an overview of retinal laser bioeffects and laser eye protection (LEP). The report was also intended to recommend methods of simulating laser bioeffects and LEP for the CTAS-2.0 exercise under both ideal conditions and given the technological limitations of the SIMNET-D system on which the CTAS-2.0 test was conducted. This document represents a window in time prior to and throughout the duration of the CTAS-2.0 exercise. Because the science of retinal laser bioeffects and LEP continues to progress rapidly, not all of the discussions contained in this report are necessarily state-of-the-art. Regardless of these limitations, this report can be used as a general summary of retinal laser bioeffects and LEP.

ACKNOWLEDGMENTS

My thanks to all my colleagues at the Armstrong Laboratory, Optical Radiation Division, KRUG Life Sciences Inc., and The Analytic Science Corporation (TASC) for their assistance in preparing the original draft of this document, which was sent to CDR McBride of ARPA in July 1990. My thanks also to Dr. Jerrold Kronenfeld of TASC for generating the laser exposure corneal irradiances to be used in CTAS-2.0, which were also part of the original draft of this document. In addition, I thank Dr. Fred Loxsom of Pentastar Support Services for his assistance in using AL/OEO's thermal model (Loxsom, 1989) to determine which laser exposures would likely produce thermal and hemorrhagic lesions, and Dr. Arthur Menendez (deceased, AL/OEO) for calculating the field of view obscured by glare using the model he developed with Peter Smith (Royal Air Force, 1990). The data generated from both of these efforts were incorporated in the original draft of this document. Finally, my thanks to Janet Pinnix (Conceptual MindWorks) for her excellent technical assistance in preparing this manuscript.

LIST OF ACRONYMS

ADATS	Air Defense Anti-Tank System
AL/OEO	Armstrong Laboratory Optical Radiation Division
atm	Atmosphere
arc-min	Minutes of Visual Arc
ARPA	Advanced Research Projects Agency
B	Background Luminance
C	Celcius
C_L	Luminance-contrast Ratio
CC	Choriocapillaris
c/d	Cycles per Degree
cd/m2	Candellas per Square-meter
CFF	Critical Fusion Frequency or Critical Flicker Fusion
CIE	Commission International de l'Eclairage
cm	Centimeter
CRT	Cathode-Ray Tube
CSF	Contrast Sensitivity Function
CTAS-2.0	Counter Target Acquisition System Test (Phase II)
cw	Continuous-Wave
EBL	Equivalent Background Luminance
EBT	Equivalent Background Theory
ED_{50}	Threshold Energy for Tissue Damage at 50% Probability
EHT	Eye-Head Tracker
EOCCM	Electro-Optical Counter-countermeasures
fL	Foot-Lambert
FOVO	Field of View Obscured
ft	Foot

HEL	High-Energy Laser
HL	Hemorrhagic Lesion
HUD	Head-Up Display
Hz	Hertz
in	Inch
I_r	Retinal Illuminance
IR	Infrared
J/cm^2	Joules per Square Centimeter
k	Threshold Contrast Ratio
km	Kilometer
LEP	Laser Eye Protection
µ	Micron
µs	Microsecond
$\mu W/cm^2$	MicroWatts per square centimeter
min	Minute
mJ/cm^2	MilliJoules per square centimeter
ms	Millisecond
MPE	Maximum Permissible Exposure
MVL	Minimum Visible Lesion
nm	Nanometer
ns	Nanosecond
OD	Optical Density
PERG	Pattern Electroretinogram
PLZT	Lead Lanthanum Doped Zirconate, Titanate
PRP	Pan-Retinal Photocoagulation
ps	Picosecond
rms	Root-Mean-Square

RPE	Retinal Pigment Epithelium
s	Second
SIMNET-D	Distributed Simulation Network used for CTAS-2.0
t	Time
T	Target of Luminence
TIE	Total Intraocular Energy (Radiant Exposure X Pupil Diameter)
USAFSAM/RZV	United States Air Force School of Aerospace Medicine Radiation Vulnerability Assessment Branch
UV	Ultraviolet Electromagnetic Radiation
VEP	Visual Evoked Potential
λ	Wavelength

REVIEW OF PERSONNEL SUSCEPTIBILITY TO LASERS: SIMULATIONS IN SIMNET-D FOR CTAS-2.0

INTRODUCTION

Background

The Optical Radiation Division of the Armstrong Laboratory (AL/OEO), formerly the Radiation Vulnerability Assessment Branch of the USAF School of Aerospace Medicine (USAFSAM/RZV), supported a project funded by the Advanced Research Projects Agency (ARPA) called Counter Target Acquisition System Test (Phase II (CTAS-2.0)). CTAS-2.0 was a simulated air-to-ground force-on-force battle test which included simulations of laser weapons, the effects of ocular laser exposures, and the perceptual consequences of laser eye protection (LEP) use by aircrews. The primary objective of the CTAS-2.0 project was to evaluate the opportunities of engagement and co-visibility between the simulated laser weapons and the pilots' eyes.

AL/OEO had two roles in supporting CTAS-2.0. The first was to provide technical information on laser bioeffects to the CTAS-2.0 sponsors and test directorate. The second was to recommend methods of simulating the laser bioeffects expected for ocular exposures to laser weapons having the physical characteristics specified for simulation in the CTAS-2.0 test. This report represents the principal mechanism by which AL/OEO provided ARPA, the CTAS-2.0 sponsors, and test directorate with this information. This document is a version of a preliminary manuscript delivered to these individuals by AL/OEO in July 1990. The purpose of this report was to educate the CTAS-2.0 sponsors and test directorate on laser bioeffects and to suggest possible ways of simulating these bioeffects on the SIMNET-D distributed simulation network.

This report also summarizes some limitations of SIMNET-D which circumscribed the bioeffects simulation possibilities. These SIMNET-D limitations were carefully considered before the final decisions about which laser bioeffects simulations would be used in the CTAS-2.0 test were made by the CTAS-2.0 test directorate. Ideal methods of simulating retinal laser bioeffects (given no technological limitations) are also recommended in this report. The recommendations for practical methods of simulating retinal bioeffects are based on the known and potential limitations of SIMNET-D, and the primary purpose of the CTAS-2.0 exercise.

The original version of this report was written prior to the final decision on which retinal laser bioeffects simulations would be used for the test was made by the CTAS-2.0 sponsors and test directorate. The information contained in this report represents AL/OEO's understanding of retinal laser bioeffects and LEP prior to the initiation of the CTAS-2.0 exercise. Therefore, this document represents a window in time in terms of AL/OEO's understanding of laser bioeffects and LEP. Because laser bioeffects and LEP research continues to progress rapidly, some of the discussions contained within this report are not state-of-the-art in terms of the scientific community's current understanding of the mechanisms of laser bioeffects or LEP technology. This document is not an interim or final report of the CTAS-2.0 exercise. Because the original report was written and delivered prior to the initiation of the CTAS-2.0 test, this manuscript is written in future tense.

General Comments on CTAS-2.0 and Laser Bioeffects

The purposes of this report are to provide an overview of retinal laser bioeffects and to document the rationale for their characterization in simulated virtual battlefield networks (i.e., SIMNET-D) for the

CTAS-2.0 exercises. Specifically, the goals of this report are to: (a) explain retinal laser bioeffects in layman's terms so that their biological and perceptual consequences can be understood by persons not having vision science backgrounds; (b) recommend methods of ideally simulating retinal laser bioeffects in computerized virtual battlefields given what is currently known about these bioeffects and the present state-of-the-art computer graphics technology; (c) propose a mapping of these ideal simulations to reasonable laser bioeffect simulations that are achievable for the CTAS-2.0 test given the capabilities the computer graphics software that SIMNET-D is known to possess; and (d) recommend methods of simulating laser bioeffects with LEP devices, called electro-optical counter-countermeasures (EOCCM), and provide the rationale for these recommendations. My intent is to provide practical information in this report that will be useful as a foundation for simulating the visualization of ocular laser exposures in future distributed simulation exercises.

Exposures to lasers can produce several different types of ocular effects. These different effects result because the tissues of the eye have different absorption properties to different wavelengths of light (see Figure 1), and can be divided into four general categories based on their major target area: dermal, corneal, lenticular, and retinal. The retina of the eye is the most vulnerable to laser damage because the laser image focused upon it by the optics of the eye (i.e., cornea and lens) has an energy density gain of approximately five to six orders of magnitude over the energy available at the cornea. Because of the retina's increased vulnerability to laser damage, and because the simulated laser weapons used in the CTAS-2.0 test are specified to emit radiation mainly within the visible portion of the electromagnetic spectrum (those wavelengths selectively absorbed by the retina, see Figure 1), my discussions will concentrate on retinal laser bioeffects.

FACTORS DETERMINING VISIBILITY

Before a good understanding of retinal laser bioeffects and their impact on visual function can be acquired, factors which generally influence visibility must be understood. These factors and their interactions influence the visibility of targets under all viewing conditions, including the period during and following laser exposures. In this report, I have divided the discussion on factors which influence visibility into five general categories: ambient environmental luminance conditions, target characteristics, retinal location, contrast sensitivity, and spectral sensitivity. Although each of these factors influence visibility independently, their interactions determine visibility in specific viewing situations.

Currently, the most prevalent form of laser eye protection (LEP) is based on absorptive dye technologies. Because these types of LEP devices, like any optical filter which selectively absorbs different wavelengths of light, can alter visual perception in the absence of laser exposures, visibility through filters which selectively absorb specific wavelengths of light will also be discussed. These discussions will provide the rationale behind AL/OEO's proposal that simulations of laser bioeffects for CTAS-2.0 EOCCM trials be identical to the simulations in the non-EOCCM trials, but scaled to represent the decrease in total laser light energy reaching the eye.

Ambient Environmental Luminance Conditions

Ambient environmental luminance conditions influence the overall visibility of a scene because the ambient background luminance (i.e., photometric equivalent of radiance typically measured in candelas per square-meter (cd/m^2)) sets the adaptation state (known as the gain in engineering terms) of the visual system. The sensitivity of the visual system changes for brightly lit (photopic) versus dimly lit (scotopic) environments. These sensitivity changes occur because, under different luminance levels, different photoreceptor systems in the eye have dominant influence over vision.

The rod photoreceptors have the greatest absolute sensitivity to light (Cornsweet, 1970) due to their better photon-capturing abilities (Hecht, Schlaer, and Pirenne, 1942). The rod photoreceptor system dominates vision in dimly lit environments. Although the rods have the greatest absolute sensitivity to light, they are not responsible for the processing of fine detail visual information. Rod photoreceptor responses saturate at moderately high luminance levels (Hood and Finkelstein, 1986). Thus, the rod system is not responsible for good visual resolution (i.e., visual acuity), and it cannot signal information about increasing brightness beyond moderate levels of illumination. The other class of retinal photoreceptors, the cones, dominates vision under higher luminance levels. The cone photoreceptors provide observers with good resolution of fine spatial detail and color vision (Cornsweet, 1970). Cone responses generally do not saturate at even the highest background luminance levels (Hood and Finkelstein, 1986).

For both the rod and cone photoreceptor systems, if background luminance is increased, target luminance must also be increased for visual detection to occur. The relationship between target and background luminance for visual detection is linear over a large range of background luminances. This linear relationship is well described by a mathematical function (with a slope of approximately 1.0) called the Weber-Fechner Law (Cornsweet, 1970; Hood and Finkelstein, 1986). Because of the mixed complement of rod and cone photoreceptors in the retina, human vision is capable of fine detail and color resolution in daytime and good visual sensitivity at nighttime.

Alterations in the adaptation state of the visual system are important to visibility for several reasons. First, as previously mentioned, at higher background luminances, greater target luminances are required for visual detection. Likewise, the brighter the environmental luminance, the brighter the glare source (e.g., lasers, search lights, or optical munitions) must generally be to obscure a visible target. Second, changes in the visual system's adaptation state from lower to higher (more scotopic to more photopic) levels, and vice versa, take time. The time required to accomplish these changes is dependent on both the level of the adaptation state prior to the change and the direction of the change. Changes in adaptation state to more photopic levels (i.e., light adaptation) can require from a few seconds to up to several minutes to occur, again, depending on the initial adaptation state of the visual system. Changes in adaptation state to lower luminance levels (i.e., dark adaptation) take longer to achieve regardless of whether the final luminance level is photopic or scotopic (Cornsweet, 1970; Hecht et al., 1942; Hood and Finkelstein, 1986; Geisler, 1982). Dark adaptation can take between a few to as many as 40 minutes to be completed, depending on the initial and final luminance levels. The time required for dark adaptation is greater in the rod-operating range of ambient luminances than in the cone-operating range (Hood & Finkelstein, 1986). Changes in the visual system's adaptation level are particularly important in understanding flashblindness and will be discussed more thoroughly in this context in subsequent sections.

In addition to setting the overall adaptation level of the visual system, the ambient luminance conditions also restrict the effective contrasts (both luminance and color) of different targets superimposed upon the background scene. Increasing the background luminance will decrease the contrast of a fixed-intensity target superimposed on it. If the reduction in target contrast falls below the contrast threshold of the observer's visual system, the target will be undetectable. This phenomenon is particularly important in laser glare situations.

Target Characteristics

Several physical target characteristics, as well as the position of the target relative to the observer, influence detection. Some of the more important of these characteristics include: (a) target luminance; (b) target contrast against the background or surround (i.e., the difference of the target luminance and the background luminance divided by the background luminance); (c) angular size subtended by the retinal image of the target; (d) the spatial frequency content of the target (particularly for complex, "real-world" targets); (e) duration or temporal frequency of the target, (f) wavelength composition (i.e., color); and (g) location of the target on the retina or within the field of view (a one-to-one mapping exists between retinal location and field of view).

The importance of these target variables in influencing visibility primarily lies in their interactions with the ambient background luminance conditions, contrast sensitivity of the observer, and retinal location of the target. For example, the duration, or temporal frequency, of a target will influence the sensitivity of the visual system for its detection. The visual system is differentially sensitive to different temporal frequencies (easily understood in terms of "flicker rates" or cycles per second measured in Hertz (Hz)). Furthermore, some regions of the retina are more sensitive to different temporal frequencies than are other regions. For example, the visibility of a high-repetition-rate laser flicker (e.g., 30 Hz) is better in the peripheral retina, in general, than in the central retina (Tyler, 1987) because the peripheral retina is more sensitive than the central retina to high frequency flicker.

The duration of a target also influences the sensitivity of the visual system to color. For example, a red target that is presented for a brief duration (e.g., 10 milliseconds (ms)) is less likely to be detected at a given luminance than if it is presented for a longer duration (e.g., 100 ms). The neural visual pathway that encodes target hue is less sensitive to very brief-duration long-wavelength (e.g., 640 nanometer (nm)) targets than long-wavelength targets having longer durations.

Precise target and background parameters, as well as other viewing conditions (e.g., central versus peripheral vision) must be specified when accurately describing visual sensitivity. This specification is essential because the interactions of these variables greatly influence visual sensitivity, and, therefore, make generalizations about visual sensitivity difficult, at best, to interpret. Because these same variables are critical for determining visual target detection in the presence and absence of laser exposures, specific target and background characteristics are crucial in assessing the impact of laser exposures on visual performance. Although these variables will be discussed at greater length in subsequent sections, for the meantime, remember that the visual system's differential sensitivity to the aforementioned variables influences both which targets are detectable, as well as which ocular laser exposures can reduce their detectability.

Retinal Location

Three retinal areas will be discussed in this document: the fovea, the macula, and the periphery or extramacular region. Definitions of the size of these three areas vary in the scientific literature, especially across scientific disciplines (i.e., anatomical versus psychophysical versus clinical definitions). According to the clinical definitions given by Green et al. (1988), the fovea is in the central 2.5° radius of the posterior pole of the eye (this corresponds to Davson's (1976) "inner fovea"), which corresponds to the endpoint of the visual axis. Centered within this region is a 1.2° diameter area (referred to as the foveola), where visual acuity is best. The 20/20 Snellen notation visual acuity (which corresponds to 1.0 arc-min of visual arc resolution power) is the standard foveolar visual acuity for normal individuals. The central 7-10° diameter of the posterior pole comprises the macula. The yellow xanthophyll pigment,

known as the macular pigment, resides in this region. The extramacular region, or retinal periphery, is everything beyond the central 10° of the posterior pole. These three regions are illustrated in Figure 2.

Visual function, including absolute sensitivity and visual acuity, varies across the retina. This variability is primarily due to the different density distributions of rods and cones, the physiological properties of their underlying neural substrates across the retina, and the differential representation of the visual field in the visual cortex (Johnson, 1986; Rovamo & Virsu, 1979; J.P. Thomas, 1987; van Esch, Koldenhof, van Doorn, & Koenderink, 1982). The highest density of photoreceptors per unit area is found within the macula. The macula contains more cone than rod photoreceptors. Cone density is highest within the central 1° of the fovea. Rod density peaks at about 20° from the center of the fovea (Ahnelt, Kolb, & Pflug, 1987; Curcio et al., 1987; Österberg, 1935). In addition, the majority of the human primary visual cortex represents the central 15° of the visual field (Hubel & Wiesel, 1968; Pearlman, 1981). Cone densities decrease dramatically from the fovea into the retinal periphery (Curcio et al., 1987). Rods are absent from the center of the fovea (500-600 micron (μ) in diameter area, corresponding to Davson's (1976) "outer fovea") and increase in density in the retinal periphery (Cornsweet, 1970; Hecht et al., 1942).

Therefore, absolute sensitivity to light is greatest in the peripheral retina (Hecht et al., 1942), and fine detail and color vision are best at the fovea (Gordon & Abramov, 1977; Hood & Finkelstein, 1986). The reduction in visual acuity associated with peripheral viewing is illustrated graphically in Figure 3, which plots visual acuity as a function of retinal eccentricity. Other aspects of visual function also vary across the retina (Raninen & Rovamo, 1987).

Under any viewing condition, information on the location of a target within the visual field, in addition to the target and background characteristics, is crucial for determining visibility because this location determines where the target is imaged on the retina. Since target visibility (and perception) varies across the retina, laser exposures imaged in different retinal regions produce different levels of visual degradation.

Contrast Sensitivity

The visual system is particularly sensitive to contrasts. Therefore, the visibility of a target in a scene is highly dependent on the contrast sensitivity of the observer. The sensitivity of the visual system to spatial contrasts is described by the spatial contrast sensitivity function (CSF). Spatial contrast sensitivity is different in scotopic and photopic environments because of the different visual abilities of the rod and cone systems. An example of the photopic spatial CSF is given in Figure 4. This function is essentially the spatial modulation transfer function of the visual system at daytime. Typically, the spatial CSF relates the logarithm of sensitivity (the inverse of logarithm of visual threshold) of the visual system to spatial frequency. Spatial frequency is usually specified in terms of cycles per degree (c/d) of sinusoidal grating patterns; however, the spatial frequency components of any target can be extracted by performing a Fourier transfer on the image. Spatial frequency can be translated into the more standard Snellen acuity notation (e.g., 20/20, etc.), or the size of the retinal area subtended by the target in some unit of visual angle (e.g., arc-min). These latter translations are also shown in Figure 4. The scotopic spatial CSF is similar in shape to the CSF in Figure 4, but it is shifted towards lower spatial frequencies due to the lower resolution ability of the rod system.

Inspection of the photopic spatial CSF indicates that the visual system is maximally sensitive to middle spatial frequencies and is less sensitive to lower and higher spatial frequencies (e.g., medium grating bars versus fat or thin grating bars). As a result, the general features of an object are more

visible at low contrast than are the fine details. The highest spatial frequency which can be perceived at the greatest overall contrast represents the cut-off of the spatial modulation transfer function and corresponds to the visual acuity of the observer. In Figure 4, this point is given by the intersection of the curve with the abscissa.

Visual acuity represents the absolute resolution capability of the visual system at any given ambient luminance level. Visual acuity decreases as ambient luminance decreases because the spatial CSF shifts from photopic to scotopic tuning. However, a person's visual acuity (e.g., 20/20) is typically measured with high-contrast targets presented on moderate-to-high luminance backgrounds. Targets of higher spatial frequencies than those corresponding to the visual acuity will be blurred or not seen, depending on the spatial frequency. The fine detail information provided by these higher spatial frequencies will not be distinguishable to the observer. Reductions in visual acuity result in a shift of the intersection of the spatial CSF and the abscissa in Figure 4 towards lower spatial frequencies, in a manner similar to changing the tuning of the function from photopic to scotopic sensitivity.

Although visual acuity is the most commonly known measure of visual function, it is not the only aspect of vision that is important to normal visual function. For example, reducing the overall contrast sensitivity of the visual system (i.e., shifting the entire CSF down vertically in Figure 4) can render previously visible low-to-moderate contrast, middle-spatial-frequency targets undetectable. Rendering a target undetectable would be far worse in some military situations than simply blurring the detail of the target in question.

Spectral Sensitivity

The three classes of cones in the human retina signal information about color. The cone classes can be distinguished by their absorption spectra, anatomical and physiological properties, and density distributions across the retina (Boynton, 1979; Cornsweet, 1970; Curcio et al., 1987; deMonasterio, 1978a, 1978b; deMonasterio & Gouras, 1975). Studies have shown that the absorption spectra of the three cone classes overlap and peak at the short- (≅ 430-440 nm), middle- (≅ 540-550 nm), and long-wavelength (≅ 570 nm) regions of the visible spectrum (Boynton, 1979; Cornsweet, 1970). Human color vision is trichromatic, which means any colored light can be matched by a combination of three primary monochromatic lights (Boynton, 1979; Cornsweet, 1970).

There are two basic categories of congenital color vision defects. Dichromatic color-defective individuals lack one or more cone visual pigments, and are commonly referred to as being "color-blind." Anomalous trichromia is the most common form of congenital color vision defects and results from one or more abnormal cone visual pigments. The absorption spectra of these abnormal cone visual pigments are shifted in wavelength from those of the color-normal population. Anomalous trichromats are typically referred to as being "color-weak" individuals. Dichromatic individuals are not capable of detecting certain visible wavelengths of light unless they are intense enough to stimulate one of the cone pigments existing in the individual's retina. These individuals cannot see certain colored numbers within the pseudo-isochromatic plates of the more common color vision tests. Anomalous trichromats use different mixture ratios of the three primaries of monochromatic light to match a colored light than do individuals with normal trichromatic color vision. Many anomalous trichromats can pass some color vision tests (e.g., Farnsworth Panel D-15 test) but they cannot distinguish many incongruous color matches (e.g., green socks and brown pants appear to be the same color).

The sensitivity of the visual system to different wavelengths of light depends on both the size (i.e., spatial frequency), duration (i.e., temporal frequency), and retinal location (i.e., eccentricity) of the

target, as well as the method used for measurement. When foveal spectral sensitivity is measured using a circular target light superimposed on a photopic white background (i.e., increment threshold), one of two spectral sensitivity functions can be obtained, depending on the target characteristics (King-Smith and Carden, 1976; Sperling and Harwerth, 1971; Thomas, 1989). If the target is small (e.g., < 0.1°) and brief-duration (e.g., < 10 ms) or flickering at approximately 25 Hz, a unimodal spectral sensitivity function with maximum sensitivity at 555-560 nm will be obtained (see Figure 5). This function, called the photopic luminosity function, is used to equate different monochromatic lights to equal visual efficiency (Wyszecki and Stiles, 1982). The photopic luminosity function is believed to represent the sensitivity of the neurophysiological channel that combines signal outputs from the three cone classes to encode changes in brightness (King-Smith and Carden, 1976; Lennie, 1980; Thomas, 1989; Wagner and Boynton, 1972; Wyszecki and Stiles, 1982). If the target is large (e.g., > 1°) and/or of long duration (e.g., > 100 ms), a three-peaked spectral sensitivity function will be obtained (see Figure 6). The peaks of this function are believed to represent the sensitivity of the three different cone classes with opponent interactions occurring between the middle- and long-wavelength-sensitive cones (Sperling and Harwerth, 1971; Thomas, 1989; Thomas and Kuyk, 1989). The neurophysiological channels presumed to underlie this three-peaked spectral sensitivity function (i.e., red-green and blue-yellow opponent-color channels) are believed to encode color differences by subtracting the outputs of different cone classes in an opponent manner (Hurvich and Jameson, 1957; King-Smith and Carden, 1976; Lennie, 1980; Sperling and Harwerth, 1971; Thomas, 1989; Thomas and Kuyk, 1989, 1990; Finkelstein and Hood, 1982).

The visual system has its best color vision at the fovea, where the highest density of cones resides (Boynton, 1979; Cornsweet, 1970; Curcio et al., 1987). Peripheral color vision is inferior to foveal color vision and actually resembles "color-blindness" for small targets (Boynton, Schafer, and Neun, 1964; Gordon and Abramov, 1977; Johnson, 1986; Kuyk, 1982; Thomas, 1989; Thomas and Kuyk, 1989). The more peripherally the target is viewed, the larger the target must be for color vision to remain trichromatic (Gordon and Abramov, 1977; Johnson, 1986; Kuyk, 1982; Thomas, 1989; Thomas and Kuyk, 1989). The scaling of a peripheral target's size to yield trichromatic color vision is similar to the cortical magnification factor relating cortical representation between the central and peripheral visual field (Abramov and Gordon, 1988; Johnson, 1986; Thomas, 1989). If the peripheral and foveal targets are equated so that they have equivalent cortical representation (i.e., stimulate the same number of cortical neurons), they will yield similar spectral sensitivity functions. Rovamo and Virsu (1979) provide an excellent review of cortical magnification and its impact of peripheral vision.

Interaction of Factors Influencing Visibility

Ambient luminance conditions (e.g., background luminance) affect contrast sensitivity in several ways; different contrast sensitivities of the rod and cone systems are one such example. Because cones are generally more sensitive to contrast than rods, contrast sensitivity, especially for moderately high spatial frequencies, is best at higher ambient luminance levels where the cone system dominates vision. In addition, different target characteristics interact with each other, as well as the ambient luminance conditions, to influence visibility and contrast sensitivity. For example, the spatial and temporal frequency components of a target influence the relative contrast sensitivity of the observer. The visual system is more sensitive to some combinations of spatial and temporal frequencies than others (e.g., targets containing low spatial frequencies and high temporal frequencies or targets containing high spatial frequencies and low temporal frequencies). This complex relationship between spatial and temporal sensitivity is believed to be due to the spatiotemporal tuning of the underlying neural elements, and it suggests that the underlying subsystems subserving these functions are interdependent. The interdependency of spatial and temporal frequency on visual detection has been described as a spatiotemporal contrast sensitivity function (Olzak and Thomas, 1986). The spatiotemporal sensitivity of

the visual system is not well understood because most vision experiments do not manipulate both spatial and temporal stimulus characteristics. The color of a target also influences contrast sensitivity because the eye has differential sensitivity to different wavelengths of light (Boynton, 1979), and because the spatial and temporal resolutions of the human color mechanisms are different (deMonasterio, 1978a, 1978b; Finkelstein and Hood, 1982; Hood and Finkelstein, 1986; Ingling and Martinez-Uriegas, 1985).

One interesting interaction of target characteristics that has recently received much scrutiny is the interaction between target size, retinal location, and contrast sensitivity. As previously mentioned, contrast sensitivity to targets of fixed spatial dimensions is progressively reduced as one uses more eccentric viewing. However, recent evidence indicates that contrast sensitivity can remain relatively constant across the retina provided that the size of the target is increased to compensate for the difference in cortical representation of different regions of the visual field (Davis, Yager, and Jones, 1987; Legge and Kersten, 1987; Thomas, 1987; Virsu and Rovamo, 1979; Watson, 1987). This scaling of target size in accordance with the increased cortical representation of the central visual field (i.e., "M-scaling") has been successfully used to yield similar foveal and peripheral sensitivities to different wavelengths of light and to different flicker frequencies (Hibino, 1990; Johnson, 1986; Legge and Kersten, 1987; Raninen and Rovamo, 1987; Thomas, 1989). These findings suggest that peripheral targets may be as visible as foveal targets provided that they are made appropriately large to compensate for cortical magnification. However, the complexity of target parameters, viewing conditions, and visual task on peripheral retinal sensitivity make it difficult to generalize the functional effects of M-scaling peripheral target sizes by the cortical magnification factor.

Models of Human Vision and Laser Bioeffects

The visibility of a target is dependent on several factors that interact with each other to modify the sensitivity of the visual system. Because of these interactions, vision scientists must perform experiments using simple targets and simple backgrounds in attempt to tease out how each of these factors independently influence the visual system's sensitivity. Models of the visual system provide a useful way of estimating the dependence of visual sensitivity upon these different factors, as well as the adverse effects of conditions such as ocular laser exposures.

Several models of human spatial vision currently exist (see Olzak and Thomas, 1986, or Graham, 1989, for an overview). These models have been primarily developed to describe the results of human visual psychophysical experiments. Most of these models describe human spatial vision as a set of difference of Gaussian or Gabor filters tuned to different spatial frequencies and orientations. The outputs of the most sensitive filters to a target determine its visibility under different viewing conditions (e.g., different luminance levels, etc.). However, at the present time, none of these models have been directly tested to see if they can accurately predict detection of complex visual targets on complex visual backgrounds (i.e., a tank on the ground) or during laser exposures. Menendez and Smith (1990) developed a model that takes such factors as the contrast ratio of the target to the background, the luminance of the laser exposure, and the retinal distribution of the laser image into account to calculate the field of view obscured (FOVO) by glare and flashblindness from a laser exposure. Thus, by manipulating any one of the factors influencing visibility, they can calculate how its interactions with the other influencing factors affect vision during and following a laser exposure.

Visibility with Selective Absorption Filters

Visors, spectacles, and goggles that are used to protect individuals in laser laboratories from potential eye damage have been developed to protect military personnel against potential battlefield laser threats. Military LEP have different criteria than laboratory LEP, such as ballistic protection requirements and environmental stability requirements. In addition, military LEP users, such as aircrew, generally have stricter visual requirements for performing job-related tasks, which results in stricter optical characteristic requirements for military LEP.

Since most lasers emit only a limited number of discrete monochromatic wavelengths, "notch" filters that selectively absorb narrow spectral bands have been used for LEP. Although neutral density filters could provide sufficient levels of protection, by design they absorb all wavelengths of visible light and, thereby, could lower the transmitted light to unacceptable levels. Notched filters are advantageous over neutral density filters for LEP because they are designed to provide adequate protection against laser threat wavelengths while maximizing transmission at all other wavelengths. The increased light transmission of visible wavelengths that are not laser threats could aid aircrew members in visual task performance. One disadvantage of notched filters for LEP is that their selective absorption characteristics may result in poor visibility of exterior and interior aircraft lighting, cockpit instruments and displays, and out-of-cockpit objects (Sulak, 1988).

Lenses that selectively filter visible wavelengths of light have the potential of adversely affecting vision. Visual acuity, contrast sensitivity, stereopsis, and color vision can all be affected by wearing selective absorption filters. Neutral density filters attenuate visible wavelengths by equivalent amounts and reduce the total amount of light entering the eye. Attenuation of the total amount of light entering the eye can result in reductions in visual acuity, contrast sensitivity, and color discrimination. The likelihood of reducing visual abilities increases if the optical density of the neutral density filter is great enough to render the observer's ambient lighting conditions mesopic (i.e., between photopic and scotopic levels where both rod and cone systems are operating) or scotopic. Rod system domination of vision in scotopic lighting conditions results in poor visual resolution and contrast sensitivity to moderate-to-high spatial frequency targets, as well as a very limited ability to distinguish differences in color. In fact, even under dim photopic lighting conditions, visual acuity, contrast sensitivity (Allen, Labo, and Mayo, 1990; Green et al., 1988; Olzak and Thomas, 1986), and color discrimination (Kuyk and Thomas, 1990) can be reduced. Because these visual abilities can also be reduced by hypoxia caused from high-altitude flights, the optical density of any eye protection given to aircrews should not be high enough to prevent significant visual reductions (Sheehy, 1989a).

In addition to reducing the overall lighting of the scene, selective absorption filters can alter the color appearance of the scene and, thereby, significantly reduce visual performance. (Berggren, 1970; Hovis et al., 1989; Kinney, Paulson, and Beare, 1979; Kuyk and Thomas, 1990; Phillips and Kondig, 1975). By selectively absorbing visible wavelengths of a multi-wavelength (i.e., broadband) environmental scene, some filters can alter the scene's color appearance to the point that certain targets are indistinguishable (Sulak, 1988). In fact, if the transmission of specific regions of the visible spectrum is sufficiently reduced, selective absorption filter use can render the color detection and color discrimination abilities of individuals with normal color vision equivalent to those demonstrated by individuals with congenital color vision defects (Hovis et al., 1989; Kuyk and Thomas, 1990; Thomas and Kuyk, 1988). Although there are reports that certain selective absorption filters can improve contrast sensitivity and depth perception, objective reports dispute this claim, showing little or no improvement (Barron and Waiss, 1987; Hellinger, 1983; Hovis et al., 1989; Kelly, Goldberg, and Banton, 1984; Kinney et al., 1979; Lynch and Brilliant, 1984; Tuper, Miller, and Miller, 1985; Zigman, 1990).

Alterations in the color appearance of broadband scenes caused by wearing selective absorption filters can be calculated by dividing the spectral reflectance of the scene with the absorption spectrum of the lenses, and mapping the changes in terms of established color metrics. Kuyk and Thomas (1990) explained a methodology of calculating shifts in the color appearance of broadband sources using the Commission Internationale de l'Eclairage (C.I.E.) color classification system. Simply, one calculates the location of the broadband source in C.I.E. space and then determines its new location after transmission through the optical filter using the filter's transmission (or absorption) characteristics. The vector shift in C.I.E. space created by transmission through the filter can then be used to provide an approximation of the change in color (e.g., dominant wavelength) by analyzing the direction and length of the color difference vector (i.e., the direction and magnitude of the color shift). This methodology can be used for any broad-band source, including the color phosphor guns on video monitors or aircraft cockpit displays. This method could also be used to calibrate and accurately simulate the appearance of an environmental scene when viewed through lenses that selectively absorb different wavelengths of light.

The limitation of this method is that the C.I.E. space, which is the international standard for describing the color of light sources, has not been completely mapped in terms of the color names associated with all locations within the space. Therefore, although certain physical characteristics of a light (or target) viewed through different filters can be accurately predicted, the color perception an observer associates with the light (or target) cannot be accurately predicted because of its subjectivity and dependence on the observer's color vision and use of color names. Establishing color appearance classification schemes and training observers on their use could help standardize the color appearance of targets or light sources of military interest.

Shifts in the color appearance of monochromatic sources through selective filters may be subtle and due to intensity-related effects (i.e., Bezold-Brücke effect). For example, Kosnik et al. (1989) have shown that the color appearances of monochromatic laser wavelengths are not significantly altered with the Glendale FV-2 LEP spectacles used primarily by the United States Navy. For a monochromatic light source, the FV-2 LEP spectacles act similar to a neutral density filter by simply reducing the total laser energy that enters the eye at that wavelength. Kosnik et al. (1989) did not measure the spectral composition of the transmitted laser light, so it is unknown whether the FV-2 spectacles physically performed like a neutral density filter. However, significant cockpit visibility problems and color discrimination problems have been reported for the FV-4 LEP spectacles, a modification of the FV-2 LEP spectacles (Perez and Flick, 1991).

The materials used to make selective filters influence the spectral composition and appearance of the transmitted light, particularly for high photon energy, short-wavelength sources (e.g., argon lasers). In general, if the spectral optical density (OD) of a filter is greater than 4.0 at a specific wavelength (or waveband), the light absorbed by the filter can be re-emitted from the material as a longer wavelength. This phenomenon is referred to as luminescence. With these high OD filters, a monochromatic light source's appearance will be different from the original color. Furthermore, if the absorption sites in the materials are saturated, as might be expected with high-energy, short-pulsed laser exposures, other fundamental frequencies of the light may be transmitted through the filters, even though the light source appears monochromatic. Kosnik et al. (1989) did not perform a spectral analysis of the laser light transmitted through the FV-2 spectacles. Therefore, they could not positively ascertain whether the spectral composition of the transmitted laser light had been altered by the filter, even though its color did not appear to be changed. Since the wavelengths Kosnik et al. (1989) used were readily passed through the filter they tested (optical density of less that 4.0 log units), it is likely that the perceptual effect of any change in wavelength composition of the light transmitted through the FV-2 spectacles would be less than that resulting from the reduction in luminance.

Technology has expanded the number of approaches that need to be taken in order to develop adequate LEP. Tunable lasers, which are capable of emitting several wavelengths (usually one at a time) have been available in the laboratory for a number of years. Agile lasers, which can be rapidly tuned to different wavelengths or which produce multiple wavelengths simultaneously, are under development. Agile lasers pose serious future battlefield threats, particularly in terms of providing adequate LEP against them which also meet with user acceptance. The concept of passive notch filter eye protection is not adequate for the future since it can be defeated by agile lasers. In addition, it is difficult to produce passive notch LEP that protect against all existing discrete-line visible laser systems without severely reducing interior and exterior aircraft lighting visibility (Sulak, 1988; Perez and Flick, 1991).

Several new LEP technologies are in development for military applications that can provide multi-line visible wavelength protection without seriously restricting aircraft lighting visibility. Some of these technologies include holograms, dielectric stacks, interference filters, and hybrid technologies. Dynamic LEP based on fast switching devices are being developed to provide sufficient protection against agile lasers. The goal of fast switching LEP is to provide sufficient optical density within a few nanoseconds (ns) or less (International Committee of the Red Cross, 1990) to limit anticipated exposures to acceptable "eye-safe" levels. Switching devices such as these are currently used to protect aircrew members from ocular exposures to thermal radiation from nuclear detonations (i.e., PLZT). However, the switching response times required to protect against laser exposures are much faster than those required for nuclear detonations, and the first pulse will likely always be transmitted by the LEP before the switches are activated. Until very fast switches can be developed, agile LEP is limited to multi-lined passive notch filters.

Another LEP option is to employ a statistical filter which is open just long enough to enable aircrews to perform their missions and not reduce the transmitted light in the "closed state" to an unacceptable level. For example, if the filter continuously switches at a fairly rapid rate (>30 Hz) and remains in the "open state" one-fifth of the time, the observer's eye protection would be similar to wearing a neutral density filter with 20% transmission. Unlike neutral density filters that have 80% light transmission all of the time, statistical filters would provide complete protection 80% of the time and no protection 20% of the time. User acceptance of LEP based on fast switches and statistical filters by aircrew has yet to be explored and remains questionable.

OVERVIEW OF LASER BIOEFFECTS

Simulations of laser bioeffects recommended for virtual battlefields, such as SIMNET-D, need to integrate what is known about retinal laser bioeffects with the technological capabilities of the distributed simulation network. Sub-optimal (reduced fidelity) simulations of laser bioeffects used for CTAS-2.0 on SIMNET-D can be justified if they produce visual degradations that are functionally equivalent to those expected from an actual ocular exposure to a laser of the specified physical characteristics. The known battlefield visual conditions must also be integrated to produce a functionally equivalent laser bioeffect simulation. This is no trivial task in that it requires knowledge of the effects of visual cues on task performance for conditions encountered in both the real and the simulated battlefield environments.

The purpose of this section is to provide a general review of retinal laser bioeffects and their impact on visual function. Investigations into laser bioeffects are still ongoing and many questions remain unanswered. The goal of this report is to provide the necessary unclassified background information to allow the reader to understand the trade-offs between ideal and achievable simulations for retinal laser bioeffects in SIMNET-D for CTAS-2.0. Remember that this overview and the proposed recommendations of simulating retinal bioeffects represent a window in time prior to the finalization of all the technical decisions concerning the CTAS-2.0 exercise. Future reports will build on this information to

critically evaluate alternative modeling and simulation approaches and will consider alternative approaches based on various interpretations of the bioeffects data and theories. This review of retinal laser bioeffects represents a relatively simple explanation of the biological damage and effects of visual function based on the literature. The explanations given in this report do not completely depict the information known about laser bioeffects and their impact on visual function.

Laser exposures can immediately reduce target detectability as a result of induced changes to the structure and/or function of the eye. Laser bioeffects that result from retinal light absorption can be divided into four general categories: glare, flashblindness, thermal (photocoagulation) lesions, and hemorrhagic lesions. Glare and flashblindness are temporary laser bioeffects that last from several seconds to several minutes in duration due to normal changes in the adaptive (sensitivity-regulating) physiological visual mechanism. Thermal lesions and hemorrhagic lesions produce permanent retinal tissue damage, although partial recovery of some of the initial symptoms usually occurs after several days to several weeks, depending on the magnitude of the damage.

Retinal laser bioeffects are not independent, distinct entities. All four retinal laser bioeffects can occur together as a result of a single ocular laser exposure. This phenomenon is due to the amounts of different energy required to initiate each of the four bioeffects, and to the typical retinal image distribution which occurs from ocular laser exposures. Due to scatter both outside and within the eye, the image of a laser point source on the retina forms a sharply-peaked light distribution, which causes differential retinal light adaptation and damage effects. For example, a certain laser pulse could produce glare while the laser light is on, flashblindness upon its extinction, and biological damage to the retinal tissues, which could cause the vision loss to persist after recovery from flashblindness.

Laser bioeffects may be source-fixed or eye-fixed effects. Source-fixed bioeffects remain in the same location in visual space as the source causing them. Therefore, source-fixed bioeffects like glare vary as a function of the eye's (or target's) displacement from the laser, and can be defeated by looking away from the laser source. Eye-fixed bioeffects remain in the same position of the visual field regardless of the subsequent displacement between the laser and the eye. Eye-fixed laser bioeffects move with the eye as the point of gaze moves across the visual field. Losses in vision that accompany eye-fixed laser bioeffects remain in the same region of the observer's field of view for the duration of the effect. The observer cannot simply look away from or block his view of the laser source and remove the visual effect. Therefore, functionally-equivalent simulations of eye-fixed effects require that the visually masked area maintain a constant retinal image (and corresponding visual field) location. In the following sections, laser glare, flashblindness, and biological damage (thermal and hemorrhagic lesions) will be reviewed and their impact on visual function discussed.

Veiling Glare

Laser glare, also referred to as dazzle, can temporarily obscure targets either partially or completely. Veiling glare is a normal visual response to visible wavelengths of light (400-760 nm) that is a result of the spatial light scattering. Studies have shown that all visible wavelengths of light have equivalent spatial scattering distributions when they are equated in terms of the visual system's differential sensitivity to visible wavelengths of light (Wooten and Geri, 1987; Varner et al., 1988). Therefore, no one visible wavelength of light has been demonstrated to be more effective at producing glare than any other. However, reports from Varner et al. (1988) indicate that an interaction between age and glare may exist which increases the glare effectiveness of short-wavelength, versus other wavelengths of visible light. This interaction is likely related to the opacification of the lens of the eye with age. The obstruction of targets by glare results from the reduction in the luminance contrast of the target's retinal image by the superimposition of a veil of light produced from spatial scattering. The media

between the glare source and the eye (e.g., atmosphere, canopy, or smoke) and within the eye itself (by the cornea and lens (Padmos, 1984)) both scatter light and contribute to glare. Glare can occur as a result of "eye-safe" and higher intensities of laser exposures. Glare can occur simultaneously with retinal damage, and glaring laser exposures can be followed by flashblindness.

Glare is primarily a concern with continuous-wave (cw) lasers but also may be possible with pulsed lasers whose repetition rates are near or greater than the temporal resolution of the visual system. Repetition rates faster than 30 Hz may be fused by the eye to appear as one continuous emission. This visual phenomenon, referred to as either the critical fusion frequency or critical flicker fusion (CFF), is a common everyday effect which perceptually removes the flicker from fluorescent lighting and causes motion picture films to appear as continuous flowing pictures instead of jumping individual frames. The CFF for lasers has not been clearly specified and is likely to be wavelength and contrast dependent. The intensity and duty-cycle of a laser may result in a high luminance contrast, which could raise the laser's CFF to as high as 90 Hz. On the other hand, the effectiveness of laser light at bleaching very large amounts of visual pigments (contained within the rods and cones) result in laser CFFs of less than 90 Hz. Rapid pulses of laser light do not necessarily have to be fused to be an effective glare source since flickering glare could be effective at obscuring a target. Glare effects can be compounded by the scattering of the laser light by other battlefield media, such as smoke. However, if such media are optically dense enough and if the laser light is of low enough intensity, these media may reduce glare effects by decreasing the luminance level of the laser light reaching the eye.

Because glare is a source-fixed effect, its effectiveness at obscuring a target rapidly decreases as one's gaze (or the target of interest) moves away from the glare source. Figure 7 illustrates this point by showing the logarithm of the effectiveness of glare from a 514-nm argon laser source at obscuring the flight path marker of a head-up display (HUD) as a function of the separation between the target and the glare source (in logarithmic degrees of visual angle). Figure 7 clearly illustrates how the effectiveness of a glare source rapidly declines with small visual angles between the target and the source. In fact, Varner and colleagues (Varner, Thomas, and Cartledge, 1991; Zuclich et al., 1988) found that there is an approximate two-decade decline in glare effectiveness for angular separations of up to, but less than, 2°.

Vos (1984) has provided one of the best theoretical discussions and mathematical descriptions of the impact of angular separation between a glare source and a target on glare effectiveness. This mathematical function, called the Vos glare function (Figure 8), only describes intraocular scattering of light and does not include scattering caused by the atmosphere or any intervening optical surfaces (e.g., windscreens). In Figure 8, the Vos function (specified as equation 4) is shown in relation to actual laboratory data collected by different investigators over the past several decades. Figure 9 shows how different added amounts of scattering increase the effectiveness of glare, (as specified by the Vos function) at different glare angles.

Field studies of atmospheric and aircraft canopy scattering of light have shown that intervening media between the light source and an observer increases the amount of glare (Padmos, 1984; Labo et al., 1990). These types of intervening media affect the glare spread function by decreasing the luminance of the central peak and increasing the luminance at the wings of the function. The result of these types of modifications to the glare spread function is that the contrast of targets spatially close to the glare source will be higher than if the intervening media were not present. Likewise, targets more distant from the glare source will be obscured more by the glare than if the intervening media were not present. Thus, the effectiveness of a glare source at obscuring targets at different locations in the visual field depends on both intraocular scattering and scattering by other media between the observer and the glaring light source.

Equivalent Background Hypothesis for Modeling Glare

Secondary superimposed light sources can interfere with an observer's ability to detect a target both during and following the light exposure. This is the basic etiology of visual disabilities produced by glare and flashblindness. One practical way of modeling and analyzing the effects of a laser exposure on target visibility is using the equivalent background theory (Stiles, 1946). This method explains a light's adaptational effects on target detection in terms of the reduction in target contrast required to produce an equivalent visual response on a background of a given luminance. The equivalent background theory (EBT) is well established and accepted as a method of understanding target detection as a function of visual adaptation, and it has been validated for many visual conditions and visual tasks (Geisler, 1979; Hood and Finkelstein, 1986; Stiles and Crawford, 1937).

When the visual system is adapted to a background scene of a specfied luminance, a superimposing light exposure will raise the luminance required to detect a target against that background scene (luminance threshold). For example, if the visual system is adapted to a specific background field of luminance (B), visual sensitivity to a target of luminance (T) is constant over time and is a function of the target's luminance-contrast ratio (C_L), where:

$$C_L = (T - B) \div B \qquad (1)$$

and where (T - B) is the absolute luminance difference between the target and background regions of the visual field or corresponding retinal images. When the eye is adapted to (B), the minimum-detectable (threshold) luminance change (T' - B) is proportional to the background luminance:

$$T' - B = k(B) \Rightarrow \text{when the eye is adapted to (B)} \qquad (2)$$

where (k) defines the threshold contrast ratio. The value of (k) is constant over a wide range of background luminance conditions (Weber-Fechner Law). The value of (k) varies with observers and as a function of a large number of target conditions, such as retinal image size, location, and duration. If (k) is known, Equation 2 can be used to predict the target luminance required to permit visual detection when the eye is fully adapted to a specific background luminance. For lower levels of (B), the Weber-Fechner law does not hold, and the (k) can vary with (B), as well as the aforementioned target parameters.

One practical way of studying glare and flashblindness is in terms of the EBT. This method explains a light's (laser or non-coherent) adaptation effects on target detection in terms of an equivalent reduction in target or scene contrast rather than as a reduction in visual sensitivity. The EBT explains target detection at a given adaptation level in terms of the reduction in target contrast required to produce an equivalent visual response on a background of a given brightness. For example, a glare source of intensity (x) reduces target contrast and raises visual adaptation similar to an equivalent background of luminance (y). Likewise, three minutes following the extinction of a light of intensity (x), target threshold contrast (k) is similar to (k) measured using an equivalent background brightness of luminance (y). Using the EBT simplifies predictions of visual performance because the probability of target detection is a function of target contrast. It also unifies our understanding of dynamic and steady-states of adaptation in that it interprets each instant during a changing adaptation state in terms of a specific condition of steady-state adaptation.

The equivalent background luminance (EBL) defines the retinal illumination required to produce a psychophysical response equivalent to that measured at a given point in time following a light exposure. One major advantage of using this approach is that it is independent of task and target conditions. The

EBL varies as a function of exposure intensity and the time elapsed since the light's extinction. The EBL is additive with the effects of actual physical background luminances. The EBL acts like a veil of light added to the retinal image of the scene to reduce its luminance and/or color contrast. The EBL varies as a function of retinal illuminance (I_r) and time (t) for both dark and light adaptation. Retinal illuminance is, therefore, integrated over the time (over ≅1 s) from the light exposure. Thus:

$$EBL = f\ (I_r, t) \qquad (3)$$

where the value of (I_r) may also vary as a function of retinal position with respect to the center of the retinal image of the laser source. For special viewing conditions, the EBL is related to the luminance which matches the brightness of afterimages seen after high-luminance light exposures (Barlow and Sparrock, 1964; Miller, 1966a, 1966b). Because the EBT is well established and validated for many visual tasks and conditions, adaptation effects of various laser exposures can be estimated for a range of target conditions using estimates of EBL obtained in studies using only one kind of target (e.g., one of a given size or shape).

Flashblindness

Flashblindness is a temporary reduction in target detectability due to the visual system's natural process of adjusting its sensitivity to new ambient luminance levels. For a specified target condition, the higher the luminance of the flashblinding light, the longer the duration of flashblindness (Brown, 1965; Miller, 1965; Menendez and Smith, 1990). Unlike glare, which occurs during a laser exposure, flashblindness occurs after the laser light is turned off. Also unlike glare, flashblindness is an eye-fixed laser bioeffect. Glare and flashblindness can be caused by a single laser pulse, but they are most commonly associated with multiple pulses or continuous-wave (cw) laser output. Glare and flashblindness can also be caused by non-coherent light sources, and both are phenomena of visual adaptation.

Visual adaptation is a normal negative-feedback physiological process which scales visual sensitivity to the level of ambient or background light. Figure 10 shows how an increase in retinal illumination causes light adaptation. Light adaptation results in a rapid decrease in visual sensitivity and increased luminance thresholds for detecting visual targets. If the high-luminance source continues to illuminate the eye, light adaptation is followed by a period where thresholds stabilize, indicating that vision is adapted to the new ambient luminance level. Glare results from both the light adaptation and the steady-state adaptation phases.

Figure 10 also shows dark adaptation following the reduction of light intensity. During dark adaptation, target detection thresholds decrease until they stabilize at a level determined by the new, lower adaptation level. This new, lower level of adaptation does not have to be scotopic to cause dark adaptation. Any change in background luminance from a higher to a lower level, even if the lower level is within the photopic range, will result in dark adaptation. Flashblindness is the period of dark adaptation which follows a high-luminance exposure. Short, repetitive high-luminance exposures interfere with vision by eliciting successive light- and dark-adaptation responses in the flashed part of the retina. The time required for dark adaptation to a specific luminance change is longer than that required for light adaptation. Dark adaptation can last from less than a second to several minutes, depending on the initial and final luminance levels (see Factors Determining Visiblility).

The brighter the ambient illuminance levels the visual system is adapted to, the brighter the flash of light must be to elicit flashblindness, and the brighter the flashblinding light, the longer the duration of

flashblindness (Brown, 1965; Miller, 1965; Menendez and Smith, 1990). The latter phenomenon is due to longer dark adaptation periods resulting from more intense light exposures (Hood & Finkelstein, 1986). Flashblindness duration also varies with the nature of visual task being performed at the time the flash occurs (Menendez & Smith, 1990). Flashblindness recovery is prolonged if the viewing of small, low-contrast targets, such as those viewed by aircrew during combat and training operations, is required (Miller, 1965; O'Mara, Stamper, Lund, & Beatrice, 1980). Increasing target brightness has been shown to speed the recovery time from flashblindness (Brown, 1965; Chisum, 1968; Chisum and Morway, 1974; Menendez and Garcia, 1985; Miller, 1966a; Rhodes, Garcia, and Cosgrove, 1989). This strategy might provide some practical assistance to aircrew for in-cockpit viewing, where the instrument brightness can be increased, but it offers no assistance for viewing targets that are out of the cockpit.

Other target variables also determine the rate of recovery from flashblindness. Recovery from flashblindness has been demonstrated to follow the spatial CSF (Harwerth and Smith, 1985; Menendez and Garcia, 1985; Rhodes et al., 1989; Yates and Harding, 1983). Specifically, for a given flash luminance and target luminance, recovery from flashblindness will be quickest for those targets containing spatial frequencies to which the visual system is most sensitive (see Figure 4) and longest for targets that contain spatial frequencies to which the visual system is least sensitive (i.e., high spatial frequencies). Given this information, one might predict that for a complex target (i.e., real-world targets such as airplanes or tanks), an observer recovering from flashblindness would first be able to make out the general form of an object, and then later, towards the end of the flashblindness recovery period, to identify the fine detail contained within the general form. Figure 11 shows a composite of several graphs that illustrate how recovery from flashblindness is dependent on the exposure luminance and other target characteristics, such as contrast and spatial frequency content.

As with glare, flashblindness occurs only for lasers whose light output is within the visible wavelengths of the spectrum. Near-infrared (IR) laser wavelengths may reach and be absorbed by retinal tissues, but are not capable of producing flashblindness. Studies have shown that intraocular structures can cause frequency doubling of near-IR wavelengths of light (Sliney, Wangemann, Franks, and Wolbarsht, 1976; Vasilenko, Chebotaev, and Troitskii, 1965), which results in visible wavelengths being produced through second harmonic generation (Zaidi and Pokorny, 1988) or some other mechanism. The middle-wavelength light ($\cong$ 530-580 nm) produced from frequency doubling of IR light could potentially produce flashblindness if the original laser intensity was great enough. However, biological damage will likely occur before flashblindness under these conditions. Because second harmonic frequency doubling of IR lasers produces low-energy visible wavelengths, it is unclear what the magnitude of any flashblindness effect would be.

As previously mentioned, the sensitivity of the visual system to different wavelengths of light depends on both the size and duration of the target and background, as well as the adaptive state of the eye (Sperling & Harwerth, 1971; Thomas, 1989; Veenhuis, 1986). When visible wavelengths are equated using the C.I.E. photopic luminosity function, no one particular wavelength appears to be better at producing flashblindness or prolonging its recovery. In fact, Previc, Allen, and Blankenstein (1985) found that flashblindness recovery times for targets of different wavelengths were equivalent, provided they had the same effective luminances and contrasts. However, for lasers of the same energy outputs but different wavelengths of light, the greatest visual effect would come from those having wavelengths at or near the peak of the photopic luminosity function (i.e., 555 nm).

Flashblindness produces a temporary scotoma. The size of the obstruction produced by this temporary scotoma depends on the luminance of the flash and the target used for its measurement. A scotoma can be described as absolute or relative and as permanent or temporary. Absolute scotomas are areas in the visual field (or retina) where no visual response can be produced. A relative scotoma is

a region of the visual field where visual sensitivity is reduced when compared with the expected norm. Both absolute and relative scotomas can be either permanent or temporary. Although flashblindness is typically associated with creating temporary relative scotomas, the possibility of flashblindness producing temporary absolute scotomas also exists.

Because the distribution of light across the retina occurring from a point source of light, (such as a laser) is sharply peaked, the retina is differentially adapted by a laser exposure. A target may be obscured for longer periods of time if its retinal position corresponds with the center of the retinal laser light distribution. Target positions further away from the center of the imaged light distribution may become visible more quickly. As the retina dark adapts following the laser flash, the size of the temporary scotoma produced by the exposure shrinks. A flash causing a uniform luminance distribution on the retina would produce an afterimage whose dimensions would not shrink with time, but would actually appear to gradually fall within the visual field, or "sink" (Miller, 1966b).

The size of a relative scotoma depends on both the luminance distribution of the flash (relative to the adaptation state of the eye prior to the flash) and the target characteristics (see Figure 12). Full recovery of visual function usually occurs following flashblindness. However, some flashblinding laser exposures, particularly those capable of producing significant flashblindness at very high daytime luminance levels, may also produce biological damage, and full recovery of visual function will not occur. This is an important point when discussing laser bioeffects. Retinal laser bioeffects are not distinct entities that are produced exclusive of one another. Multiple effects are possible, especially from intense ocular laser exposures. An individual may experience glare while the laser is on, flashblindness following the termination of the laser output, and permanent biological damage following recovery from flashblindness (see Figure 12).

Menendez and Smith's (1990) model provides a good, general way of approximating the amount of time required to recover from flashblindness for different light exposures. Because this model is still being developed to encompass more target-related conditions into its underlying mathematical equations, it is only a first approximation of the recovery rate. Models of this sort are essential for trying to answer general questions regarding flashblindness durations.

General Comments on Biological Damage

As with flashblindness, biological damage produced from laser exposures are eye-fixed laser bioeffects that can result in significant reductions in vision. However, unlike flashblindness, where vision will recover within minutes, the visual effects from biological damage may improve with time (days or months), but a portion of the loss will not recover. The amount of vision recovered following biological damage is dependent on the amount of healing of the biological tissue. If flashblindness is accompanied by biological damage, full visual function will not be completely restored. In this report, biological damage will be categorized into two general types of lesions which contain subtypes within their respective categories: lesions and hemorrhages.

Biological damage can produce both relative and absolute permanent and temporary scotomas. However, all biological damage can potentially result in absolute, permanent scotomas. The impact of scotomas on visual function depends on both the location of the lesion (i.e., biological damage) on the retina (which corresponds to its location in the visual field, see Cornsweet, 1970, pp. 10, 40, and 43 for examples) and its size. Because visual function varies across the retina, biological damage to the retina produces varying effects of visual function depending on the location. Furthermore, the higher levels of the visual system (i.e., cortical areas controlling vision) are capable of "filling in" areas of the visual field where scotomas are present to produce the perception of a continuous field of vision (Gille, Larimer,

Piantanida, and Landham, 1990). This same phenomenon of the visual system describes people's unawareness of their natural scotomas where the optic nerves leave the eyes (known as the "blindspots"), and it explains why many glaucoma and retinitis pigmentosa patients are unaware that they have lost portions of their visual field until tests to measure their visual field size are performed.

The cortical "filling in" process is useful in providing an observer with a continuous scene. However, it does not help the observer detect objects actually located in the scotomatous region. Scotomas produced by biological damage are size-fixed areas of retinal necrosis and are, therefore, not capable of visual response, regardless of the higher visual system's (i.e., visual cortex) "filling in" processes (Gille et al., 1990). The size of the scotoma produced by biological damage is not always the same size as the actual lesion on the retina. Although the minimum size of the scotoma can be calculated by transforming the retinal lesion size (millimeters (mm) on the retina) into the visual field scotoma size (degrees of visual angle), the observer may report that the perceived scotoma is larger than that predicted from this calculation. Studies on glaucoma and retinitis pigmentosa patients have shown that several factors influence the size of the perceived scotoma, which makes predictions of scotoma size difficult to estimate by lesion size. For example, the size of measured scotomas can vary for different target characteristics (e.g., target size and brightness) and across testing sessions (Kuyk, Norden, and Ehrnst, 1986; Pokorny, Mith, Verriest, and Pinkers, 1979; Spalton, Hitchings, and Hunter, 1985). Also, in some cases, scotomas may be relative and not absolute.

An observer's visual abilities can also vary depending on the strategy used in the attempt to visualize a target with a visual deficit. For example, if an observer receives a lesion that covers the entire fovea (as opposed to just the foveola described in Factors Determining Visibility), visual acuity will be no better than 20/200 if a target is centrally fixated and the target is imaged on the lesioned fovea. If the subject eccentrically views the target so that the target is imaged on the macular retinal area adjacent to the lesion (see Figure 13), acuity may improve to as good as 20/40. Because there is a natural tendency to foveate a target of interest (Dodge, 1903; Leigh and Zee, 1985), eccentric viewing is a difficult technique which requires concentration and practice. In addition, image fading is difficult to avoid when eccentrically viewing targets (i.e., Troxler effect). Therefore, overall visual functioning will be greatly impaired, visual efficiency will be greatly reduced, and tracking performance will be affected (see "Other Discussions of Biological Damage Effects on Visual Function" section) if the fovea is damaged by a laser exposure.

Following trauma, retinal tissues tend to accumulate plasma fluids and swell. This swelling, or edema, can distort vision by misaligning the photoreceptors or interfering with the optical focus of light to the retina (Spalton et al., 1985). Retinal edema can often immediately follow small foveal lesions, and it can reduce visual acuity of the adjacent retinal areas to below 20/40.

Unlike glare and flashblindness, where the wavelength of the laser light (when equated for luminous efficiency of the eye) does not significantly affect the extent of the bioeffect, the wavelength of the laser light does significantly affect the type and severity of biological damage. Ocular tissue absorption is wavelength dependent. The cornea, lens, retina, and choroid of the eye have different absorption characteristics. In addition, the mechanisms of retinal laser damage are also wavelength dependent. Therefore, the wavelength of the laser will influence the site and the type of laser damage.

Short-wavelength light (< 500 nm) is absorbed more by the hemoglobin in the intraretinal layers, where the photoreceptors and underlying nerve cells are located (Spalton et al., 1985). The yellow xanthophyll pigment located in the central 7-10° of the visual axis (the macula) also selectively absorbs short-wavelength light. Short-wavelength laser exposures can, therefore, affect these retinal layers more so than others. Furthermore, the absorption of short-wavelength light can cause photochemical retinal

tissue disruption. Photochemical damage processes, which occur over hours to days, are slower than the thermal damage processes, which occur immediately following laser exposure that produces a thermal (photocoagulation) lesion (Ham, Mueller, Ruffolo, and Clarke, 1979; International Committee of the Red Cross, 1990). Longer-wavelength laser light (> 600 nm) is absorbed more by the choroid of the eye, which is beneath the intraretinal layers. In fact, ophthalmologists performing laser surgery on the fovea and macular regions of the eye use the 647-nm emission line of krypton lasers to avoid damage to the retinal layers containing the photoreceptors (rods and cones) and their associated nerve cells (Spalton et al., 1985).

Discussions of visual performance measured with real and simulated scotomas will be discussed further in this section in relation to the type of biological damage produced. These discussions of the different types of biological damage will include general descriptions of the biological damage, as well as known laser energy levels (in terms of corneal irradiance given in Joules per square centimeter (J/cm^2)), which produce such lesions.

Classifications of Laser Energy and Damage

Laser energy levels required to produce biological damage can be specified relative to the maximum permissible exposure (MPE) energy, defined in current laser safety standards (AFOSH Standard 161-10, 1980; ANSI Z136.1, 1986). On the average, the MPE is one-tenth of the energy required to produce a minimum visible lesion (MVL) with a 50% probability. The MPE is determined by several laser characteristics, which include the wavelength, pulsewidth, image size, and mode of laser output (i.e., pulsed or cw). Two exposures made at the same MPE level may actually produce different retinal illuminances. For example, because of the lower MPE for shorter pulsewidth exposures, the retinal illuminance of a 10-ns exposure at 60% of the MPE may be considerably less than that for a 10-ms exposure at 60% of the MPE. The MPEs for direct ocular exposures to a collimated laser beam (intrabeam viewing) are shown in Figure 14. The Army has proposed a classification scheme for the severity of laser lesions referred to as the Wolfe grades of laser retinal injury (Wolfe, 1984).

Classifications of Biological Damage

Photocoagulation lesions appear as "whitish spots" on the retina and are primarily the result of thermal damage to one or more retinal layers. Photocoagulation lesions are commonly referred to as thermal lesions, and they are the types of lesions made during laser eye surgery. Visible wavelengths of laser light are absorbed by the intraretinal layers, which contain the photoreceptors and associated nerve cells, and the retinal pigment epithelium (RPE). The RPE contains the melanin pigment cells, and it provides nutritive substances to the retina and photoreceptors. The choroid, its underlying vasculature, and the choriocapillaris (CC), are also susceptible to laser damage. However, of these three areas, the RPE is generally the most vulnerable because approximately 60% of all incoming visible light is absorbed by the RPE (Boettner and Wolter, 1962). In fact, the "whitish" appearance of the photocoagulation lesions is primarily due to reflectance changes in the RPE, as opposed to retinal or choroidal changes. The exception to this circumstance is for very high retinal irradiances, where all of these tissues are heated (Glickman, personal communication, March 1991). Because the RPE is beneath the retina, hemorrhages that bleed in between the RPE and the retina are called subretinal hemorrhages.

Threshold photocoagulation lesions, or minimum visible lesions, are formally defined as "minimally ophthalmoscopically visible lesions of about 30-50 microns (μ) in diameter that form within one hour of the laser exposure" (AFOSH Standard 161-10, 1980; ANSI Z136.1, 1986; Sanders and Zuclich,

1975; Wolbarsht and Allen, 1986; Zuclich et al., 1988). Photocoagulation lesions are the type produced by clinicians performing photocoagulation laser surgery on diabetic eyes, and, thus, can be medically beneficial when administered under the proper circumstances and conditions. Surgical photocoagulation lesions are produced at energy levels considerably above threshold, and, in contrast to MVLs, may be several hundred μ in diameter (L'Esperance, 1989).

More severe retinal lesions are those which result in choroidal bleeding that remains beneath the retina or spreads within or throughout the retina and into the vitreal chamber. These hemorrhagic lesions (HLs) can vary in severity depending on the energy and pulsewidth of the laser exposure. Some HLs have bleeding that remains contained within a certain area, usually beneath the retina. These types of HLs are called contained hemorrhages. Other HLs may bleed through the retinal layers into the vitreous chamber, where the blood may become mixed with the jelly-like vitreous substance (i.e., vitreous humor). Hemorrhages that bleed into the vitreal chamber are called vitreal hemorrhages.

Figure 15 shows a monkey eye containing all four of the types of lesions discussed in this report. The HL on the far right of the photograph is a vitreal hemorrhage. The human vitreous humor liquefies with age and becomes thinner (Spalton et al., 1985). This aging process causes blood from vitreal hemorrhages to bleed into the vitreal chamber more easily, unlike the vitreal hemorrhages shown in this photograph. In this photograph, the blood flows through the retina until it reaches the vitreal-retinal interface and then flows downward due to the pull of gravity. This same lesion in humans would likely bleed into the vitreal chamber (Glickman, personal communication, June 1990).

Subjective reports indicate that hemorrhages that mix with the vitreous humor appear as though one is looking through a red cloudy filter (Zuclich, personal communication, June 1990), or as if the blood is in the front of the eye. In addition, because of the inversion of the visual field relative to the retina, hemorrhages whose blood flows downward due to the pull of gravity would appear to the observer as though the blood were moving upwards.

Mechanisms of Biological Damage

Mechanisms of biological damage can be discussed in terms of three general processes: thermal, photochemical, and thermoacoustic/mechanical damage. These general mechanisms represent only a subset of the potential mechanisms of biological damage. However, for the purpose of providing an overview for non-vision scientists, dividing the mechanisms of biological damage into these general categories provides a simple yet good explanation of the basic underlying biophysiological processes that cause laser lesions.

The absorption of high-energy photons emitted from lasers, especially from short-wavelength lasers, can initiate many chemical reactions in retinal tissue that otherwise would not be energetically favored (International Committee of the Red Cross, 1990). The result of these chemical reactions is photochemical damage. Since photochemical processes are just as efficient for long, low-intensity exposures as for short, high-intensity pulses (with equivalent photon energies), they are typically the only damage mechanisms operative with low-intensity, long-duration laser exposures. These chemical reactions produce toxic free radicals which can injure or destroy the cells' metabolic activities and lead to cell death (International Committee of the Red Cross, 1990).

Thermal damage is caused by the transformation of the absorbed laser energy into heat that raises the temperature of the surrounding tissue to a level that denatures biological molecules. The magnitude and duration of the temperature rise, as well as the thermal conductivity of the retinal tissue,

determine the extent of thermal damage. The point at which the protein destruction rate exceeds the repair rate is the lower threshold of thermal damage. When the rise in tissue temperature is very fast and exceeds the boiling point of water, rapidly expanding steam is produced, causing additional mechanical damage. This vaporization process, which can result in carbonization and charring of the tissue, is the upper threshold of thermal damage (International Committee of the Red Cross, 1990).

Thermoacoustic/mechanical damage results from short pulsewidth (< a few microseconds (μs)) laser energy exposures where photon energy absorption greatly exceeds energy dissipation by thermal conduction. The rapidly heated retinal tissues expand so quickly that a compressive pressure acoustic pulse is generated onto the surrounding tissue. As mentioned for thermal damage, resulting tissue temperature increases above the boiling point of water will cause steam to form. The rapidly expanding steam causes an explosive tissue expansion which also generates an acoustic impulse. The ensuing mechanical damage is extensive and of great magnitude. Acoustic pulses travel away from their origins at the speed of sound and cause tearing of subretinal tissue membranes and the CC vessels. Subretinal and vitreal hemorrhages are the consequence of these processes. Furthermore, for even shorter, high-energy laser exposures (> 1014 W/m^2), ionization of the tissue can occur. Tissue ionization can ultimately result in plasmas (an effect of optical breakdown, see Birngruber et al., 1987, or Zysset, Fujimoto, Puliafito, Birngruber, and Deutsch, 1989, for more detail on plasmas) containing gaseous products being produced. The gaseous products of the plasma combine with the steam produced by the high tissue temperatures and form a cavitation bubble in the tissues which can expand and then collapse very violently, causing damage far away from the original absorption site. The resulting mechanical damage area can be as much as 200 times larger than the thermal damage size (International Committee of the Red Cross, 1990).

The mechanism of biological damage, whether photochemical, thermal, or thermoacoustic/mechanical, is interdependent on the wavelength, energy, and duration of the laser exposure. For exposures in the seconds (s)-to-minutes (min) range, photochemical damage is more likely to occur at lower energies of short-wavelength (< 514 nm) light versus longer-wavelength light. As the duration of the exposure decreases (μs - s), thermal damage is more likely to occur for short- and long-wavelength exposures. For laser exposures of less than a microsecond (μs), thermoacoustic/mechanical damage is likely to result for all visible and near-IR wavelengths, especially if they are high-energy exposures (Zuclich, personal communications, June 1990). Dividing the mechanisms of laser damage by wavelength is difficult because the regions are not well-defined. Considerable overlap exists between the different damage mechanisms as a function of wavelength due to their strong dependencies on exposure duration and available energy. Both thermal and photochemical damage can occur for exposures in the s-to-min duration range, with the photochemical damage dominating for long-duration, low-intensity exposures to shorter wavelengths. The thermal mechanism becomes relatively more efficient at higher intensities for all wavelengths. Short-pulsewidth (10^{-9} - 10^{-12} s) exposures can produce nonlinear effects which can lead to acoustic/mechanical shock events, as described above. These nonlinear effects may include: 2-photon absorption, frequency doubling, Raman and Brillouin scattering, and re-radiation by black-body emission. Pressures as high as 100 atmospheres (atm) can be generated in the vicinity of the absorption site, which is probably the melanin pigment granules in the choroid (Ham, Ruffolo, Mueller, and Guerry, 1980). Mixtures of both thermal and acoustic/mechanical events probably take place in the ns to μs range of laser exposures (Allen, Blankenstein, and Zuclich, 1986).

Minimum Visible and Photocoagulation Lesions

Thresholds for minimum visible lesions (MVL) have been established at selected points from the near ultraviolet (UV) to near IR. These threshold energies are part of the baseline data used to establish MPE values for the safe use of lasers (see Figure 14). Some representative MVL threshold (ED_{50}) values for wavelengths of interest are given below in terms of total intraocular energy (TIE). These values were calculated by multiplying the energy of the laser exposure at the cornea by the area of the pupil. Thus:

TIE = (radiant exposure in J/cm^2) X (pupil area in cm^2) (4)

The values given below are for collimated, intrabeam viewing exposures and generally represent the TIEs as calculated with a nominal, 0.7-cm diameter (i.e., dilated) pupil. These TIEs should be adjusted downward for the smaller pupil sizes expected for high-luminance viewing conditions (i.e., daytime).

Long-Pulse Exposures:

476 nm, 250 ms: 8.69 x 10-3 to 8.86 x 10-3 J (Sanders and Zuclich, 1975)
514.5 nm, 500 ms: 4.62 x 10-3 J (Gibbons and Egbert, 1974)
647.1 nm, 40 ms, 6.88 x 10-4 J (Sanders and Zuclich, 1975)

Short-Pulse Exposures:

530 nm, 15 ns: 3.03 x 10-6 J (Gibbons, 1973)
532 nm, 250 ns: 1.61 x 10-6 J (Gallagher and MacKenzie, 1974)
694 nm, 10 ns: 2.20 x 10-5 J (Vassiliades et al, 1970)
1060 nm, 30 ns: 2.81 x 10-4 J (Vassiliades et al., 1970)
1064 nm, 30 ns: 3.27 x 10-4 J (Zuclich and Blankenstein, 1983)

Thermal tissue damage is the primary mechanism for photocoagulation lesions (Mainster, 1989). When temperature rises sufficiently over the ambient tissue temperature (> 10°Celcius (C)), complex proteins in the retina are coagulated (Ham et al., 1980). The resulting change in RPE and retinal tissue reflectivity causes the whitish appearance of the photocoagulation lesion spots.

Figure 14 shows the MPE curve and its dependence on wavelength, pulsewidth, and retinal illuminance[1]. Threshold energies required to produce MVLs at the macula are lower than those for the periphery (extramacular). These lower macular threshold energies may be due to the decreased thickness of some of the neural retinal layers in the macula (Allen et al., 1986). Threshold estimates have been found to show a high degree of variability, and may differ by as much as factors of 2-10 across different laboratories (Allen et al., 1986).

MVL and Photocoagulation Lesions Effects on Visual Function. Most studies of lesions on visual function have carefully controlled the placement of the lesions on the retina. Foveal and macular lesion sites have been chosen for most of the carefully controlled experiments on the effects of biological damage on visual function. Other than clinical studies on the effects of pan-retinal photocoagulation (PRP) on visual function, little data has been reported on the effects of extramacular lesions on visual function. PRP has been shown to have temporary effects on spatial contrast sensitivity, but Snellen acuity remained stable at the pre-laser surgery level (Higgins et al, 1986). However, dark adaptation has been demonstrated to

[1]In this report, discussions will be limited to biological damage produced by collimated laser beams.

be affected by PRP (Pender, Benson, Compton, and Cox, 1981; Russell, Sekuler, and Fetkenhour, 1985). Thus, extramacular MVLs would be expected to have little or no impact on foveally dominated visual abilities, such as visual acuity, fixation, and tracking. Hemorrhagic lesions could affect these abilities if the spread of the hemorrhage covered the fovea (Green et al., 1988). Due to the limited information on the effects of extramacular lesions on visual function, the effects of different types of biological damage on foveal or macular visual function will only be discussed unless otherwise specified.

Behavioral studies of nonhuman primates have demonstrated that detrimental effects on visual acuity and contrast sensitivity result from punctuate foveal lesions. Rhesus monkeys trained in a visual acuity task experienced permanent acuity losses from two 11 mW, 633-nm laser exposures, and transient losses from exposures below this power level have also occurred (Robbins, Zwick, and Holst, 1974). Likewise, small, punctuate macular lesions produced by several exposures to a very short-pulsewidth (20 ns), frequency-doubled laser (532-nm 11-3 mJ corneal irradiance per pulse) produced transient changes in contrast sensitivity and acuity for rhesus monkeys performing a visually guided task (Zwick, Bloom, and Beatrice, 1988). Recovery from the effects of the exposure was apparent by 16-min post-exposure. Changes in spectral sensitivity and contrast sensitivity have also been reported (Zwick and Beatrice, 1978). Central macular lesions in primates produced relatively short-term losses in visual acuity losses and what appeared to be permanent alterations in spectral sensitivity (Zwick, Bedell, and Bloom, 1974).

Electrophysiological measures (i.e., electrical recordings of brain activity) of the local effects of retinal lesions resulting from single, very short-pulsewidth (15 ns) macular exposures to a doubled Nd:YAG (532-nm) laser were studied in rhesus monkeys (Cartledge, Allen, Previc, Glickman, and Mehaffey, 1988; Zuclich et al., 1988). Pattern electroretinogram (PERG) and visually evoked potential (VEP) measures were used to assess visual function. PERG and VEP recordings, represent retinal and cortical electrical activity, respectively, over an approximate 1° visual field. Suprathreshold (i.e., above threshold) laser exposures, ranging from 52.5-91.0 mJ of corneal irradiance, produced either white, coagulated lesions or small local hemorrhages. Following lesion placement, the PERG and VEP declined transiently, with recovery occurring in 1.0 min. Notably, even lesions producing small local hemorrhages did not cause any permanent vision loss within their local retinal area that could be determined by the VEP. The effects of the exposure were diminished markedly at sites more than 4° from the exposure site. The transient effects observed were likely due to the flashblinding component of the laser exposure (Zuclich et al., 1988).

Hemorrhagic Lesions

HLs result from trauma causing blood to leak from retinal or CC blood vessels. The blood can pool within the retina (i.e., retinal hemorrhage), between the retina and choroid (i.e., subretinal hemorrhage), in the vitreous humor (i.e., vitreal hemorrhage) (Sliney, 1986). Because HLs result primarily from mechanical damage processes, they are difficult to produce with long-pulsewidth laser exposures. As previously mentioned, ns to picosecond ((ps) 10^{-9} to 10^{-12} s) exposures can produce nonlinear effects and optical breakdown that are the basis for thermoacoustic/mechanical damage. For these reasons, long-pulse laser exposures rarely produce HLs. Because most current military laser systems emit short pulses (International Committee of the Red Cross, 1990), the following discussion will be limited to the effects of short-pulsed (i.e., Q-switched) exposures.

For ns laser pulses, the ED_{50} exposure for a hemorrhagic lesion is near the MVL threshold. Compared to long exposure durations, the amount of energy required for the various damage endpoints is relatively small. Short-pulse HLs have been produced by exposures 10 times the MVL threshold in the

near IR and between 20-100 times the MVL thresholds in the visible spectrum (Blankenstein et al., 1986; Zuclich, work in progress) when the peak power of the laser on exposure was high. For example, Blankenstein et al. (1986) found that for a 1064-nm, 30-ns exposure from the Nd:YAG laser, the ED_{50} for a subretinal hemorrhage was approximately 1.9 mJ, whereas the ED_{50} for a vitreal hemorrhage was about 4.2 mJ. However, ongoing work by Glickman indicates that these energy values may be too high. For the frequency-doubled, 532-nm output of this laser, the energy values are about an order of magnitude lower ($\cong$ 0.25 mJ) for non-contained HLs.

Hemorrhagic Lesions Effects on Visual Function. Current behavioral studies (Rhodes and Garcia, work in progress; Wolfe, 1984) confirm that visual acuity can be significantly and permanently reduced by HLs which directly or indirectly (i.e., through edema or the spreading of the hemorrhage) affect the fovea. For example, foveal HLs produced an initial visual acuity reduction in one subject from 20/20 to 20/35 (Rhodes and Garcia, work in progress). Macular laser exposures outside the fovea have resulted in immediate central visual acuity reductions as great as 20/60 to 20/200. In some instances, visual acuity improved to a near-baseline level over time; however, in other cases, it did not (Wolfe, 1984). Others have reported that both the severity of the vision loss and the recovery of visual function following HL-producing laser exposures vary from individual to individual (Green et al., 1988; Zuclich et al., 1988). In general, foveal damage has the greatest impact on high spatial frequency detection (fine detail vision). This probably explains why Rhodes and Garcia (work in progress) have found that retinal lesions that do not directly or indirectly affect the central fovea, and are not HLs, have a minimal effect on visual acuity.

The effects of foveal and extrafoveal suprathreshold laser HLs on visual function were studied in rhesus monkeys using the VEP to record cortical activity. In one study, doubled Nd:YAG (532 nm, 15-ns pulse) laser exposures were delivered at a minimum corneal irradiance of 182 μJ to produced large subretinal hemorrhages. The severity of these HLs varied considerably depending on the lesion location and individual's susceptibility (Zuclich et al., 1988). The VEP arising from the lesioned retina (as indicated by the response at the corresponding cortical electrode) was totally abolished for periods lasting up to several weeks (Zuclich et al., 1988) if large spreading foveal or parafoveal HLs were produced. Only partial recovery of the VEP signal occurred. This partial recovery was possibly related to the resorption of the retinal hemorrhage by the ocular tissue. The effect of these severe suprathreshold HLs extended beyond the physical boundary of the laser impact (Zuclich et al., 1988). At a site 4° from the lesion, the VEP was reduced by 50%; whereas at locations 6-8° off-axis, an essentially normal VEP was obtained. The spread of the lesion effect may have been due to tissue edema and/or shock processes emanating from the lesion site (Zuclich et al., 1988).

More recently, the effects of hemorrhagic foveal lesions on visual acuity in the rhesus monkey were studied by a modification of the VEP technique. By "sweeping" the spatial frequencies in the luminance grating stimulus used to elicit the VEP, a real-time measure of acuity can be derived with a time resolution of a few seconds. Vitreal hemorrhages were produced from single, 15-ns, 1064-nm Nd:YAG laser pulses (TIEs of 1.34-1.85 mJ). In less than 12 s following hemorrhage production, acuity had declined to less than 10/150, and remained at this low level for 20 - 30 min. Limited recovery to 20/80 - 20/100 acuity was observed by 1-hr after the exposure. Over the next several months, acuity recovered to within the 20/60 - 20/100 range in the three animals studied (Glickman, Rhodes, and Smith, 1991; Smith, Glickman, and Coffey, 1990). Other changes, such as loss of temporal sensitivity, were noted in the visual responses of some of these animals. All of these effects appeared to be permanent (Glickman, work in progress).

Other Discussions of Biological Damage Effects on Visual Function

Losses in visual acuity associated with retinal laser lesions do not necessarily predict the observer's ability to detect a target. Visual acuity, by definition, only predicts the ability to resolve high-contrast, high-spatial-frequency targets. Visual acuity does not necessarily correlate with flying performance (Ginsburg, Evans, Sekuler, and Harp, 1982). In fact, one study indicated that contrast sensitivity appeared to be a better predictor of a pilot's normal detection of ground targets (Ginsburg et al., 1982). However, another study contradicted this assertion by showing that contrast sensitivity was not a good predictor of pilots' normal ability to detect T-37 aircraft on the ground (O'Neal and Miller, 1988). Other visual performance measures may be more predictive of one's ability to perform a task such as flying. Contrast thresholds for ground target discrimination (as opposed to detection) as a function of range, and dynamic visual acuity are two examples of other measures of visual performance that may correlate with visual requirements when flying.

Visual performance measures, such as the observer's ability to track an object or aim at a target with an artificial scotoma, are two examples of ways of assessing pilots' visual abilities with laser-induced visual impairment. Figure 16 illustrates how tracking and aiming abilities are affected by foveal artificial scotomas of different size. Tracking abilities are more severely affected by foveal artificial scotomas than are aiming abilities. Furthermore, tracking abilities are also more dramatically affected by the size of the artificial scotoma (Burbeck and Boman, 1988). In general, a 1° scotoma centered on the fovea has very little effect on tracking. One-degree lesions located around the fovea at distances 1° from its center also do not dramatically affect tracking abilities. Conclusions from tracking studies have indicated that a minimum impact on tracking performance will be observed, unless about 90% of the central 2° of vision is impaired (Burbeck and Boman, 1989).

Individuals with central retinal lesions have good mobility while those with substantial peripheral visual field losses have difficulties in mobility (Kuyk, personal communication, June 1990). This fact explains why retinitis pigmentosa patients, who usually have good central visual acuity and deteriorating peripheral visual fields, have difficulties with mobility (Ehrnst, personal communication, June 1986; Marron and Bailey, 1982; Robinson, Story, and Kuyk, 1991).

Multiple Lesions

If two laser exposures follow each other at a rate so fast that the eye is unable to recover from the thermal changes induced by the first exposure, retinal damage is likely to occur for the second exposure, even if the two exposures in and of themselves are not intense enough to produce retinal lesions. Thus, multiple-pulse laser exposures provide a significant risk to military personnel, especially those laser systems with high repetition rates.

Studies have shown that the compactness of the artificial scotomas may be critical in determining the visual impact (Burbeck and Boman, 1988) they induce. Macular artificial scotomas that are spread further apart have less of an impact on visual function than those spaced closer together. Figure 17 illustrates how different spacings of artificial scotomas have different effects on visual tracking abilities.

When a multiple-pulse laser is propagated towards an observer, the eye-movement strategy used to avoid the laser threat may determine the number of lesions. Kosnik (1988) has developed a model that can predict, for a given laser exposure train hitting the retina at several different locations, how many lesions will be produced for several different laser-evasion strategies. The laser-threat strategies included: (a) lid closure, (b) acquisition saccades (looking towards the laser), (c) avoidance saccades

(looking away from the laser), and (d) fixation (continually staring at the laser). Acquisition saccades differ from fixation in that with acquisition saccades, the laser exposure did not necessarily initially present in the central visual field, so an eye movement towards the target was required to put the laser flash into the central visual field. With fixation strategies, the laser exposures always presented in the central visual field. Kosnik (1988) found that a pilot's reaction to a short-duration, multiple-pulse laser exposure significantly influenced the degree of retinal damage. The most effective strategy for minimizing retinal damage was a lid closure, yielding an 80-87% rate of lesion avoidance. However, in a practical sense, closing eyes, even briefly, could be extremely detrimental to a pilot flying a military mission. Looking away from the laser by means of an avoidance saccade was another effective way of minimizing injury. Avoidance saccades were found to displace a significant portion of the laser pulses to the periphery of the retina, which would generally result in less visual impact than foveal lesions. The other two eye movement strategies were found to increase the risk of eye injury in the central visual field. An eye movement towards the laser source increased the probability of serious visual loss by irradiating the fovea and, thus, forcing the pilot to resort to eccentric fixation. One possible successful strategy that was not examined in Kosnik's (1988) model was putting one's hand in between the laser source and the eye. This strategy would also block laser radiation from reaching the eye. However, if the repetition rate was very fast, significant damage could occur before the hand could block the beam. In addition, placing one's hand in front of their eyes could also impact a military pilot's mission performance (particularly for single-seat fighter aircraft), and if the energy of the laser source was sufficiently intense and of the appropriate wavelength, it could result in dermal laser injury to the hand.

Summary of Retinal Laser Bioeffects

In summary, retinal laser bioeffects can be divided into four general categories: veiling glare, flashblindness, MVL and photocoagulation lesions, and hemorrhagic lesions. These four general categories can be grouped by the relative persistence of their associated vision losses. Veiling glare and flashblindness produce temporary, though potentially significant, vision losses, whereas biological tissue damage from photocoagulation and hemorrhagic lesions results in more long-term reductions in vision, some of which are permanent. These four categories of retinal laser bioeffects can also be grouped into those which are source-fixed, or vary in severity as a function of the separation between the eye (or target) and the laser source, and those which are eye-fixed, or move with the eye's movements. Eye-fixed bioeffects keep the visual disruption within the same location of the observer's visual field, regardless of the laser's position, once the bioeffect has occurred. Veiling glare is a source-fixed bioeffect and flashblindness and all types of biological damage are eye-fixed bioeffects.

One of the most important points concerning retinal laser bioeffects is that certain laser exposures can produce multiple effects simultaneously. While the laser is on, veiling glare, which is essentially a reduction in the target-background contrast ratio, can occur. The effectiveness of laser veiling glare is dependent on the environmental luminance conditions, the physical characteristics of the target and laser, and the location of the laser in the observer's visual field. Once the laser exposure has ended, flashblindness could occur, resulting in up to several minutes of a partial or complete (depending on the target, background, and laser characteristics) obscuration of vision. Because flashblindness is an eye-fixed bioeffect, the visual loss produced by it would move with the observer's eye movements and keep the visual disruption within the same location of the visual field. During flashblindness recovery, vision is gradually restored. However, if the laser characteristics are appropriate, recovery from flashblindness may not culminate in the original level of visual abilities, due to the occurrence of biological damage to the retina. Because biological damage is also an eye-fixed bioeffect, vision losses resulting from it would also follow eye gaze. Retinal edema produced from MVL and photocoagulation lesions would likely occur rapidly and would increase the size of the affected area of reduced visual acuity. The spread of blood from HLs typically results in larger areas of vision loss than would be expected from the size of the lesion sites, and could affect the entire visual field if a vitreal hemorrhage is produced.

The energy output, wavelength, pulsewidth of the laser, and the size and location of the retinal laser image are all critical factors which determine the different mechanisms of biological damage, as well as the expected visual consequences of a given laser exposure. For example, HLs typically only originate from very short (< 10^{-7}-s) pulse durations. Because different wavelengths of laser light play a decisive role in the different mechanisms of biological damage, they influence the type of biological damage expected for a given laser exposure. The wavelength of light is not as critical at influencing magnitude of veiling glare and flashblindness. Comparisons of different wavelengths equated for equal visual luminous efficiency using the C.I.E. photopic luminosity function have not been found to differ significantly at affecting the severity of veiling glare or flashblindness.

Because there is a one-to-one mapping between the visual field and retinal location, and because visual capabilities vary across the retina, laser bioeffects in different regions of the retina result in visual degradation of different levels of severity. Laser bioeffects affecting foveal vision generally have the most severe effect on visual performance. Foveal vision is generally better than peripheral vision, and it is primarily used for most visual tasks. Other than large HLs or vitreal lesions, laser bioeffects affecting the peripheral retina are not expected to produce significant effects on visual performance provided adequate foveal vision remains. However, some visual tasks are more dependent of peripheral vision than others, and they may be more affected by peripheral laser exposures.

INFLUENCE OF SIMNET WORLD AMBIENT CONDITIONS ON PREDICTED LASER BIOEFFECTS FOR CTAS-2.0

As previously discussed, many visual abilities and temporary laser bioeffects (glare and flashblindness), are dependent on the ambient environmental luminance. This is particularly true for flashblindness, where the degree of visual light adaptation produced by a laser flash depends on the initial adaptation state of the visual system. For high-luminance ambient conditions, very intense laser exposures will be required to produce flashblindness. This section concentrates on how the ambient background conditions proposed to be simulated in SIMNET-D for the CTAS-2.0 exercises (i.e., Fort Knox, Kentucky, with high-luminance, clear skies) will influence and constrain the types of laser bioeffects expected for the different simulated laser exposures. These discussions will also address how these same limitations apply to laser bioeffects that would be expected when eye protection is worn. The discussions in this section are based on our knowledge of the battlefield environment for the CTAS-2.0 exercise during a window in time prior to the exercise's initiation. Therefore, these discussions represent our recommendations to ARPA and the CTAS-2.0 sponsors about how the environmental conditions we believed were going to be simulated in CTAS-2.0 affect the types and severities of retinal laser bioeffects that would be expected for the simulated laser weapons. These discussions do not necessarily reflect the actual conditions used for CTAS-2.0.

Our current understanding is that the United States version of SIMNET-D has only one environmental viewing condition. This is a high-luminance (≅10,000-20,000 cd/m^2) condition with the sun in the sky in such a position that no shadows are cast by objects on the ground. We casually refer to these lighting conditions as "high noon in Texas." Actual brightness values associated with "high noon in Texas" lighting conditions can vary greatly depending upon the object viewed. For example, measurements made at Brooks Air Force Base, Texas, in the early afternoon of June 7, 1990, were as follows: a radar unit (desert paint), 6000-8000 cd/m^2; trees and grass, 1200-4000 cd/m^2; cars, 4000-9000 cd/m^2; and sky/clouds, 3000-20,000 cd/m^2 (Labo, personal communication, June 1990). Although these were "rough" measurements made under specific environmental conditions, they do indicate the actual range of background luminances that can be encountered at "high noon in Texas" environments.

Thus, when considering the ambient environmental conditions of the SIMNET-D world and how they influence laser bioeffects, there is a great deal of variability that must be generalized to a specific set of predictions.

One study which examined laser bioeffects under high-luminance background conditions is that conducted by Labo et al. (1990). They measured the FOVO by a low-power, cw, argon-ion laser beam after transmission through the atmosphere (1.5-kilometer (km) path) and an F-16A aircraft canopy in daytime. The laser exposures in this study were 75% of the 24-hr cumulative exposure MPE. Labo et al. (1990) found it was impractical to measure the FOVO for high-luminance targets under daytime conditions because the laser irradiances required to produce a measurable FOVO were too high to permit repeated trials while remaining under the maximum daily exposure limit. For example, the maximum daily exposure of 7.5 milliJoules per square centimeter (mJ/cm^2) per subject was reached within a 37.5-s exposure, with an average corneal irradiance of 200 microWatts per square centimeter ($\mu W/cm^2$).

Table 1 shows Labo et al.'s (1990) data relating the angle obscured by the laser glare, in both day- and nighttime conditions, to target luminance and corneal irradiance. Large corneal irradiances of laser light were required to obscure the central 10° of vision for high-luminance targets during late afternoon, October daytime conditions. These data are further illustrated in Figure 18. Labo et al. (1990) also reported that a clear F-16A aircraft canopy caused the laser glare to appear "star-like" with "streaks" of light extending from the laser source. This appearance is a common perception of laser glare striking a canopy, which has been observed both in the laboratory and the field. These streaks of laser glare served to broaden the retinal image of the laser source and increase the size of the FOVO. The general conclusion from Labo et al.'s study was that under their experimental conditions, while viewing a relatively bright target, the laser glare did not produce an afterimage when the light was extinguished. Labo concluded from this study that glare generated from low-luminance, sub-MPE laser exposures is generally a problem only at night. However, the FOVO measured by Labo et al. (1990) was greater than that which would be expected from intraocular scatter alone, and it was dependent on both the laser irradiance and the target conditions.

Sheehy (1989b) also showed that argon laser glare (528.7-nm) impaired visual function under high-luminance conditions, but that laser glare was more effective at obscuring small target visibility under lower ambient luminances. He concluded that the relationship between glare intensity and ambient illumination was not linear. In contrast, Varner et al. (1991) found that laser glare was a problem in both simulated daytime (1700 cd/m^2) and simulated nighttime conditions. Their study found that an F-16 HUD flight path marker (of fixed intensity) could be effectively obscured by glare produced by an argon (514-nm) laser passing through an F-16 gold-tinted canopy. Contrary to Sheehy's (1989b) findings, Varner et al. (1991) found glare effectiveness to be better under simulated daytime conditions than nighttime conditions. Their explanation for this result was that the greater high-spatial-frequency contrast sensitivity provided by the increased ambient luminance did not sufficiently compensate for the reduced target contrast caused by the glare superimposed on the higher background luminance.[2] Regardless of the discrepancies in these two studies' findings, many of which could be contributed to the differences in their techniques and targets (see Varner et al., 1991), it is clear that ambient background luminance is a key variable in determining whether or not glare will disrupt visual performance as well as whether or not a laser exposure will produce glare and/or flashblindness. Glare can be a problem in photopic as well as scotopic ambient conditions. The amount of an observer's field of view that is obscured by glare is dependent on several other factors, such as the laser irradiance and the target characteristics.

---

[2]Contrast = $\frac{\text{HUD Luminance - (Glare Luminance + Outside World Luminance)}}{\text{(Glare Luminance + Outside World Luminance)}}$

Table 2 provides a description of different single Q-switched laser exposures (at several wavelengths) that will produce various laser bioeffects under different ambient conditions (Allen et al., 1990). Notice how low-power, MPE to ED_{50} (MVL), exposures of a laser wavelength of high photopic wavelength efficiency are not expected to produce flashblindness during daytime conditions. By the time flashblindness would be predicted at other than nighttime luminance conditions, biological damage could occur. With the laser pulsewidths in Table 2, a point has been reached under daytime conditions where the damage levels are close to the levels which cause flashblindness. Because the gap between the damage and flashblindness levels is diminished or, in some cases, absent, flashblindness is less likely to occur for Q-switched pulses in high ambient environmental luminances than it is for longer laser pulsewidths or under nighttime conditions. With short-pulsewidth laser exposures, biological damage can be produced at energy levels that are lower than those required to produce flashblindness if the ambient environmental luminances are high.

One question that has not been completely answered is what bioeffects can be presented on the video monitors for the CTAS-2.0 exercises? Specifically, how will the simulation of "high noon in Texas" viewing conditions be done? These questions impact the laser bioeffects simulations. Because the simulated visual field is often physically different in many ways from the real world, it is necessary to scale the simulations to the simulator conditions. For example, the luminance levels and spatial detail which can be displayed in simulators are significantly lower than what exists for many outdoor conditions, particularly "high noon in Texas" conditions. These differences alone can reduce target visibility in the simulator relative to the real world. The challenge, then, is to simulate the degradation of vision produced by laser exposures by altering the simulator display to produce an equivalent drop in target detectability, and hope this simulated degradation has an equivalent effect on mission performance as an actual laser bioeffect. Such simulations might give the CTAS-2.0 participants the appropriate relative visual effect, but it is possible that absolute effects, which may be important to certain aspects of mission performance, may be lost. This situation, of course, is the trade-off between real versus virtual battlefield training, and it is a question that will be dealt with by post-exercise analysis.

TECHNICAL CONSIDERATIONS AND SUGGESTIONS FOR THE SIMULATION OF LASER BIOEFFECTS ON SIMNET FOR CTAS-2.0

Technical Considerations for Simulating Laser Bioeffects[3]

The primary goal of CTAS-2.0 is to investigate opportunities for engagement between a simulated laser weapon system and pilots' eyes. To successfully accomplish this goal, the pilots' eye positions must be known at all times, in real time during the exercise. Furthermore, it is important to simulate laser glare and other expected bioeffects so that the aircrew may be introduced to some of the frustration associated with laser-induced visual disruption. To adequately calculate[4] the proper type and severity of the laser bioeffects, the pilot's eye position in relation to the laser beam is required. CTAS-2.0 will use a combined head/eyetracking system to determine and record the pilots' eye positions, in relation to the laser weapons' beam, in real time during the course of the battlefield scenarios. Ideally, the CTAS-2.0 Test Directorate would like to produce laser bioeffects simulations which are realistic enough that the effects of laser-induced visual disruption on mission performance could be examined. However, the

[3]These discussions and ideas were presented to Cmdr McBride of ARPA and the CTAS-2.0 Test Directorate prior to the final decisions about how the laser bioeffects would be simulated in the exercise were made. Therefore, the information within this section does not necessarily represent how the laser bioeffects were simulated in CTAS-2.0.
[4]Lookup tables derived from experimental and theoretical data will be used in CTAS-2.0 to make these calculations.

database of many of the laser bioeffects effects described in Overview of Laser Bioeffects (especially flashblindness) and the present SIMNET-D computer technology is not capable of producing eye-fixed bioeffects simulations of sufficient quality to conduct this type of a laser bioeffects performance test with any reasonable level of confidence. Some of the bioeffects (both source-fixed and eye-fixed) can be simulated and integrated with the head/eyetracking device well enough to examine their effects on the opportunities of engagement and the sensitivity of the mission to having pilots exposed to these bioeffects. These bioeffects simulations can also provide some feedback or "penalty" (in terms of visual disruption) to the aircrew that is associated with ocular laser exposures.

The purpose of this section is to provide ARPA with information concerning technical issues associated with the SIMNET-D network and the CTAS-2.0 battle scenario that place limitations on the types of laser bioeffects that can be simulated. In addition, recommendations on different ways of ideally and practically simulating retinal laser bioeffects, with and without laser eye protection, for the CTAS-2.0 exercise are given. These discussions and recommendations are based on our knowledge of laser bioeffects and the SIMNET-D network prior to the finalization of all technical issues associated with the CTAS-2.0 exercise. Therefore, this section represents the recommendations AL/OEO made to ARPA during a window in time prior to the CTAS-2.0 exercise. The discussions and recommendations made in this section do not necessarily reflect the simulations used in the exercises or the final capabilities of the simulator during the CTAS-2.0 exercise.

Before describing ideal and more practically achieved simulation possibilities for the different laser bioeffects, some of the technical issues concerning current (and future) computer graphics capabilities, especially in regard to producing simulations that are integrated to eye-head tracking (EHT) equipment, must be addressed. Combination eyetracking/headtracking systems will monitor and record the pilots' eye movements and head positions during the CTAS-2.0 exercise. The software and log tapes used for the exercise can extract the head and eye position information and use it to determine when a simulated laser system is aiming in the region of the pilot's eye (i.e., co-visibility). Calculations can then be made to determine the region of the retina exposed to the laser radiation so that the proper laser bioeffect "penalty" can be displayed on the participant's simulator screen(s) during the exercises. Several parameters of the EHT and the visual display of the SIMNET-D simulators must be taken into account before decisions on laser bioeffect simulation strategies can be properly made. The parameters for visual display in simulators such as SIMNET-D include: (a) luminance, (b) color, (c) resolution, (d) contrast, and (e) saturation. The AIRNET facility at Fort Rucker, Alabama, uses Sony Trinitron cathode-ray tube (CRT) tubes, which are common in commercial televisions. The highest brightness of this type of CRT tube is around 20 foot-Lamberts (fL). The real image on the Trinitron is viewed directly by an observer as a virtual image. Because the CRT monitor is not bright, there is a limited dynamic range of the presented scene. This finite dynamic range of luminance on the CRT monitors is the source of the most significant scaling limitations for video effects presentation in SIMNET-D. The color of the Sony tube is not specified; however, it is most likely the P-22 red-green-blue phosphor set used on most commercial CRT monitors. Spectral plots of this and other tubes' phosphors are shown in Figure 19 (Diakides, 1975). These phosphors limit the colors that may be produced in an additive color system such as television. In addition, the phosphors selected may not be ideal for high luminance. For high-brightness use, a monochrome tube is optimal.

The resolution of the Sony monitor is 640-pixels by 400-lines, and the half-field rate is 640-pixels by 200-lines. The AIRNET fixed-wing aircraft platform simulator uses a monitor as an approximation to a 20° by 15° field of view from the cockpit. In resolution terms, a 25-in. diagonal monitor has a 20-in. horizontal view that represents a 20° horizontal field of view. The resolution of this monitor will produce 32 pixels per degree, or about 2-min of visual arc per pixel (i.e., ≅20/40 visual acuity). This monitor resolution prediction assumes a 5-foot (ft) viewing distance. For the ideal presentation to the human

observer, it is necessary to present one pixel per 0.5-min of visual arc so that 20/20 visual acuity can be achieved at the 5-ft viewing distance. This resolution requirement translates to 2560 pixels per Trinitron tube, which requires a high-resolution monitor.

The limiting factor for high contrast on the simulator CRT monitors is light reflection from the back of the CRT glass surface. This reflection problem serves to limit contrast in most CRTs to about 80% or 90% luminance contrast. When the CRT is operating at low luminance and low contrast, the factor limiting the quality of the visual image is the CRT's ability to modulate the video beam as it is swept across the monitor. This type of limitation is usually associated with the electronics capabilities of the CRT monitor. How well SIMNET-D CRT monitors operate for low-brightness, low-contrast situations is unknown. For example, as monitor brightness decreases, does contrast also decrease? Because many video effects intended for CTAS-2.0 should involve the manipulation of contrast, the electronics behind the monitor are a key component in determining the best simulation representations.

SIMNET-D relies on electronics to create the video virtual world. The appropriateness of the current configuration is apparent. Only under conditions of viewing the jet aircraft modeled on SIMNET-D do observers notice any jerkiness or unevenness in the movement of the aircraft. There are temporal properties associated with both the manipulation of the scene generated from the "scene data base" and the video link itself. Currently, the actual extent of these time delays or lags in the video channels of SIMNET-D has not been specified, but they are known to exist. These delays will add to any latency contributed by the EHT systems and will limit the ability of laser bioeffect simulations integrated to the EHT system to accurately follow the pilot's eye movements (i.e., be truly "eye-fixed" effects). The SIMNET-D software contractor (BBN) has stated that the scene is updated at 15 Hz, and the total delay through the video channel is 100 ms. The EHT delay may be up to 200 ms. Therefore, the total time lag between the pilot's actual eye movement and the corresponding movement of the bioeffect simulation on the monitors may be 250 to 300 ms. This response time is insufficient to produce a small (e.g., 1°) eye-fixed central scotoma that is perceptually realistic in terms of its movement with the eye. Westheimer and Conover (1954) determined that 2% of the population could perceive time lags shorter than 125 ms, and none of this population could perceive time lags of less than about 100 ms. Given this data, time lags less than 100 ms would be optimal since the time lags associated with the video refresh rate, coupled with time lags associated with the EHT, can significantly affect the quality of the eye-fixed laser bioeffects simulated for CTAS-2.0.

In addition, for a small eye-fixed bioeffect, such as a 1° scotoma, the accuracy of the placement of the scotoma within the pilot's visual field is also critical. If the goal is to keep the central 1-2° of the pilot's visual field continuously obscured with a scotoma simulation, any inaccuracy in the placement of that simulated scotoma that is caused by integrating the simulation with the EHT will become significant. If there is even a small (1°) inaccuracy, the pilot will be able to use his[5] central foveal vision and defeat the simulated laser bioeffect "penalty." Therefore, the spatial and temporal integration between the simulation software and the EHT must be perfected before very small eye-fixed bioeffect simulations can be accurately displayed for a dynamic force-on-force simulation exercise such as CTAS-2.0.

Simulations of scenes viewed through protective eyewear need to reflect the color shifts associated with the altered transmission of the scene lighting. In addition, any battlefield performance trials whose goal is to attempt to determine the value of protective eyewear (such as specified for CTAS-2.0) should first contain baseline trials from which information on how mission performance is altered by simply wearing the eye protection alone (without simulated laser exposures). The various laser sources can be introduced in subsequent tests. Shifts in color appearance and changes in color contrasts

[5] All pilots participating in the CTAS-2.0 study will be male.

between targets and their dynamic backgrounds could serve to reduce, or even enhance in some instances (i.e., camouflaged targets), the detectability of the targets. Without these baseline trials, interpretations of the eye protection's impact on mission performance could be confounded by possible significant alterations in performance caused by simply wearing the filters.

Because these types of baseline trials are not planned for the CTAS-2.0 exercise, and because some selective filters have been shown from a perceptual standpoint to effectively lower the energy reaching the eye from monochromatic (laser) sources, we recommend that simulations of laser bioeffects with eye protection be considered as scaled versions (i.e., reduced in magnitude) of those simulations of laser bioeffects without eye protection. These recommended simulations will only represent the reduced energy of the laser light entering the eye due to absorption by the eye-protective lenses. This recommendation is not only the simplest way to simulate laser bioeffects with eye protection, but it is rational given mentioned scientific results. This recommendation for eye protection simulations also sidesteps issues concerning the visual quality of the colors produced on SIMNET-D video monitors compared to real-world scenes, and how to accurately represent those colors after transmission through selective filters. However, recommendations for ideal ways of simulating laser bioeffects with EOCCM that selectively filter light will be discussed in this section.

Actual Bioeffects Versus Ideal Simulations

Ideal ways (technology unlimited) of simulating laser bioeffects in virtual worlds will be proposed in this section, and their impact on visual perception will be discussed. The discussions in this section will compare and contrast the AL/OEO's views on what ideal simulations of the laser bioeffects should represent as compared to those which have been suggested in preliminary CTAS-2.0 technical meetings. Simpler laser bioeffect simulations may be more practical given the limitations of the current computer technology and the time constraints to begin the CTAS-2.0 on schedule. These more achievable, but sub-optimal, laser bioeffect simulations can be used for CTAS-2.0 to provide the pilots in the exercise with a consequential penalty for receiving a simulated retinal laser exposure, yet also permit the exercise to run on schedule. Suggestions for simpler laser bioeffects simulations will be offered in a subsequent section.

Ideal Simulations of Glare

Veiling glare effectively reduces the contrast of a target against a background. Reports of laser glare transmitted through aircraft canopies during daytime indicate that the appearance is of a central bright spot of light surrounded by "spokes" of light that move around the canopy (Labo et al., 1990). This glare gives the overall appearance of a star-like pattern. An ideal simulation of laser glare would reproduce this perception. A central bright spot of an appropriate color (to represent the wavelength of the laser) with randomly moving spokes of light radiating from the central spot would reproduce the daytime glare perception. In addition, the glare icon would have to effectively reduce the contrast ratio of the target against the background scene by amounts similar to an actual glare source of the same intensity. Because the ambient luminance of a scene determines, in part, how effective a glare source is at reducing the contrast of a target, the brightness of the glare icon (or the effective contrast reduction of the scene) would have to be scaled depending on the simulated scene's luminance. Since the space-averaged simulated scene luminance is likely to remain constant within and across CTAS-2.0 trials, the effective contrast reduction produced by the glare icons could be generalized and put into a standard database look-up table.

Glare simulations do not have to be coordinated with the EHT because they are not eye-fixed bioeffects. However, they will require intensity and size modifications as a function of the angular separation between the simulated laser source and the eye position. The effectiveness of glare is known to decrease significantly with very small angles between the source and the target (or the eye). Ideal simulations would have to properly represent this effect. The laser glare simulation would have to show small "breaks" in the glare icon for multiple laser emissions at frequencies of less than at least 30 Hz. The frequency at which pulsed laser irradiation is fused by the visual system is not precisely known, so this 30 Hz temporal frequency may be too low. However, it does offer a relatively good initial estimate. Repetition rates faster than the cut-off temporal frequency used in the simulations should appear as a single glare icon that is removed from the screen when the laser no longer illuminates the aircraft canopy.

Simulations of laser glare through eye protection (EOCCM) would cause the glare icon to lose its spoke-like appendages, as well as reduce the area of the central bright spot. This effect has been termed a "beacon." The beacon simulation would either decrease in intensity with angular separation between the source and the target or completely disappear. The color of the beacon would need to be representative of the laser wavelength after transmission and/or predicted re-emission through the EOCCM. Proper intensity reductions in laser glare due to EOCCM absorption would also have to be portrayed. Ideally, the simulation of the viewer's scene with the EOCCM in absence of laser exposures would also be represented. Any appropriate hue shifts, magnification of the scene by the EOCCM optical enhancement, and luminance and/or contrast reductions that are expected given the transmission spectra of the EOCCM would need to be depicted in these simulations. EOCCM that have photodiode-detected polarizing shutters (e.g., PLZT) would be simulated by blanking the screen while the laser is on to represent the closure of the shutter (i.e., light being absorbed by the material due to changing the polarization). SIMNET-D's database would then have to keep track of the shutter position in order to determine whether or not a laser light was able to reach the eye.

Simulations of laser glare have been recommended during the preliminary CTAS-2.0 Test Directorate meetings to try to represent actual laser glare photographed hitting a canopy at night. How the glare icon should effectively reduce the contrast of the scene or how the daytime ambient luminance should serve to attenuate the glare icons as a function of the laser energy have not been specified within these recommendations. In addition, no mention of simulations through EOCCM with polarizing "shutters" was made even though a "switching" EOCCM has been specified for the CTAS-2.0 exercise. This latter simulation will require that the monitors' colors shift in order to reflect the change in the scene's appearance when the EOCCM filters are "switched on" following a laser emission.

A "beaconing effect," or pencil of light emanating from a laser through the atmosphere for off-axis (i.e., not entering the eye) exposures, has been proposed for implementation in CTAS-2.0. This simulation was proposed to provide a penalty to the air defense anti-tank system (ADATS) crew for firing a laser off-axis and becoming detectable to pilots who may not have previously acquired them (the pilot's primary target). Visualization of the "beaconing effect" is dependent on the ambient luminance of the scene and the visual system's sensitivity to targets superimposed on bright backgrounds. Given the high ambient luminance conditions to be simulated for CTAS-2.0 (10,000-20,000 cd/m^2) and the increased target (off-axis laser exposure) intensities required for detection on bright backgrounds, it is unlikely that the "beaconing effect" would be observed in a comparable field operation. Therefore, implementation of the "beaconing effect" is not required for CTAS II.

Ideal Simulations of Flashblindness

Flashblindness is a temporary obscuration of targets caused by the reduction of the target-background contrast ratio or by the production of a relative scotoma. Whether a relative scotoma is

visualized as a complete or partial obscuration of a target (i.e., the latter being a central area where the target-background contrast ratio is reduced) depends on the energy of the laser reaching the eye and the adaptation level of the visual system. Likewise, the size of the relative scotoma and the recovery rate of the flashblindness are also dependent on the laser energy reaching the eye, the adaptation level of the visual system, and the original target-background ratio. Flashblindness is an eye-fixed bioeffect.

Ideal simulations of flashblindness would produce EHT-integrated relative scotomas which would decay in size and/or magnitude (i.e., effective contrast reduction) with time. The relative scotoma would appear as a central bright spot on the screen whose size and intensity (effective contrast reduction as well as brightness) would decay with time. The initial size of the relative scotoma and the decay rate would depend on the laser energy reaching the eye, the original adaptation state of the eye (the ambient luminance), the target-background contrast, and the target size. Targets with higher contrast and low spatial frequencies would appear visible more quickly than those with lower contrasts and high spatial frequencies. In addition, ideal simulations of flashblindness should try to capture some of the other perceptual changes associated with afterimages (e.g., hue changes and contrast reversals of the afterimage, see Miller, 1965). The EHT-integrated flashblindness icons should also, ideally, obscure the pilot's instrument panel and other targets not displayed on the video screens.

Flashblindness simulations with EOCCM would appear less intense, smaller in size, and faster in recovery rate for any given amount of available laser energy. As mentioned for ideal glare simulations with EOCCM, ideal flashblindness simulations with EOCCM should also produce any screen hue shifts, reductions in luminance, and target contrasts expected given the transmission spectra of the EOCCM filters. "Switching" EOCCM simulations for flashblindness would be similar to previous descriptions for glare with these EOCCM.

Because flashblindness recovery is dependent on so many target and background factors, it is very difficult to model for a simulated battlefield exercise. Therefore, the CTAS-2.0 sponsors chose to forego flashblindness simulations for the exercise. However, flashblindness simulations are envisioned for future CTAS exercises. Therefore, suggestions for practical flashblindness simulations will be discussed in a later section.

Ideal Simulations of Biological Damage

Ideal simulations of biological damage would need to produce blanked-out portions of the screen to represent absolute scotomas. Ideally, these blanked-out regions would remove a portion of the scene and fuse the surrounding areas in order to simulate the "filling in" process done by the visual cortex. However, laser accident victims have described these regions as "blacked-out" and "appearing as a bright spot," so blanking a portion of the monitor would be suitable. All assumptions concerning the procedure for mapping the size of the scotoma from the size of the lesion would have to be specified. Ideal simulations would also represent visual acuity changes associated with damage in the fovea or macula (due to edema) by changing the visual resolution on the monitors to simulate either peripheral viewing (for foveal scotomas) or blurred central vision (for macular edema). These types of visual resolution alterations have been produced at the AL/OEO by changing the pixel resolution on different parts of the monitors and by blurring the image with Gaussian filters.

The scotoma icons would have to be placed in an appropriate area of the monitor to represent the lesion location in the visual field and they would have to be carefully integrated with eye-gaze. As with flashblindness, ideal scotoma simulations should obscure all targets in the simulator regardless of whether they were located on or off the video monitors. Wearing EOCCM would serve to lower the total energy reaching the eye and, therefore, could be simulated by producing smaller scotomas or different

types of biological damage on the monitors (e.g., threshold MVL versus suprathreshold photocoagulation lesions), if any biological damage simulations at all for laser exposure.

For CTAS-2.0, two types of biological damage could be simulated. MVL simulations could be used to demonstrate to the pilots how relatively minor, yet permanent, biological damage can result from laser exposures. Hemorrhagic lesion simulations could be used to demonstrate severe biological damage and how a single laser exposure can result in significant reductions in vision. Simulations for MVLs and hemorrhagic lesions will, therefore, be discussed separately in greater detail.

Ideal Simulations for Minimum Visible Lesions. Foveal and macular MVLs can reduce visual acuity and spatial contrast sensitivity due to actual tissue destruction or tissue swelling from edema. Small, focal scotomas can result from MVLs. Except for the immediate blurring of vision from edema, MVLs are not likely to be perceived by the observer unless they are present in the fovea. Even foveal MVLs may not be noticeable if they are very small and the foveola is not damaged. Therefore, ideal simulations of MVLs would change the pixel resolution on the central screen to represent the reduction in visual acuity associated with edema. The size of the blurred area would not exceed the size of a single monitor. Another approach would be to incorporate a model of human spatial vision to filter the image (using difference of Gaussian filters) and then display the output of all the filters except those whose spatial tuning matched the higher spatial frequencies expected to be undetectable with the acuity and spatial contrast sensitivity loss (this capability is also present at AL/OEO).

Regardless of the simulation chosen, it is important to remember that blurring an image to a lower resolution level will not necessarily simulate all the effects on visual function produced by having a central lesion. This fact is particularly true if the scotoma produced by the laser exposure is large enough to interfere with tracking, visual search, and visual acquisition abilities. Ideally, the chosen MVL simulation would be integrated to the EHT and would affect all targets on and off the simulator monitors. EOCCM simulations would either lower the extent of visual acuity and contrast sensitivity reductions or fail to produce an MVL altogether. The energy of the exposure would determine which of these two options should be simulated.

Ideal Simulations for Hemorrhagic Lesions. HLs produce absolute scotomas at the lesion site and reductions in visual sensitivity in the portion of the visual field corresponding to the areas of blood obscuring the retina. Vitreal HLs have been described by accident victims to appear as though the observer is looking through a cloudy red filter or as if blood were in front of the eyeball. Ideal HL simulations would blank the portion of the monitor corresponding to the lesion's location (in order to represent the scotoma) and reduce the screen's pixel resolution (or totally blank the screen) over the area surrounding the lesion, where the blood would be expected to flow due to the pull of gravity. Ideally, the SIMNET-D system would be able to produce extra spreading of the hemorrhage simulation if very fast "jerky" eye movements followed the HL simulation, since this type of observer response would likely increase the spread of blood in a real laser injury.

By turning up all the red phosphor guns on the monitor to their maximum firing output, vitreal hemorrhage simulations could represent the perceptual effect of "looking through a red filter." The blue and green phosphor guns might also need to be reduced to produce a more effective "looking through a red filter" simulation, as well as to simulate the reduction in light reaching the retina due to absorption by the blood in front of it. If the HL spreads into a significant portion of the vitreous and is sufficiently dense, it is likely that the observer would only be able to "perceive light." Simulations of these HLs would best be represented by simply blanking the monitor. All these ideal simulations would have to be integrated with the EHT, and objects that are not on the video monitors (such as the pilot's instrument panel) should be obscured by the HL simulations.

Ideal Versus Achievable Simulations of Laser Bioeffects

Although ideal simulations would be best for indicating the appearance and impact of laser exposures to military personnel during training exercises, ideal simulations may not be achievable at the level required for the CTAS-2.0 exercise. One factor contributing to these limitations is that the computer technology may not be sufficiently advanced to integrate many of these ideal simulations to the head position and eye gaze without significant time delay across the SIMNET-D network. With such time delays, the participants in CTAS-2.0 could possibly avoid the simulated bioeffect "penalty." In addition, time limitations make screen changes impossible for the production of ideal simulations. BBN has informed AL/OEO of certain simpler, albeit feasible, simulations, which although not ideal, can be effective in providing laser bioeffect "penalties" to the participants during the CTAS-2.0 exercise. The following sections will discuss these options for each different laser bioeffect.

Achievable Laser Glare Simulations. BBN has indicated that they can produce video effects on a monitor-wide basis and integrate them with the EHT. Reductions in monitor contrast and additions of visual spatiotemporal Gaussian noise (white noise integrated over space and time) are achievable for the CTAS-2.0 exercise. Since glare effectively reduces the target-background contrast ratio, achievable simulations of laser glare could either reduce the monitor's target-background contrast or add spatiotemporal noise to the monitor to effectively reduce its contrast. These simulations would be psychophysically similar to the actual laser bioeffect, in that target detection would be reduced as a function of the reduction in the target-background contrast ratio predicted for the laser glare exposure. Attenuation of the contrast reduction using either of these two methods could be accomplished by calculating the angular separation between the simulated laser glare source and the eye. Larger angular separations would result in less contrast reduction or the absence of the simulation. Proper calibrations could yield tables relating contrast reduction levels to different amounts of root mean squared (rms) space-averaged luminance associated with the added spatiotemporal visual noise. These tables would provide an easy way for different laser exposure energies to produce different amounts of contrast reduction for the glare simulations.

Achievable Flashblindness Simulations. Achievable simulations for flashblindness would be similar to those for glare except that they would occur after the laser is turned off and the reduction in contrast (using either method previously described) would fade with time. In other words, following a simulated laser exposure's extinction, the appropriate monitor's contrast would be dramatically reduced, but the contrast would gradually recover over time. The simulation could be integrated with the EHT on a monitor by monitor basis. By avoiding partial screen bioeffect simulations, delay times caused by the slow network/EHT update rates could be minimized. This strategy might also minimize any observer confusion or aggravation caused by long delay times in integrating the simulation with the EHT.

Altering the simulator room lighting could provide a method of integrating the simulation to targets that are not on the video monitors. For example, for flashblindness, the room lights could either be lowered or turned off and then slowly increased back to their original levels. This latter simulation would depend on the lighting control of the aircraft simulator and whether a light dimmer could be controlled by the SIMNET-D network.

Achievable Biological Damage Simulations. Achievable simulations for biological damage would entail blanking an appropriate screen to represent a scotoma in a particular portion of the observer's visual field. For MVLs outside the fovea, it is not necessary to simulate any bioeffects. For MVLs near the fovea, reductions of monitor contrast, produced by either reducing the actual contrast or by adding spatiotemporal visual noise, could be used to represent the loss of visual acuity. The contrast reductions could be calibrated so that they correspond, in some way, with reducing target detectability of higher spatial frequencies within the video scene. In other words, the reduction in contrast would shift the cut-off

frequency of the spatial CSF to lower spatial frequencies (towards the left in Figure 4), as well as shift the entire CSF function vertically downward on the sensitivity scale. For vitreous hemorrhages, the whole monitor could be turned red or blanked completely to simulate spreading of a dense hemorrhage. These simulations could be integrated with the EHT on a monitor-by-monitor basis. The room lights could be lowered to provide some simulation of the reduction in vision for targets not present on the video monitors.

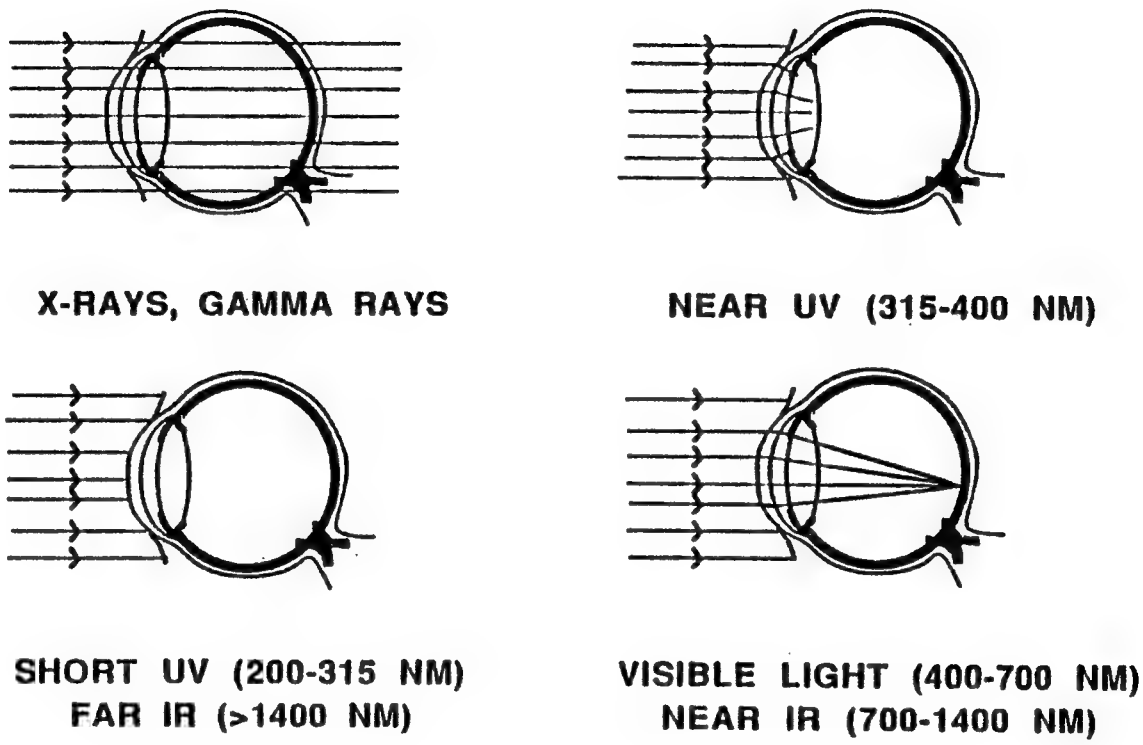

Figure 1. Ocular tissue absorption of electromagnetic radiation. The tissues of the eye selectively absorb different wavelengths of electromagnetic radiation. X-rays and gamma rays are not selectively absorbed (upper left) by the eye. Ultraviolet, visible, and infrared radiation are selectively absorbed by the different ocular layers. The cornea and lens of the eye selectively absorb most ultraviolet radiation (upper right and lower left), as well as wavelengths in the far infrared. Visible and near-infrared radiation are primarily absorbed by the retinal layers (lower right).

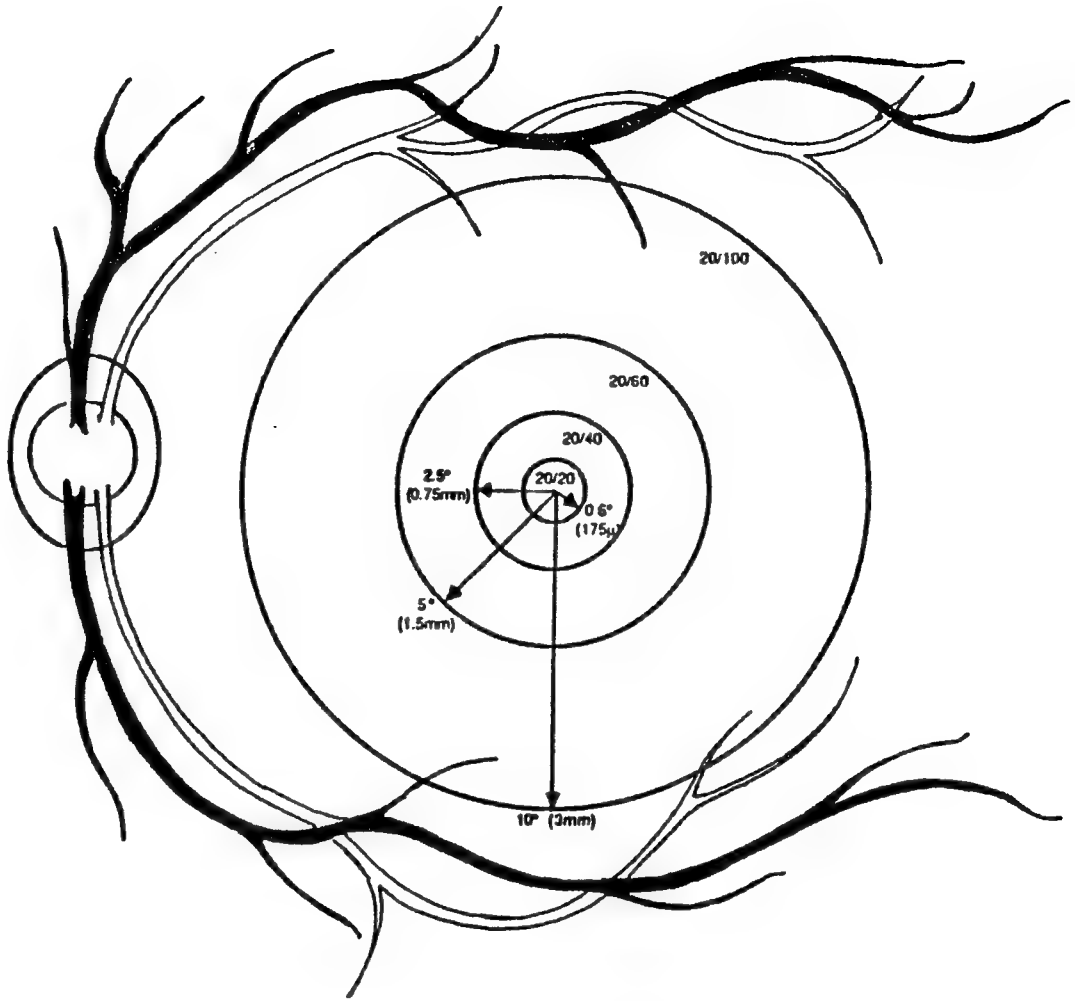

Figure 2. Diagram of the different regions of the retina. The retina can be divided into three different regions–fovea, macular, and extramacular regions. The fovea encompasses the central 2.5° radius from the visual axis of the eye. Within the fovea is the central 0.6° radius that comprises the foveola, where visual acuity is 20/20. The central 10° portion of the retina comprises the macula, where the yellow xanthophyll pigment resides. Visual acuity varies between 20/40 - 20/60 in the macular region. Beyond the central 10° of the retina is the extramacular region, where visual acuity is below 20/100 (Adapted from Green et al., 1988).

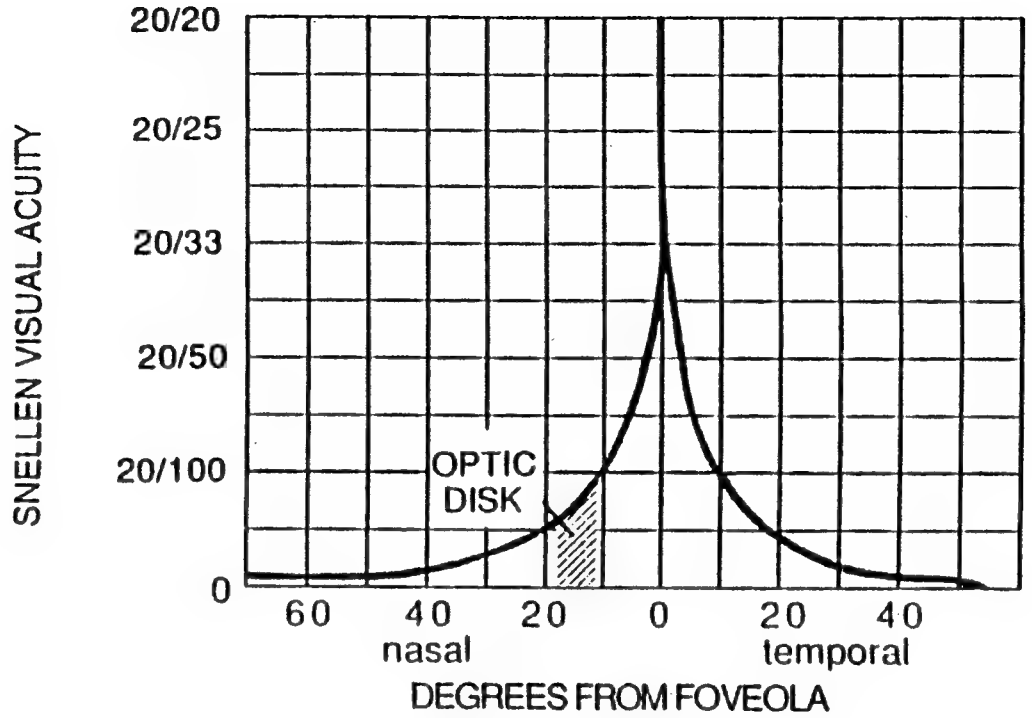

Figure 3. Visual acuity across the retina. Visual acuity varies across the retina and is best at the foveola. The fall off in visual acuity is relative to the observer's maximal foveal acuity and varies across individuals (Adapted from Green et al., 1988).

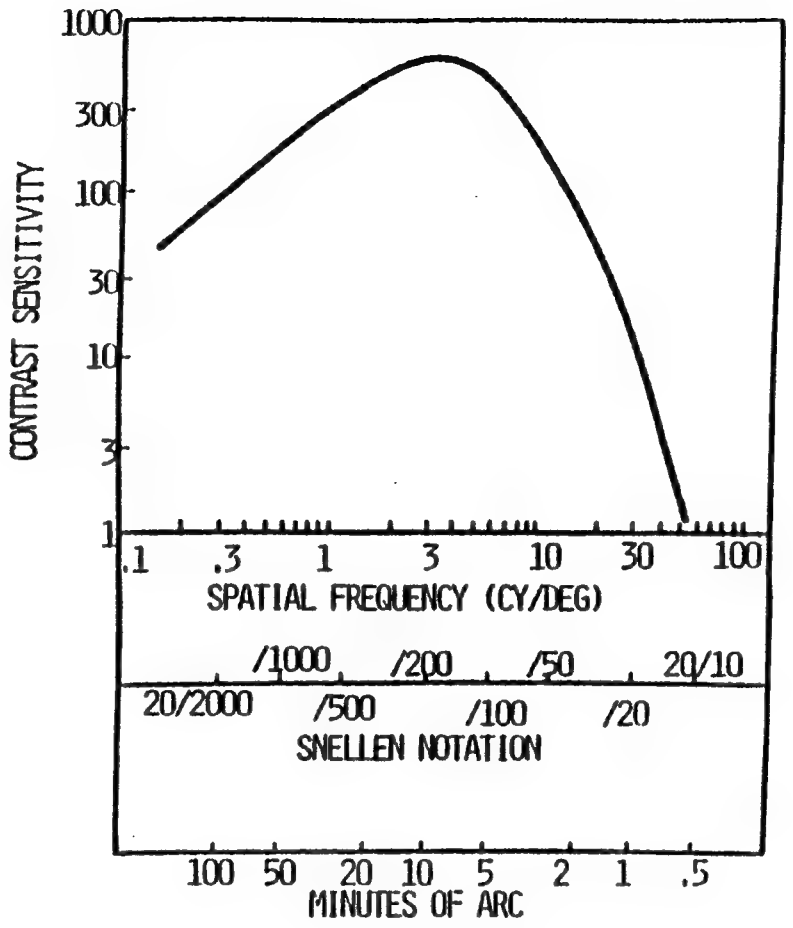

Figure 4. Sensitivity of the visual system to contrast. The sensitivity of the visual system varies for targets containing different spatial frequencies (usually measured with square or sinusoidal gratings). Lower contrasts are required to see medium spatial frequencies between 3-6 c/d. Thus, contrast sensitivity is highest for these spatial frequencies, as indicated by the peak in the function. Contrast sensitivity is lower for low and high spatial frequencies. The intersection of the right endpoint of the function with the abscissa represents the visual acuity of the observer. Visual acuity represents the highest spatial frequency that can be detected at high (usually 90 - 100%) contrast and is shown here to be approximately 60 c/d, or roughly 20/10 Snellen acuity. This is equivalent to the detection of 0.5-min of arc target.

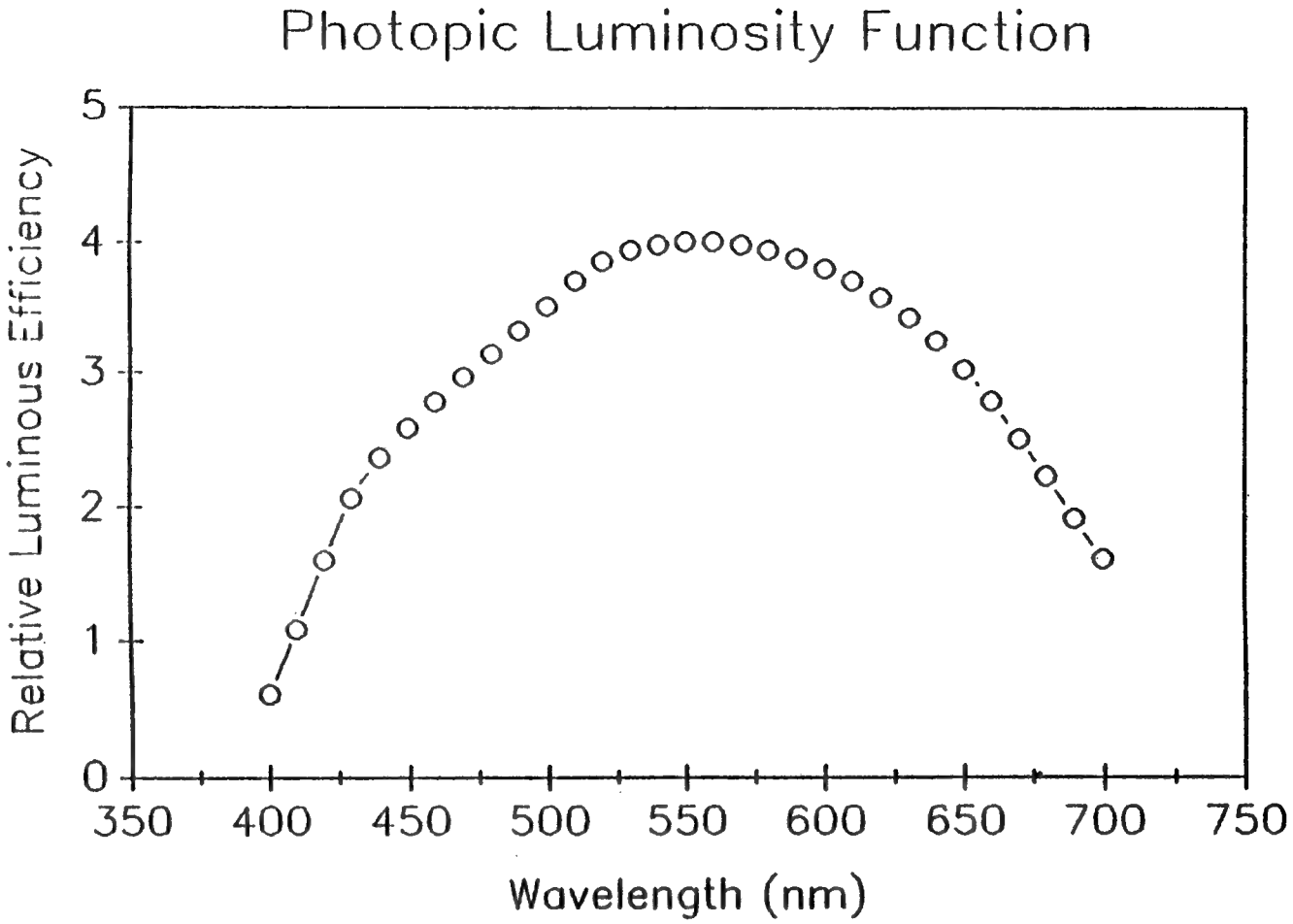

Figure 5. The photopic luminosity function. Visual sensitivity varies for different wavelengths of light, with peak sensitivity at 555 nm. This function is used to equate wavelengths of light for visual luminous efficiency. The photopic luminosity function is typically measured using a critical flicker frequency (CFF) paradigm where subjects are asked to minimize the flicker of a temporally modulating target (25 Hz) or by measuring detection thresholds for small (0.05°), brief (10 ms) targets superimposed on photopic neutral (white) backgrounds.

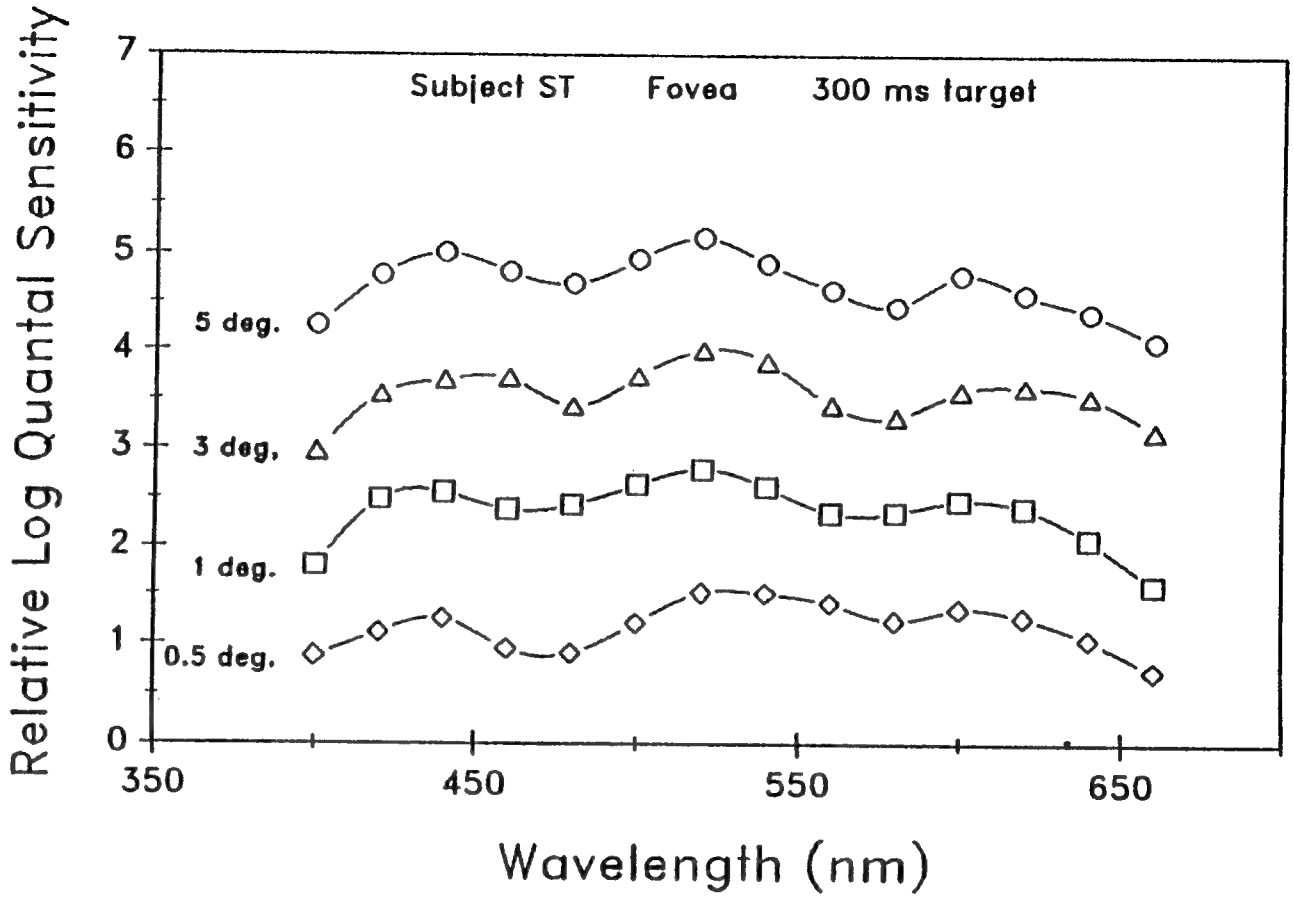

Figure 6. Increment threshold spectral sensitivity as a function of target size. Foveal spectral sensitivity to long-duration targets superimposed on photopic neutral backgrounds have three peaks in the short-, middle-, and long-wavelength regions. This function has been modeled using the underlying cone absorption function and assumes opponent interactions between the middle- and long-wavelength-sensitive cones. (Adapted from Thomas, 1989).

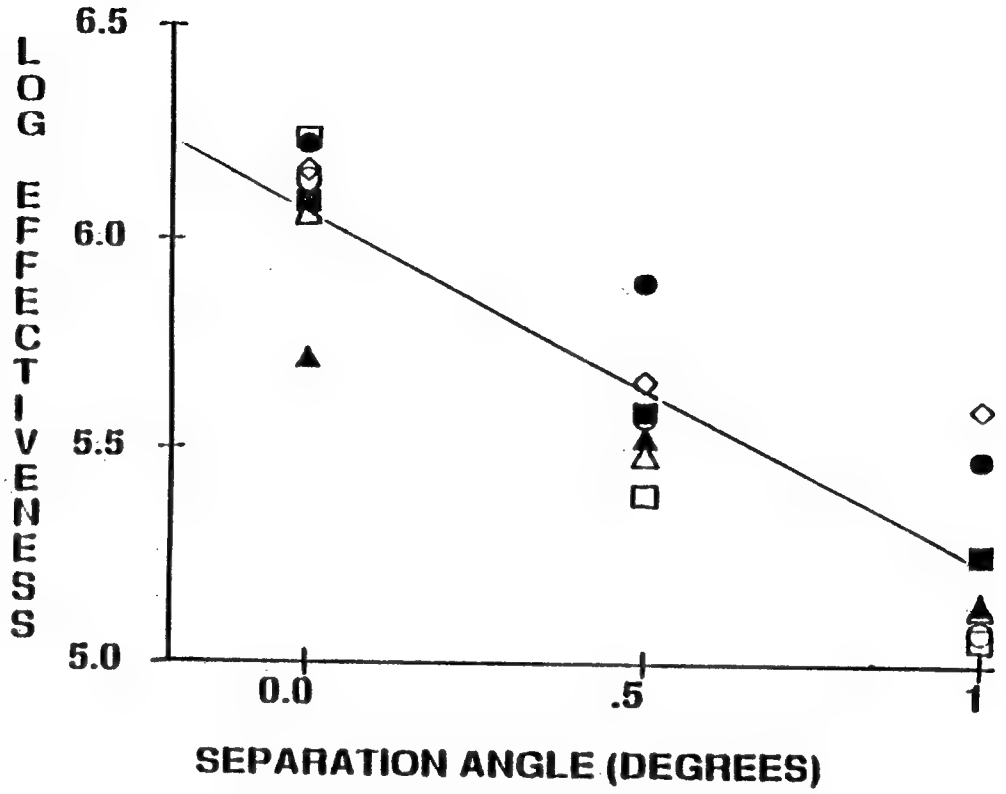

Figure 7. Glare effectiveness as a function of angular separation. The effectiveness of glare decreases dramatically as the angular separation between the target and the laser glare source increases. The separation between a HUD flight path marker target and an argon laser (514-nm) is represented in degrees of visual angle. Glare effectiveness is reduced by over 1.0 log units between 0° - 1° of angular separation between the target and the source.

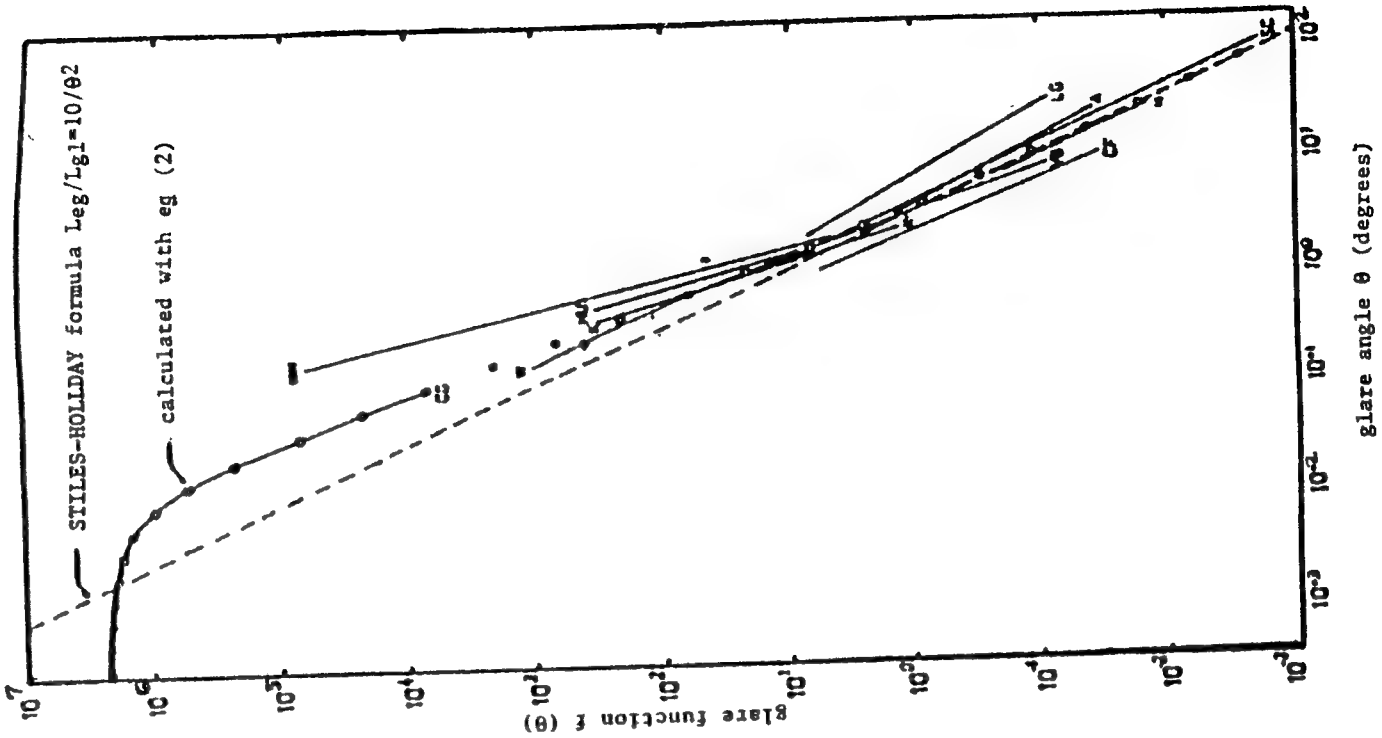

Figure 8. The Vos function of glare. Vos (1984) has described a mathematical function to describe glare effectiveness as a function of angular separation between the visual axis and the glare source. This function is represented by the open symbols and it is shown in relation to data collected in several psychophysical experiments. (Modified from Vos, 1984).

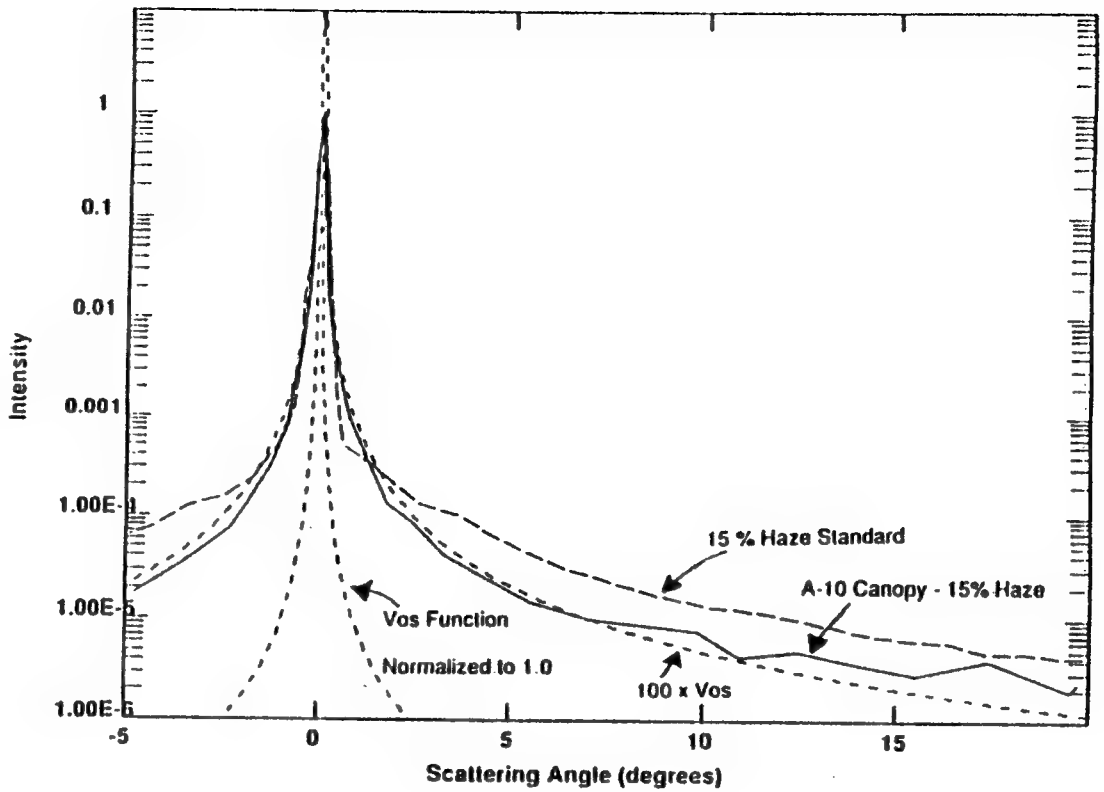

Figure 9. Extraocular scatter effects on the Vos function. The Vos glare function is shown with and without modification by extraocular scatter by the atmosphere and an A-10 canopy. glare effectiveness declines with visual angle, but extraocular media scatter tends to improve its efficiency.

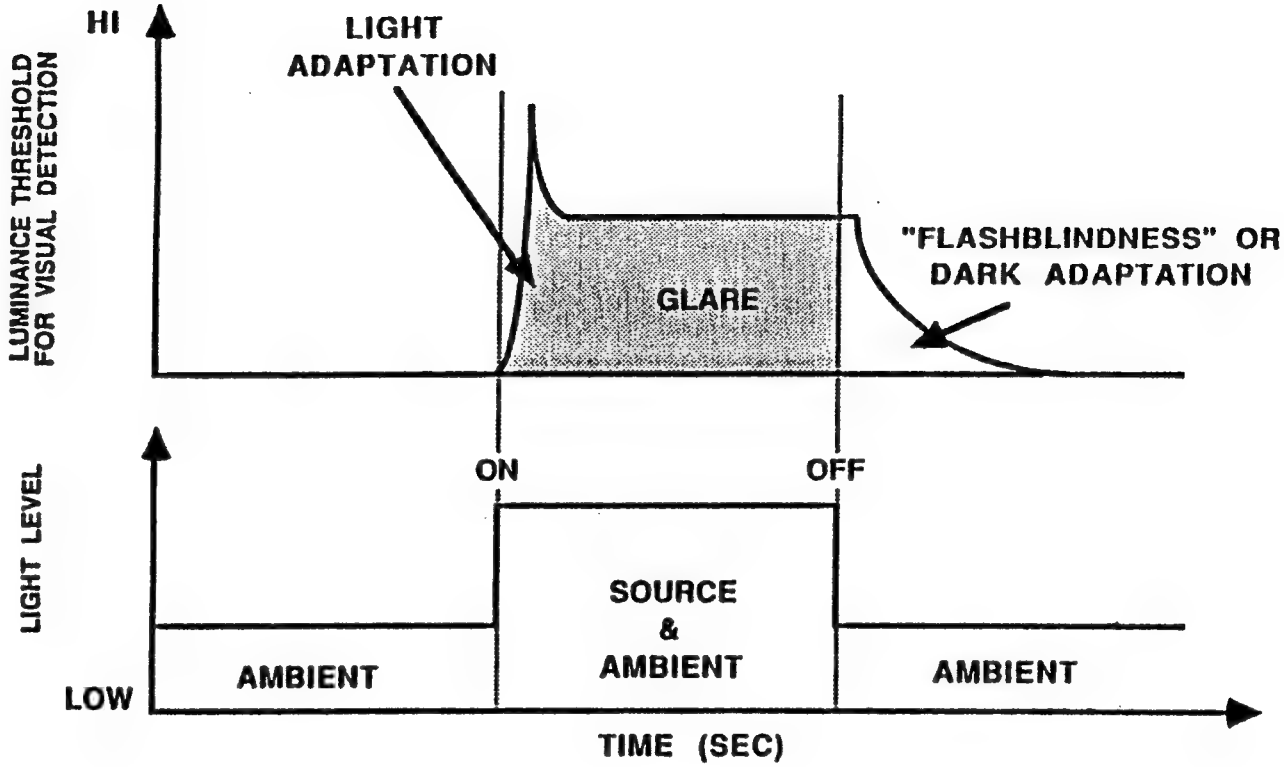

Figure 10. Physiological mechanisms for glare and flashblindness. Glare and flashblindness can be explained in terms of changes in retinal illumination and light- and dark-adaptation responses. (From Menendez and Smith, 1990).

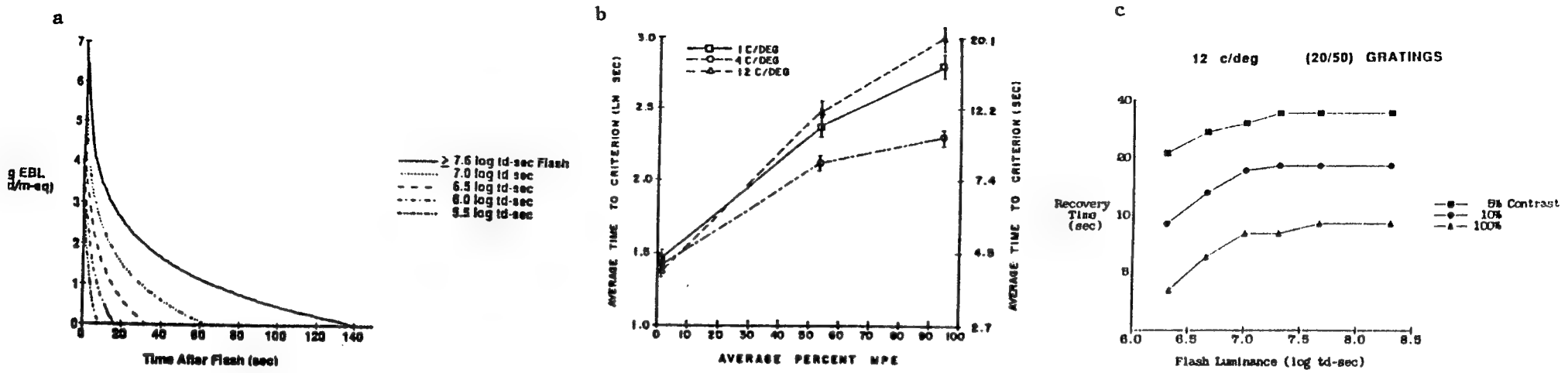

Figure 11. Variables effecting recover from flashblindness. Several target and source variables can slow the recovery rate of flashblindness. The retinal illuminance of the exposure (a) and the spatial frequency (b) and contrast (c) of the target are three such examples of these variables. Data in (a) and (c) were collected by Menendez and Smith (1990) and data in (b) were collected by Rhodes et al. (1988).

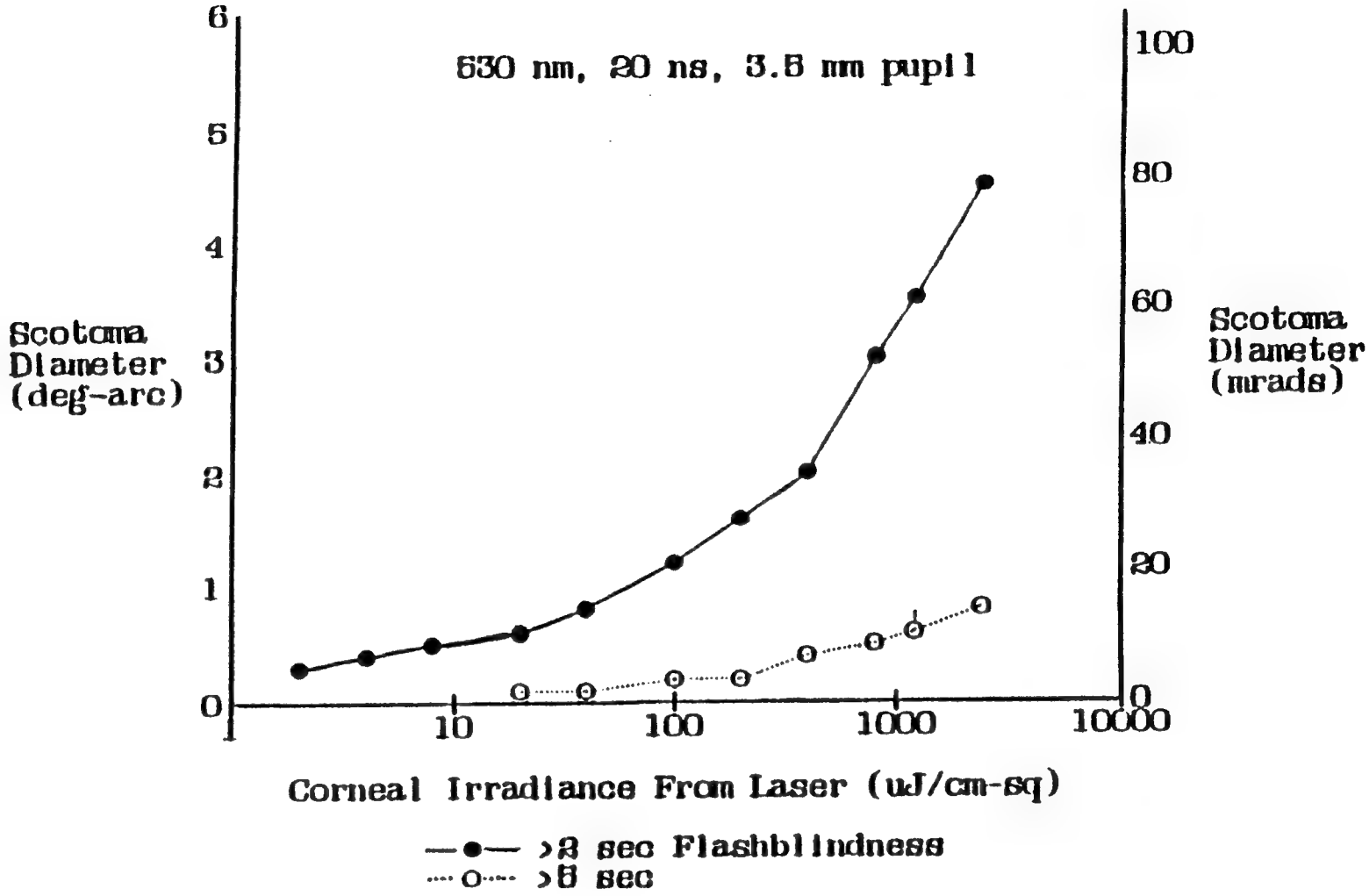

Figure 12. Flashblindness scotoma size as a function of corneal irradiance of the laser exposure. The diameter of the relative scotoma produced by flashblindness (abscissa) is dependent on the corneal irradiance of the flash (ordinate). For a 530-nm, 20ns pulsewidth argon laser flash that produces either 2-s (closed symbols) or 5-s (open symbols) of flashblindesss, the calculated diameter of the relative scotoma increases nonlinearly with the corneal irradiance of the laser exposure. A 3.5-mm pupil size was used in these calculations.

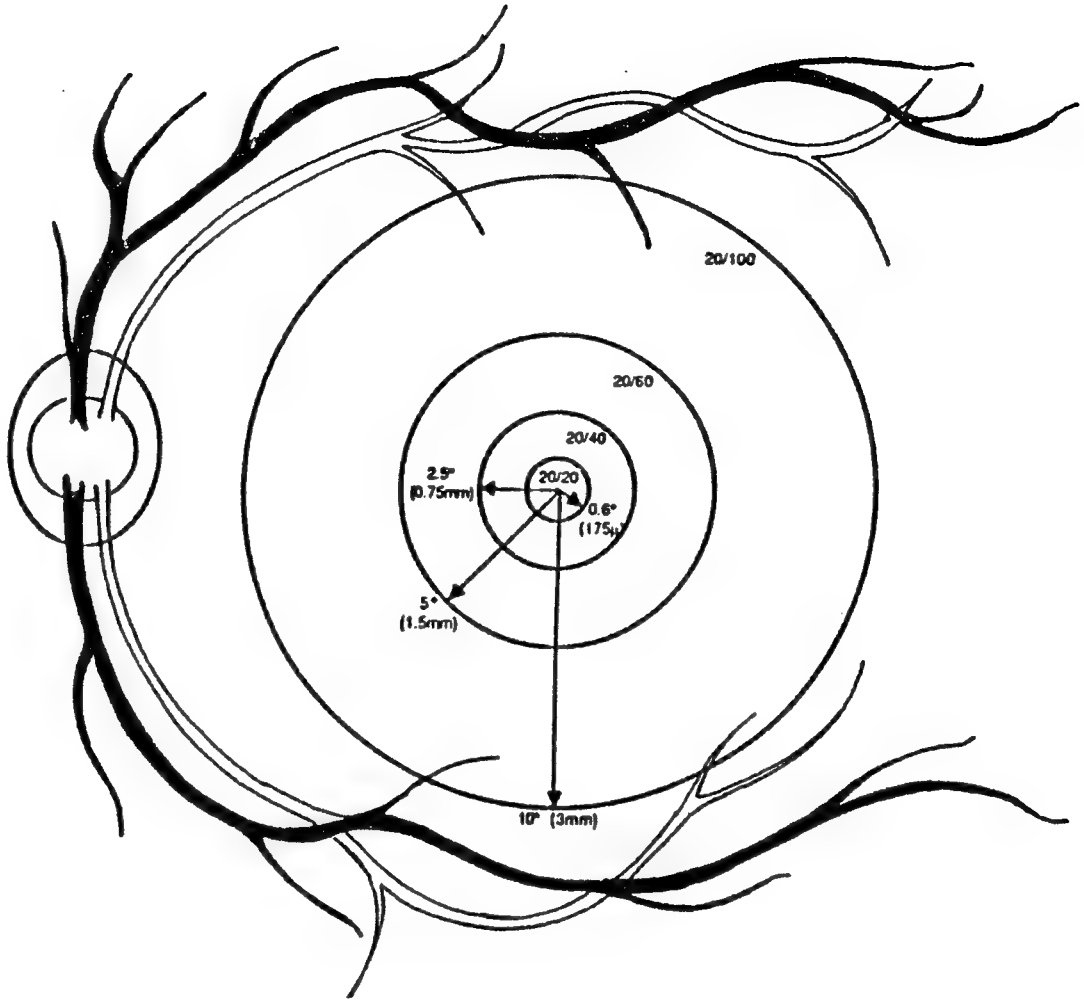

Figure 13. The visual acuity of the posterior pole. Visual acuity of the posterior pole varies with retinal location. As described in Figure 3, visual acuity and contrast sensitivity are best in the foveola and worst in the extramacular region outside the central 10° of the visual axis. Therefore, biological damage occurring in the foveal will have the most profound effects on visual function. Hemorrhagic lesions that occlude the fovea will likely impair vision even if the lesion site is extramacular. The entire central 10° of the retina does not have to be impaired to reduce visual function.

Figure 14. Several types of laser lesions. MVLs and HLs are shown with varying degrees of severity in this monkey fundus photograph. The hemorrhage to the far left has spread into the intraretinal layers and has two MVLs along its right border. The central hemorrhage has also spread into the intraretinal lasers but has a considerable amount of subretinal fluid accumulation. Below the central hemorrhage, several photocoagulation lesions can be seen forming a vertical line. To the far right is a vitreal hemorrhage. Because the interface between the monkey retina and vitreous humor is very tight, the bold does not easily penetrate into the vitreous humor. Instead, it reaches the vireoretinal interface and then flows downward due to the pull of gravity. In humans, where the vitreoretinal interface is not as tight, the hemorrhage would likely spread into the vitreous humor.

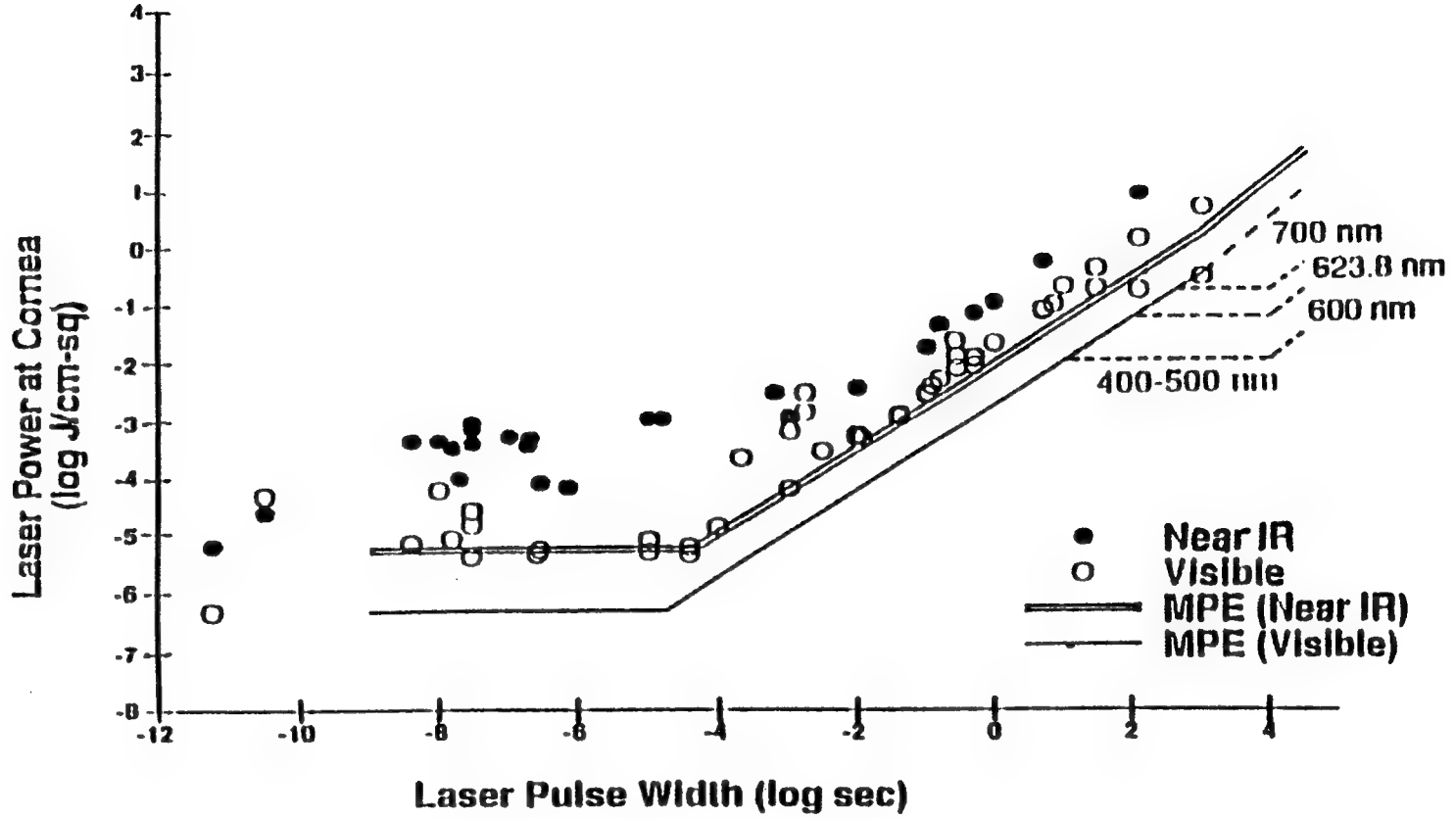

Figure 15. The MPE energy for visible and near IR wavelengths. The MPE is a probabilistic exposure level that is based on experimental data determining hazardous laser exposure energies to the eye or skin. The MPE criteria is set at 10% of the energy levels shown to produce MVLs with at 50% probability. The MPE varies as a function of several variables, including wavelength and pulsewidth.

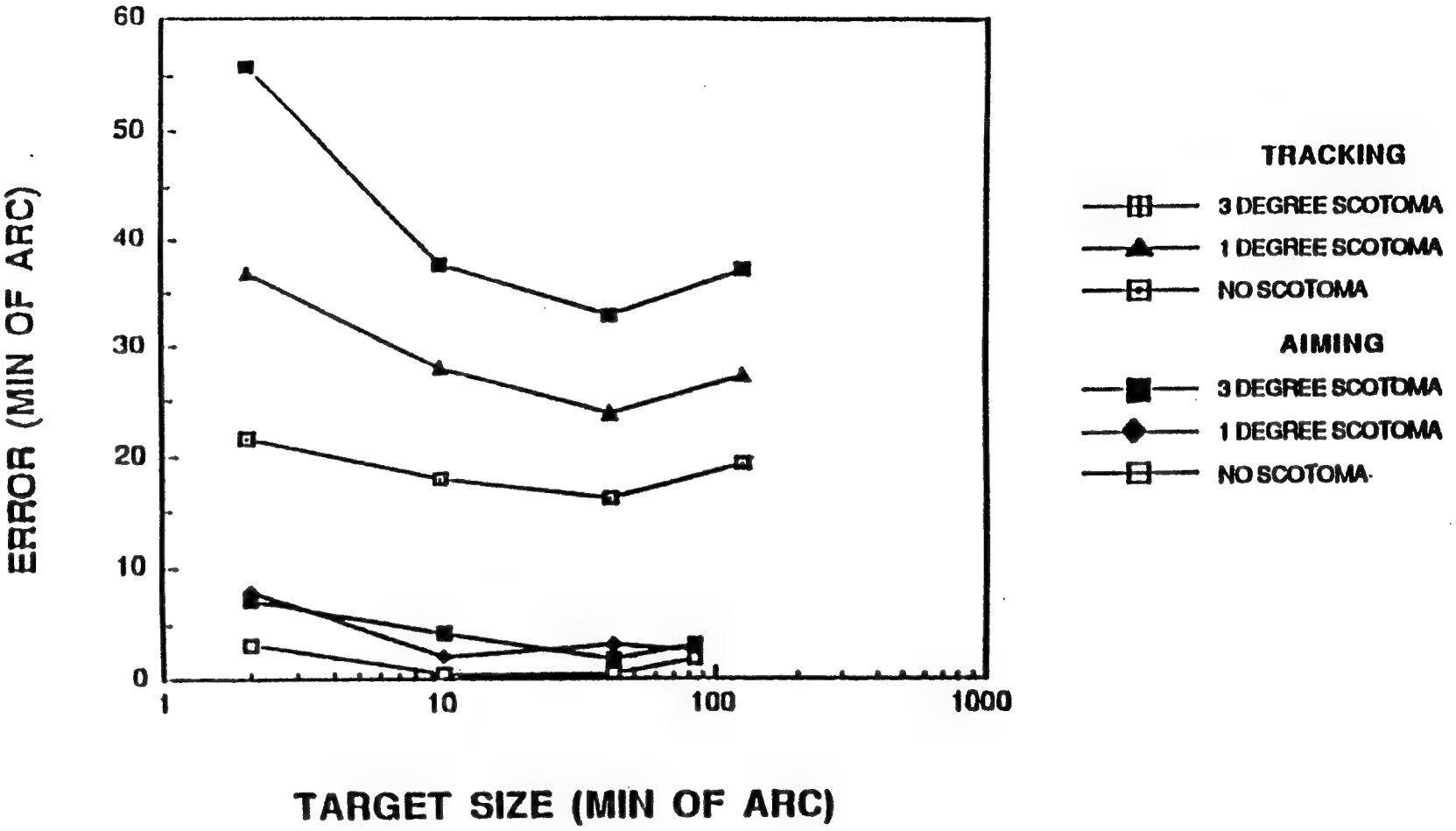

Figure 16. The effect of a foveal scotoma on aiming and tracking. Tracking and aiming abilities can be affected by foveal scotomas. The error of the offset of these abilities (ordinate) is related to both the size of the target (abscissa) and the size of the scotoma (symbol type). In general, tracking is more adversely affected than aiming for small foveal scotomas. For tracking abilities, the larger the foveal scotoma, the worse the performance. Both 1° and 3° scotomas had similar effects on aiming abilities. (Data were collected by Burbeck et al., 1988).

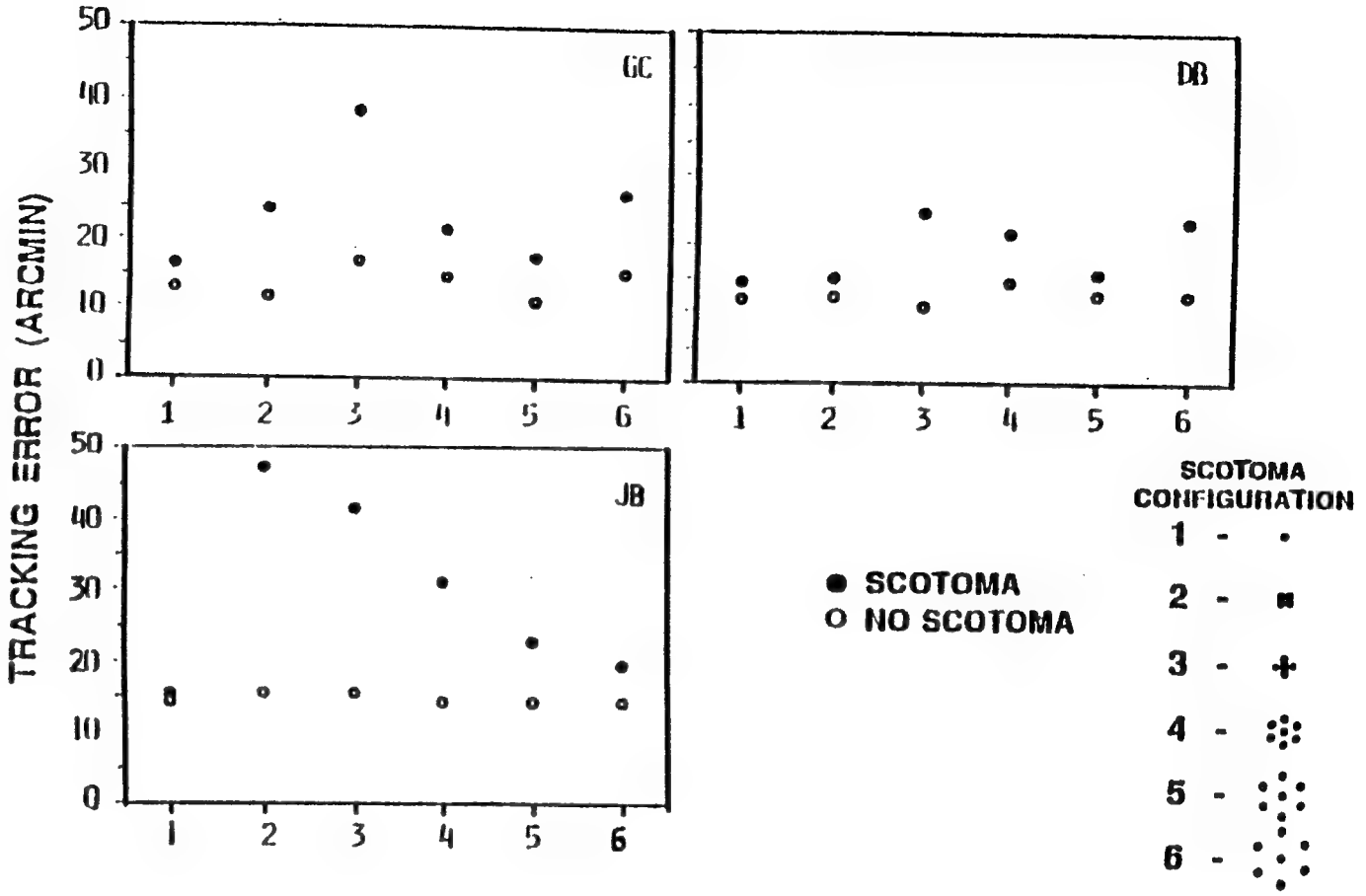

Figure 17. The effect of multiple scotomas on tracking. The error of offset of tracking a target (ordinate) is also affected by the spacing of multiple small scotomas at the fovea (abscissa). The closer the scotomas are to each other, the more adversely effected are the tracking abilities. (Data were collected by Burbeck and Boman, 1987).

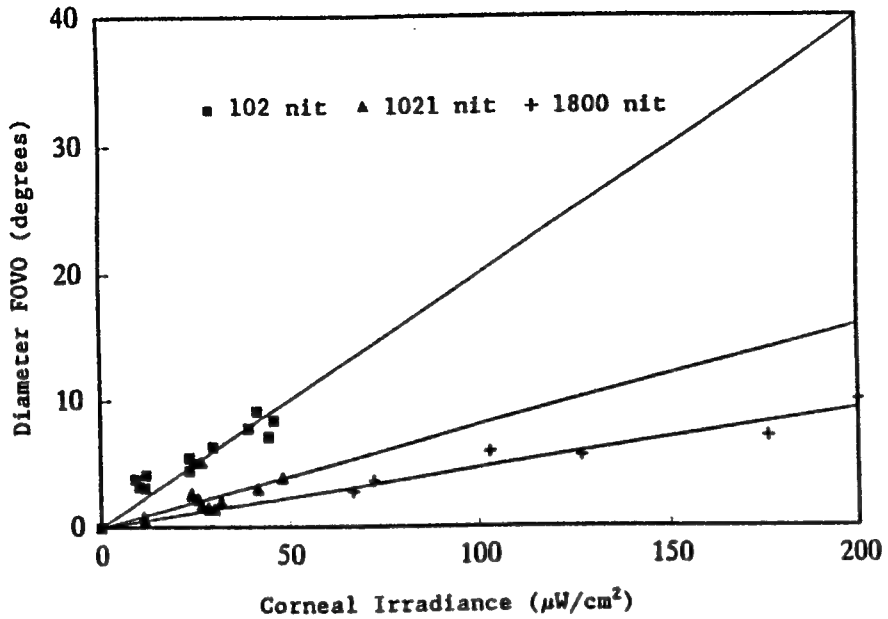

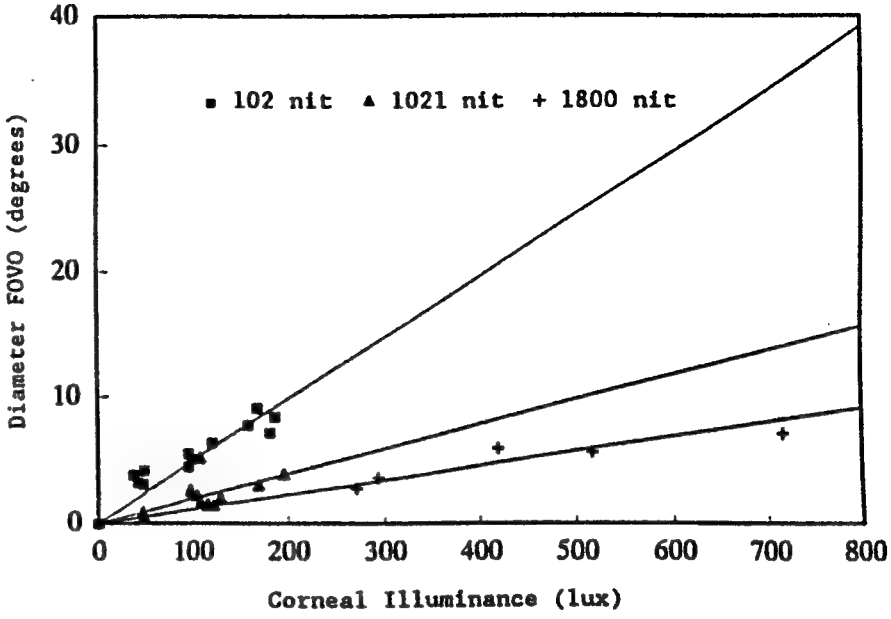

Figure 18. The size of the FOVO by cw laser glare. The diameter of the FOVO (ordinate) by a 514.5-nm cw argon laser is dependent on the corneal irradiance of the laser (abscissa) and the target luminance (symbol type). In general, larger FOVOs are measured for brighter corneal irradiances and with dimmer ambient luminances. The data are fit well by linear regression functions (solid lines). Data were collected by Labo et al., 1990.

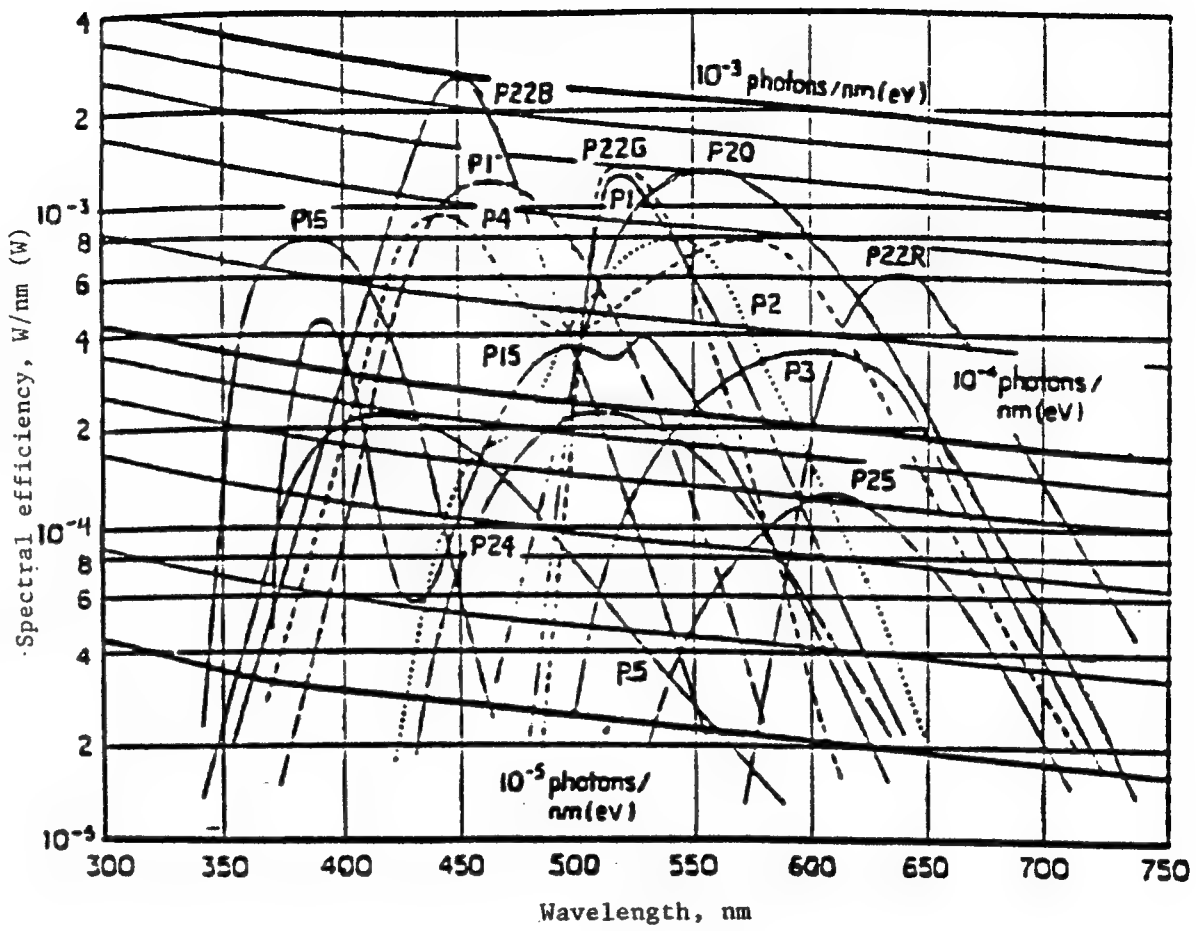

Figure 19. Spectral characteristics of several commercial phosphors. The spectral efficiency of several commercial phosphors is shown as a function of wavelength. The different line types represent different phosphor types. (From "Reference Data for Radio Engineers" (5th ed.), Howard W. Sams & Co., Inc., Indianapolis, Indiana, 1968).

Subjects were exposed to different corneal irradiances.

TABLE 1. AVERAGE VALUES OF SUBJECT TRIALS

SUBJECT (Num)	RUN (Num)	CORNEAL IRRADIANCE ($\mu W/cm^2$)	CORNEAL ILLUMINANCE (lux)	ANGLE OBSCURED (deg)	TARGET LUMINANCE (nit)	REMARKS
3	1	9.1	36.8	3.80	102	24 Sep 86
4	2	10.2	41.5	3.21	102	Canopy
5	3	11.6	47.0	3.11	102	Night
6	4	11.9	48.5	4.13	102	Background
5	19	23.6	96.1	4.47	102	
6	20	23.6	96.1	5.48	102	
4	18	24.6	100.2	5.09	102	
3	17	29.8	121.3	6.32	102	
5	15	39.2	159.6	7.74	102	
6	16	41.4	168.6	9.06	102	
4	14	44.6	181.6	7.07	102	
3	13	45.9	186.9	8.37	102	
3	5	11.4	46.3	0.87	1021	
5	7	11.7	47.5	0.60	1021	
6	24	24.1	98.1	2.67	1021	
3	21	25.8	105.0	2.22	1021	
4	22	26.7	108.7	1.78	1021	
4	10	30.1	122.6	1.43	1021	
5	11	31.9	129.9	2.02	1021	
3	9	41.6	169.5	2.99	1021	
6	12	48.1	195.8	3.90	1021	
3	1	24.3	98.9	2.52	1021	01 Oct 86
1	2	26.7	108.7	5.16	1021	Canopy
5	3	28.5	115.3	1.44	1021	Night
4	4	28.5	116.0	1.54	1021	Background
3	6	66.5	270.8	2.79	1800	10 Oct 86
1	7	72.0	293.2	3.61	1800	Canopy
1	3	103.0	419.4	5.92	1800	Late
3	2	127.0	517.1	5.60	1800	Afternoon
2	5	176.0	716.6	7.08	1800	Background
4	4	200.0	814.6	10.00	1800	

TABLE 2. MEASURED SIZES OF ADATS ON VIDEO DISPLAY

Range (meters):	ADATS Size (Inches) Height	(Width)
48	6 1/2	4
100	3 3/4	2
149	2 3/4	1 1/2
249	1 3/4	3/4
500	1	3/4
1000	1/2	5/16
1250	5/16	1/4
1500	1/4	3/16
2000	3/16	1/4
2500	1/4	1/4
3000	11/16	11/16
3500	not distinguishable	

REFERENCES

Abramov, I., & Gordon, J. (1988). Color appearance in peripheral retina: naso-temporal asymmetries. Invest. Ophthal. Vis. Sci. (ARVO abst.), 29, 300.

Air Force Occupational Safety and Health Standard 161-10. (1980). Health hazards control for laser radiation. Department of the Air Force.

Ahnelt, P. K., Kolb, H., & Pflug, R. (1987). Identification of a subtype of cone photoreceptor, likely to be blue sensitive, in the human retina. J. Comparative Neurol., 255, 18-34.

Allen, R. G., Blankenstein, M., & Zuclich, J. A. (1986). Dose quantification of some retinal effects produced by Q-switched laser radiation. In L. A. Court, A. Duchene, & D. Courant (Eds.), Lasers and Protection Standards, Proceedings of the First International Symposium on Laser Biological Effects and Exposure Limits, Commisariat a l'Energie Atomique, Cedex, France.

Allen, R. G., Labo, J. A., & Mayo, M. W. (1990). Laser eye protection. International Society for Optical Engineering (S.P.I.E.) Proceedings, 1207, Technical Conference on "Laser Safety, Eyesafe Laser Systems, and Laser Eye Protection," Los Angeles, CA.

American National Standards Institute, Inc. (1986). American national standard for the safe use of lasers. Standard Z136.1. New York.

Barlow, H. B., & Sparrock, J. M. B. (1964). The role of after-images in dark adaptation. Science, 144, 1309-1314.

Barron, C., & Waiss, B. (1987). An evaluation of visual acuity with the Corning CPF 527 lens. J. Am. Opt. Assoc., 58, 50-54.

Berggren, L. (1970). Coloured glasses and colour vision, with reference to car driving. Acta Ophthal., 48, 537-545.

Birngruber, R., Puliafito, C. A., Gawande, A., Lin, W. Z., Schoenlein, R. T., & Fujimoto, J. G. (1987). Femtosecond laser-tissue interactions: Retinal injury studies. I.E.E.E. J. Quantum Electronics, QE-23, 1836-1844.

Blankenstein, M. F., Zuclich, J. A., Allen, R. G., Davis, H., Thomas, S. J., & Harrison, R. F. (1986). Retinal hemorrhage thresholds for Q-switched neodymium-YAG laser exposures. Invest. Ophthal. Vis. Sci., 27, 1176-1179.

Boettner, E. A., & Wolter, J. R. (1962). Transmission of the ocular media. Invest. Ophthal., 1, 776-783.

Boynton, R. M. (1979). Human color vision. New York: Holt, Rinehart, & Winston.

Boynton, R. M., Schafer, W., & Neun, M. E. (1964). Hue-wavelength relation measured by color naming method for three retinal locations. Science, 146, 666-668.

Brown, J. L. (1965). Flashblindness. Am. J. Ophthalmol., 60, 505-520.

Burbeck, C. A., & Boman, D. K. (1988, March). Final report on SRI project 5556 for the period September 1986 to October 1987. California: SRI International.

Burbeck, C. A., & Boman, D. K. (1989, March). Tracking with a foveal obscuration. Final report overing the period November 1987 to December 1988 (SRI project 5556). California: SRI International.

Cartledge, R. M., Allen, R. G., Previc, F. H., Glickman, R. D., & Mehaffey, L. (1988). Alterations in visual evoked potentials and pattern electroretinograms following multiple laser pulses and off-axis lesions. In L. A. Court, A. Duchene, & D. Courant (Eds.), Lasers and protection standards, Proceedings of the First International Symposium on Laser Biological Effects and Exposure Limits. Commisariat a l'Energie Atomique, Cedex, France.

Chisum, G. T. (1968). Intraocular effects on flashblindness. Aerosp. Med., 39, 860-868.

Chisum, G. T., & Morway, P. E. (1974). Flashblindness following double flash exposures. Aerosp. Med., 45, 1013-1016.

Cornsweet, T. N. (1970). Visual perception. Orlando: Academic Press.

Curcio, C. A., Sloan, K. R., Packer, O., Hendrickson, A. E., & Kalina, R. E. (1987). Distribution of cones in human and monkey retina: individual variability and radial asymmetry. Science, 236, 579-582.

Davis, E. T., Yager, D., & Jones, B. J. (1987). Comparison of perceived spatial frequency between the fovea and the periphery. J. Opt. Soc. Am., 4(8), 1606-1611.

Davson, H. (1976). The physiology of the eye. New York: Academic Press.

deMonasterio, F. M. (1978a). Properties of concentrically organized X and Y ganglion cells of macaque retina. J. Neurophysiol., 41(6), 1394-1417.

deMonasterio, F. M. (1978b). Center and surround mechanisms of opponent-color X and Y ganglion cells of retina of macaques. J. Neurophysiol., 41(6), 1418-1434.

deMonasterio, F. M., & Gouras, P. (1975). Functional properties of ganglion cells of the rhesus monkey retina. J. Physiol., 251, 167-195.

Diakides, N. A. (1975). Phosphor screens. In D. G. Fink & A. A. McKenzie (Eds.), Electronic engineer's handbook, (pp. 11-33 - 11-45). New York: McGraw Hill.

Dodge, R. (1903). Five types of eye movement in the horizontal meridian plane of the field of regard. Am. J. Physiol., 8, 307.

Finkelstein, M. A., & Hood, D. C. (1982). Detection and discrimination of small, brief lights: variable tuning of opponent channels. Vision Res., 24, 175-181.

Gallagher, J. T., & MacKenzie, W. F. Retinal subthreshold laser exposures: cumulative effect. USAFSAM-TR-74-39, September 1974.

Geisler, W. S. (1979). Evidence for the equivalent-background hypothesis in cones. Vision Res., 19, 799-805.

Geisler, W. S. (1981). Effects of bleaching and backgrounds on the flash response of the cone system. J. Physiol., 312, 413-434.

Gibbons, W. D. Retinal burn thresholds for exposure to a frequency-doubled neodymium laser. USAFSAM-TR-73-45, November 1973.

Gibbons, W. D., & Egbert, D. E. Ocular damage thresholds for repetitive pulsed argon laser exposures. USAFSAM-TR-74-1, February 1974.

Gille, J., Larimer, J., Piantanida, T., & Landham, J. (1990). Geometry of perceptual fields across naturally occurring scotomas: is the evidence for perceptual distortions? Invest. Ophthal. Vis. Sci. (ARVO abstr.), 31(4), 410.

Ginsburg, A. P., Evans, D. W., Sekuler, R., & Harp, S. A. (1982). Contrast sensitivity predicts pilots' performance in aircraft simulators. Am. J. Optom. Physiol. Optics, 59, 105-109.

Glickman, R. D. (work in progress). Contract F33615-88-C-0631, USAF Armstrong Laboratory.

Glickman, R. G., Rhodes, W. R., & Smith, P. (1991). Visual acuity following hemorrhagic lesions in the eye I. Lesions resulting from laser exposures to the fovea. Submitted to USAF Armstrong Laboratory, Brooks AFB, Texas.

Gordon, J., & Abramov, I. (1977). Color vision in the peripheral retina. II. Hue and saturation. J. Opt. Soc. Am., 67(2), 202-207.

Graham, N. V. S. (1989). Visual pattern analyzers. New York: Oxford University Press.

Green, R. P., Cartledge, R. M., Cheney, F. E., & Menendez, A. R. Medical management of combat laser eye injuries. USAFSAM-TR-88-21, October 1988.

Ham, W. T., Jr., Ruffolo, J. J., Jr., Mueller, H. A., & Guerry, D. (1980). The nature of retinal radiation damage: dependence on wavelength, power level, and exposure time. Vision Res., 20, 1105-1111.

Ham, W. T., Jr., Mueller, H. A., Ruffolo, J. J., Jr., & Clarke, A. M. (1979). Sensitivity of the retina to radiation damage as a function of wavelength. Photochem. Photobiol., 29, 735-743.

Harwerth, R. S., & Smith, E. L. III. (1985). Rhesus monkey as a model for normal vision in humans. Am. J. Optom. Physiol. Optics, 62, 626-632.

Hecht, S., Schlaer, S., & Pirenne, M. H. (1942). Energy, quanta, and vision. J. Gen. Physiol., 25, 819-840.

Hellinger, G. (1983). Use of the CPF lenses for light sensitive individuals. J. Vis. Impairment & Blindness, 77, 449.

Hibino, H. (1990). R-G and Y-B opponent-color responses as a function of human retinal eccentricity. Invest. Ophthal. Vis. Sci. (ARVO suppl.), 31(4), 262.

Higgins, K. E., Meyers, S. M., Jaffe, M. J., Roy, M. S., & deMonasterio, F. M. (1986). Temporary loss of foveal contrast sensitivity associated with panretinal photocoagulation. Arch. Ophthalmol., 104, 997-1003.

Hood, D. C., & Finkelstein, M.A. (1986). Sensitivity to light. In K. R. Boff, L. Kaufman, and J. P. Thomas (Eds.), Handbook of perception and human performance (pp. 5-5 - 5-59). New York: Wiley & Sons.

Hovis, J. K., Lovasik, J. V., Cullen, A. P., & Kothe, A. C. (1989). Physical characteristics and perceptual effects of "blue-blocking" lenses. Optom. & Vis. Sci., 66, 682-689.

Hubel, D. H., & Wiesel, T. N. (1968). Receptive fields and functional architecture of monkey striate cortex. J. Physiol., 160, 106-154.

Hurvich, L. M., & Jameson, D. (1957). An opponent-process theory of color vision. J. Psychol. Review, 64(1), 384-404.

Ingling, C. R., & Martinez-Uriegas, E. (1985). The spatiotemporal properties of the r-g X-cell channel. Vision Res., 25, 33-38.

International Committee of the Red Cross. Proceedings of the first working group of experts of lasers in the modern battlefield, Geneva, Switzerland, May 1990.

Johnson, M. A. (1986). Color vision in the peripheral retina. Am. J. Optom. Physiol. Optics., 63, 97-103.

Kelly, S. A., Goldberg, S. E., & Banton, T. A. (1984). Effect of yellow-tinted lenses on contrast sensitivity. Am. J. Optom. Physiol. Optics, 61, 657-662.

King-Smith, P. E., & Carden, D. (1976). Luminance and opponent contributions to visual detection and adaptation and to temporal and spatial integration. J. Opt. Soc. Am., 66, 709-717.

Kinney, J. A., Paulson, H. M., & Beare, A. N. (1979). The ability of color defectives to judge signal lights at sea. J. Opt. Soc. Am., 69, 106-113.

Kosnik, W. D. A preliminary model of the distribution of laser-induced retinal lesions resulting from eye and head responses. USAFSAM-TR-88-19, November 1988.

Kosnik, W., Cheney, F., Cartledge, R., Rhodes, J., Elliott, W. R., & Myers, M. Color appearance of monochromatic and broadband light sources through LGB+2 spectacles. USAFSAM in-house report, November 1989.

Kuyk, T. K. (1982). Spectral sensitivity of the peripheral retina to large and small stimuli. Vision Res., 22, 1293-1297.

Kuyk, T. K., Norden, L. Z., & Ehrnst, S. S. (1986, September). An evaluation of visual field testing methods on measured visual fields. Presented at the Annual Meeting of Veterans Administration Health Services Research and Development Scientific Advisory Committee, Little Rock, AR.

Kuyk, T. K., & Thomas, S. R. (1990). Effect of short wavelength absorbing filters on Farnsworth-Munsell 100-hue test and hue identification task performance. Optom. & Vis. Sci., 29, 522-525.

Labo, J. A., Menendez, A. R., Allen, R. G., Edmonds, B. P., & Turner, M. D. Outdoor measures of laser veiling glare effects on the visual field: a preliminary study. USAFSAM-TR-90-9, March 1990.

Legge, G. E., & Kersten, D. (1987). Contrast discrimination in peripheral vision. J. Opt. Soc. Am., 4(8), 1594-1598.

Leigh, R. J., & Zee, D. S. (1985). The neurology of eye movements. Philadelphia: F. A. Davis Company.

Lennie, P. (1980). Parallel visual pathways: a review. Vision Res., 20, 561-594.

L'Esperance, F. A. (1989). Ophthalmic lasers. St. Louis: The C. V. Mosby Company.

Loxsom, F. (1989, June). Retinal thermal simulation of laser-induced damage. User Guide. Final Report. USAF School of Aerospace Medicine, Aerospace Medical Division (AFSC), Brooks Air Force Base, TX.

Lynch, D. M., & Brilliant, R. (1984). An evaluation of the Corning CPF 550 lens. Optom. Monthly, 75(1), 36-42.

Mainster, M. A. (1989). Laser light, interactions, and clinical systems. In F. A. L'Esperance, Jr. (Ed.), Ophthalmic lasers, (pp. 61-77). St. Louis: C. V. Mosby Company.

Marron, J. A., & Bailey, I. L. (1982). Visual factors and orientation-mobility performance. Am. J. Opt. Physiol. Optics, 59(5), 413-426.

Menendez, A. R., & Garcia, P. V. (1985). Human psychophysics--contrast sensitivity measures of flashblindness. In USAFSAM-TR-85-13, Effects of laser radiation on the eye: Volume IV. (Distribution Statement: Distribution limited to DoD components only; software documentation; 31 January 1985. Other requests for this document must be referred to USAFSAM/TSK-D [STINFO].)

Menendez, A. R., & Smith, P. (1990). Model for predicting the effects of laser exposures and eye protection on vision. S.P.I.E. Proceedings, Laser Safety, Eyesafe Laser Systems, and Laser Eye Protection, 1207, 21-33, Los Angeles, CA.

Miller, N. D. (1965). Visual recovery from brief exposures to high luminance. J. Opt. Soc. Am., 55, 1661-1669.

Miller, N. D. (1966a). Positive after-image following brief high-intensity flashes. J. Opt. Soc. Am., 56, 802-806.

Miller, N. D. (1966b). Positive after-image as a background luminance. J. Opt. Soc. Am., 56, 1616-1620.

Olzak, L. A., & Thomas, J. P. (1986). Seeing spatial patterns. In K. R. Boff, L. Kaufman, and J.P. Thomas (Eds.), Handbook of perception and human performance (pp. 7-1 - 7-54). New York: Wiley & Sons.

O'Mara, P. A., Stamper, D. A., Lund, D. J., & Beatrice, E. S. (1980). Chromatic strobe flash disruption of pursuit tracking performance. Letterman Army Institute of Research, Report # 88.

O'Neal, M. R. & Miller, R. E. (1988). Further investigation of contrast sensitivity and visual acuity in pilot detection of aircraft. AAMRL-TR- 88-002, Armstrong Aerospace Medical Research Laboratory, Wright- Patterson AFB, OH.

Österberg, G. (1935). Topography of the layer of rods and cones in the human retina. Acta Ophthal. Suppl. 6.

Padmos, P. (1984). Glare and tunnel entrance lighting: effects of stray light from eye, atmosphere, and windscreen. C.I.E. Journal, 3, 1-24.

Pearlman, A. L. (1981). Anatomy and physiology of central visual pathways. In R. A. Moses (Ed.), Adler's physiology of the eye clinical application (pp. 427-465). St. Louis: C. V. Mosby Company.

Pender, P. M., Benson, W. E., Compton, H., & Cox, G. B. (1981). The effects of panretinal photocoagulation of dark adaptation in diabetics with proliferative retinopathy. Am. Acad. Ophthal., 20, 635-637.

Perez, E.J., & Flick, C. (1991). FV-4 laser eye protection (LEP) spectacle test report. Modern Technology Corporation Report Number 90-029-03.

Phillips, R. A., & Kondig, W. (1975). Recognition of traffic signals viewed through colored filters. J. Opt. Soc. Am., 65, 1106-1113.

Pokorny, J., Smith, V. C., Verriest, G., & Pinkers, A. J. L. C. (1979). Congenital and acquired color vision defects. New York: Grune and Stratton.

Previc, F. H., Allen, R. G., & Blankenstein, M. F. (1985). Visual evoked potential correlates of laser flashblindness in rhesus monkeys II. Doubled-neodymium laser flashes. Am. J. Optom. Physiol. Optics, 62(9), 626-632.

Raninen, A., & Rovamo, J. (1987). Retinal ganglion-cell density and receptive-field size as determinants of photopic flicker sensitivity across the human visual field. J. Opt. Soc. Am., 4(8), 1620-1626.

Rhodes, J. W., & Garcia, P. V. (work in progress). Visual acuity and spatial contrast sensitivity as a function of retinal lesions. (Contract F33615-88-C-0631) USAF Armstrong Laboratory.

Rhodes, J. W., Garcia, P. V., & Cosgrove, D. J. (1989). Behavioral measurement of laser flashblindness in rhesus monkeys. Aviat. Space, & Environ. Med., 60, 34-39.

Robbins, D. O., Zwick, H., & Holst, G. C. (1974). Functional assessment of laser exposures in awake task-oriented rhesus monkeys. Mod. Probl. Ophthal., 13, 284-290.

Robinson, J., Story, S. M., & Kuyk, T. K. (1991). Evaluation of the Nite Lite as a night vision aide. J. Vis. Impair. & Blindness.

Rovamo, J., & Virsu, V. (1979). An estimation and application of the human cortical magnification factor. Exp. Brain Res., 37, 495-510.

Russell, P. W., Sekuler, R., & Fetkenhour, C. (1985). Visual function after pan-retinal photocoagulation: a survey. Diabetes Care, 8, 57-63.

Sanders, V. E., & Zuclich, J. A. Research on the eye effects of laser radiation, Annual Report, Contract F41609-73-C-0017. Technology Incorporated, San Antonio, Texas, Part I, February, 1974, & Part V, February, 1975.

Sheehy, J. B. (1989a). An overview of laser eye protection. NADC-89074-60, Naval Air Development Center, Warninster, PA.

Sheehy, J. B. (1989b). Dazzling glare: protection criteria versus visual performance. NADC-89076-60, Naval Air Development Center, Warminster, PA.

Sliney, D. H. (1986). Interaction mechanisms of laser radiation with ocular tissues. In L. A. Court, A. Duchene, & D. Courant (Eds.), Lasers and Protection Standards, Proceedings of the First International Symposium on Laser Biological Effects and Exposure Limits, Commisariat a l'Energie Atomique, Cedex, France.

Sliney, D. H., Wangemann, T. T., Franks, J. M., & Wolbarsht, M. L. (1976). Visual sensitivity of the eye to infrared laser radiation. J. Opt. Soc. Am., 66, 339.

Smith, P. A., Glickman, R. D., & Coffey, D. J. (1990). Visual acuity following hemorrhagic laser lesions. Proc. XI Conf. Lasers Mod. Battlefield, Letterman Army Institute of Research, Presidio of San Francisco, CA.

Spalton, D. J., Hitchings, R. A., & Hunter, P. A. (1985). Atlas of clinical ophthalmology. Philadelphia: J. B. Lippincott Company.

Sperling, H. G., & Harwerth, R. S. (1971). Red-green cone interactions in the increment threshold spectral sensitivity of primates. Science, 173, 180-182.

Stiles, W. S., & Crawford, B. H. (1937). The effect of a glaring light source on extra-foveal vision. Proceed. Roy. Soc. (Lond.), B122, 255-280.

Stiles, W.S. (1946). A modified Helmholtz line element in brigthness-colour space. Proc. Phys. Soc (London).

Sulak, D.E. (1988). Aircrew ocular laser protection QOT&E. USAF Tactical Air Warfare Center Project 87B-052T, Eglin AFB, Florida.

Thomas, J. P. (1987). Effect of eccentricity on the relationship between detection and identification. J. Opt. Soc. Am., 4(8), 1599-1606.

Thomas, S. R. (1989). Spatiotemporal properties of peripheral color mechanisms. Unpublished doctoral dissertation, University of Alabama at Birmingham, Birmingham, Alabama.

Thomas, S. R., & Kuyk, T. K. (1988). D-15 performance with short wavelength absorbing filters in normals. Am. J. Optom. Physiol. Optics, 65(9), 697-702.

Thomas, S. R., & Kuyk, T. (1989). Foveal and peripheral spectral sensitivity functions and bichromatic mixture thresholds of normal. Invest. Ophthal. Vis. Sci. (ARVO abst.), 30(3), 128.

Thomas, S.R., & Kuyk, T. (1990). The effect of stimulus size & duration on spectral sensitivity in the peripheral retina. Submitted to Vision Res., September 1990.

Tuper, V., Miller, D., & Miller, R. (1985). The effect of a 550 nm cutoff filter on the vision of cataract patients. Ann. Ophthal., 17, 67-73.

Tyler, C.W. (1987). Analysis of visual modulation sensitivity III. Meridianal variations in peripheral flicker sensitivity. J. Opt. Soc. Am., 8(4), 1612-1619.

van Esch, J. A., Koldenhof, E. E., van Doorn, A. J., & Koenderink, J. J. (1982). Spectral sensitivity and wavelength discrimination of the human peripheral visual field. J. Opt. Soc. Am., 1(5), 443-450.

Varner, D. C., Cartledge, R. M., Elliott, W. R., Menendez, A. R., Carrier, R., & Richter, M. J. Wavelength-dependent and-independent effects of veiling glare on the visibility of head-up display (HUD) symbology. USAFSAM-TR-88-15, September 1988.

Varner, D. C., Thomas, S. R., & Cartledge, R. M. (1991). The effects of glare angle, aircraft canopy, and ambient luminance on HUD symbol detection. Submitted to Human Factors.

Vasilenko, L. S., Chebotaev, V. P., & Troitskii, Y. V. (1965). Visual observation of infrared laser emission. Sov. Phys. JETP, 21, 513.

Vassiliades, A., Zweng, H. C., Peppers, N. A., Peabody, R. R., & Honey, R. C. (1970). Thresholds of laser eye hazards. Arch. Environ. Health, 20, 161-170.

Veenhuis, M. E. (1986). Human brightness and color vision: An investigation of two systems of photopic light adaptation using a double threshold technique. Unpublished masters thesis, University of Alabama at Birmingham, Birmingham, Alabama.

Virsu, V., & Rovamo, J. (1979). Visual resolution, contrast sensitivity, and the cortical magnification factor. Exp. Brain Res., 37, 475-594.

Vos, J. J. (1984). Disability glare--a state-of-the-art report. C.I.E. Journal, 3, 39-53.

Wagner, G., & Boynton, R. M. (1972). Comparison of four methods of heterochromatic photometry. J. Opt. Soc. Am., 62(12), 1508-1515.

Walls, G.C. (1942). The vertebrate eye and its adaptive radiation. Cranbrook Inst. Sci. Bull., 19, Broomfield Hills, MI.

Watson, A. B. (1987). Estimation of local spatial scale. J. Opt. Soc. Am., 4(8), 1579-1582.

Westheimer, G., & Conover, D. W. (1954). Smooth eye movements in the absence of a moving visual stimulus. J. Exp. Psych., 47(4), 283-284.

Wolbarsht, M. L., & Allen, R. G. (1986). New laser device for ophthalmology: comment. Applied Optics, 25(10), 1533-1534.

Wolfe, J. A. (1984). Laser retinal injury. Institute Report # 177, Letterman Army Institute of Research, Presidio of San Francisco, CA.

Wooten, B. R., & Geri, G. A. (1987). Psychophysical determination of intraocular light scatter as a function of wavelength. Vision Res., 27(8), 1291-1298.

Wyszecki, G., & Stiles, W. S. (1982). Color science. New York: Wiley & Sons.

Yates, T. J., & Harding, T. H. (1983). Primate spatial vision: psychophysical studies of macaque monkey and humans. Presented at the annual meeting of the Aerospace Medical Association, Houston, TX. 93

Zaidi, Q., & Pokorny, J. (1988). Appearance of pulsed infrared light: second harmonic generation in the eye. Applied Optics, 27, 1064-1068.

Zigman, S. (1990). Vision enhancement using a short wavelength light-absorbing filter. Optom. & Vision Sci., 67, 100-104.

Zuclich, J. A. (work in progress). Contract F33615-88-C-0631, USAF Armstrong Laboratory.

Zuclich, J. A., & Blankenstein, M. F. (1983, September). Ocular effects of laser radiation, Part I, Third Annual Report (Contract F33615-80-C-0610). San Antonio, TX: Technology Incorporated.

Zuclich, J. A., Glickman, R. D., Varner, D. C., Kosnik, W. D., & Brakefield, J. C. Research on the ocular effects of laser radiation. Executive Summary. USAFSAM-TP-88-8, September 1988.

Zwick, H., & Beatrice, E. S. (1978). Long-term changes in spectral sensitivity after low-level laser (514 nm) exposure. Mod. Probl. Opthal., 19, 319-325.

Zwick, H., Bedell, R. B., & Bloom, K. R. (1974). Spectral and visual eficits associated with laser irradiation. Mod. Probl. Ophthal., 13, 99-306.

Zwick, H., Bloom, K. R., & Beatrice, E. S. (1988). Permanent visual change associated with unctate foveal lesions. In L. A. Court, A. Duchene, and D. Courant (Eds.), Lasers and Protection Standards, Proceedings of the First International Symposium on LaserBiological Effects and Exposure Limits. Commisariat a l'Energie Atomique, Cedex, France.

Zysset, B., Fujimoto, J. G., Puliafito, C. A., Birngruber, R., Deutsch, T. F. (1989). Picosecond optical breakdown: Tissue effects and reduction of collateral damage. Lasers in surgery and medicine, 9, 193-204.

☆U.S. GOVERNMENT PRINTING OFFICE: 1995 - 660-049/00034